

Posterior Cranial Base Growth and Development Changes as Assessed Through CBCT Imaging  
in Adolescents

by

Kristopher Scott Currie

A thesis submitted in partial fulfillment of the requirements for the degree of

Master of Science

Medical Sciences – Orthodontics

University of Alberta

©Kristopher Currie, 2017

## **ABSTRACT**

**Introduction:** Understanding craniofacial growth and development is important for accurate diagnosis, treatment planning and post treatment evaluation of orthodontic cases. Paramount to this is knowledge of the cranial base growth and development, since it is the foundation upon which the remaining facial structures develop.

In this study, a systematic review was conducted to gather knowledge about previous data on growth changes in the posterior cranial base. Inter-rater, intra-rater and accuracy of 33 selected landmarks in the posterior cranial base and surrounding area were then evaluated via three-dimensional (3D) cone beam computed tomography (CBCT). An adolescent population was then used to assess growth related dimensional changes of the previously selected landmarks.

**Methods:** Systematic review was conducted via the PRISMA guidelines. Reliability and accuracy were assessed using CBCT's of 10 dry skulls. Sixty (60) CBCT images of the adolescent population at two time-points were used to assess growth related dimensional changes using the 33 selected landmarks.

**Results:** The selected landmarks in the posterior cranial base and surrounding area were found to be reliably and accurately located in 3D. Over the growth period studied (17.5months), minor statistically significant changes occurred, but they were deemed clinically irrelevant.

**Conclusions:** The studied landmarks in the posterior cranial base and surrounding area showed minor, but potentially important, clinically insignificant changes over the relatively study period. The observed changes could be attributed to measurement error. The posterior cranial base is

deemed to be stable in all three dimensions of study during the adolescent growth period studied, but over a longer time frame may show continued growth.

## **PREFACE**

This thesis is an original work by Kristopher Currie. Research ethics approval from the University of Alberta Research Ethics Board, project name “Posterior Cranial base changes assessed through CBCT”.

## **ACKNOWLEDGEMENTS**

Thank you to my supervisor Dr. Manuel Lagravère-Vich. I appreciate all your guidance, mentoring and knowledge that you bestowed upon me over the past three years. Completing this research project was a larger task than originally thought but I thank you for the assistance. I would also like to thank Dr. Carlos Flores-Mir and Dr. Heesoo Oh. You all contributed so much to the process. Your suggestions and guidance were welcomed contributions to the completion of this thesis project.

I would also like to thank my family. My parents for always supporting me and encouraging me to follow my dreams. My wife Maeva, thank you for being there for me, supporting me, loving me, and always believing in me. Finally to my baby Mila; you are the reason I get up every morning, your laughter always brightens my day. Papa loves you.

## Table of Contents

Chapter 1: Introduction and Systematic review .....	1
1.1 Statement of the Problem .....	1
1.1.1 Research questions .....	1
1.2 Systematic review of literature: Posterior Cranial base natural growth and development .....	2
1.2.1 Introduction .....	2
1.2.2 Materials and Methods .....	3
1.2.3 Results .....	5
1.2.4 Discussion .....	8
1.2.5 Conclusions .....	13
1.2.6 Appendix 1. Articles excluded in phase 2 .....	25
Chapter 2: Reliability and Accuracy of Posterior Cranial base and surrounding area landmarks assessed through CBCT .....	26
2.1 Introduction .....	26
2.2 Materials and Methods .....	29
2.3 Statistical Analysis .....	33
2.4 Results .....	34
2.5 Discussion .....	44
2.6 Conclusions .....	56
2.7 Appendices .....	56
Chapter 3: Posterior Cranial base and surrounding area changes assessed through CBCT Imaging in adolescents .....	70
2.1 Introduction .....	70
2.2 Methods and Materials .....	71
2.3 Statistical Analysis .....	74
2.4 Results .....	76
2.5 Discussion .....	81
2.6 Conclusions .....	88

2.7	Appendices.....	88
CHAPTER 4: General Discussion .....		95
4.1	Discussion .....	95
4.2	Limitations .....	96
4.3	Future recommendations.....	98

**List of Tables**

Table 1.1	Search strategy for MEDLINE via OVIDSP (1950 to present).....	16
Table 1.2	Summary of characteristics of included articles .....	17
Table 1.3	Methodological scoring for the included studies.....	22
Table 1.4	Risk of bias among the selected articles (Y=yes, N=no, p=partial).....	23
Table 2.1	Definitions of the chosen distance.....	32
Table 2.2	ICC of intra-rater reliability for landmarks in X, Y, Z axes.....	35
Table 2.3	Intra-rater absolute mean differences (mm) in X, Y, and Z axes.....	36
Table 2.4	Inter-rater reliability ICC values .....	37
Table 2.5	Mean error inter-rater (mm) in X, Y, and Z axes.....	39
Table 2.6	ICC for accuracy of linear measurements.....	40
Table 2.7	Mean Error for difference in linear measurements (mm).....	42
Table 3.1.1	Mean, standard deviation, minimum, maximum at T1, T2 and difference (in years) .....	72
Table 3.1.2	Male and Female Demographics.....	72
Table 3.2	Linear measurements .....	73
Table 3.3	MANOVA pairwise comparisons for growth.....	76
Table 3.4	MANOVA Pairwise comparisons for percentage change.....	78
Table 3.5	pairwise comparisons that showed statistical significance for growth (difference in distances from T1 to T2) when treatment time was considered as a covariate .....,79	79
Table 3.6	Metlab values in all axis (in mm). Highlighted values above the clinically significant value of 1.5mm.....	80

**List of figures**

Figure 1	Flow Diagram of the Study Selection.....	24
Figure 2	Skull set up in ICAT machine.....	30

Figure 3	Close-up of landmarks.....	31
Figure 4	Posterior cranial area of study.....	46

# **Chapter 1: Introduction and Systematic review**

## **1.1 Statement of the Problem**

When assessing growth or treatment outcomes using multiple time points, stable reference structures are required. The cranial base has been used on traditional two-dimensional cephalometric images as this stable reference structure.<sup>1-3</sup> The stability of the posterior cranial base is in question for this study. To the best of our knowledge, three-dimensional (3D) investigation on displacement of the posterior cranial base and surrounding area structures has yet to be reported. Thus, review of the literature needs to take place to better understand what we know, landmarks need to be identified on dry skulls, reliability and accuracy examined, then growth related changes, if they exist, investigated on cone beam computed tomography (CBCT) images on a patient sample.

### **1.1.1 Research questions**

Question #1:

- a) Within the posterior cranial base and surrounding area, which identified landmarks are reproducible and repeatable when viewed in 3D CBCT images?
- b) Are these landmarks accurate and representative of true regional anatomical structures?

Question #2:

Are structures within the posterior cranial base and surrounding area dimensionally stable during the adolescence years?

## 1.2 Systematic review of literature: Posterior Cranial base natural growth and development

### 1.2.1 Introduction

Understanding craniofacial growth and development is important for accurate diagnosis, treatment planning and post treatment evaluation of orthodontic cases. Paramount to this is knowledge of the cranial base growth and development, since it is the foundation upon which the remaining facial structures develop.<sup>4-7</sup> Various methods to assess and analyze craniofacial growth and development have been described in the literature. These include craniometry, anthropometry, cephalometric x-rays, and most recently three-dimensional (3-D) cone-beam computed tomography (CBCT).<sup>8,9</sup>

The cranial base, for orthodontic purposes, is divided into two regions: the anterior, delimited between *Sella* and *Nasion* (S-N), and the posterior, delimited between *Sella* and *Basion* (S-Ba). The cranial base is said to reach 87% of its growth by 2 years and 98% by 15 years of age.<sup>6</sup> Around age 5 the cranial base has completed 90% of its growth and from then on can be considered relatively stable as the remaining 10% of change occurs in the next 10 years.<sup>7</sup> It is known that the maturation of different components of the craniofacial skeleton reach their completion at different time points.<sup>10</sup> It is also considered that some components of the anterior cranial base are the earliest structures in the skull to reach maturity in shape and size at about 7-8 years of age.<sup>11</sup>

A previous report on the posterior cranial base changes has shown that its length and angulation are differentially affected in different vertical facial types.<sup>6</sup> It was also shown that within the posterior cranial base, the spheno-occipital synchondrosis is a cornerstone structure for the growth of the cranial vault as well as craniofacial growth.<sup>12</sup> The spheno-occipital synchondrosis

connects the occipital and sphenoid bones and is located anterior and superior to the foramen magnum and below the pituitary fossa.<sup>13</sup> To date, there are numerous reports that have studied growth of the posterior cranial base and the spheno-occipital synchondrosis,<sup>14-17</sup> but there is no certainty as for when it completes its fusion and consequently stops growing.

As it has been stated the cranial base influences the growth and development of the remaining craniofacial structures. Knowledge of its stability is vital for proper diagnosis and treatment planning by orthodontists because what happens at the cranial base affects the position, size, angles and structure of the overlying face.<sup>6</sup> A previous systematic review synthesized the changes in the anterior cranial base,<sup>18</sup> but did not consider changes in the posterior cranial base. As such, this systematic review aims to provide a synthesis of the published studies evaluating the growth and development of the posterior cranial base.

## **1.2.2 Materials and Methods**

### ***Protocol and Registration***

The PRISMA<sup>19</sup> checklist was used as a template when reporting this systematic review. Neither systematic review registration nor a review protocol was completed.

### ***Information Sources***

With the assistance of a health-sciences librarian, a computerized systematic search was performed up to July 17, 2016 in the following electronic databases: MEDLINE (Via OvidSP), Embase (via Ovid SP), PubMed, and All EBM Reviews databases (Cochrane Database of Systematic Reviews, Database of Abstracts of Reviews of Effects, and Cochrane Methodology Register). Using Google Scholar, a limited grey literature search was also performed, which

consisted of keyword searches with the first 15 webpages of hits reviewed. The bibliographies of the finally selected articles were also hand searched for additional studies that may have been missed during the database searches. Related articles were also searched from the suggested article menu when an article was searched online. Additional articles were added as suggested by an expert in the field (H.O). No language limitations were applied, but the searches were limited to craniofacial studies in humans.

### ***Searches***

When performing the above searches, specific subject headings and keywords were used first in MEDLINE. (Table I) The additional searches were modifications from this search, directed for the specific database.

### ***Study Selection***

Two reviewers (K.C and D.S) independently reviewed the articles in both steps of the review process based on the decided inclusion and exclusion criteria. Disagreements in article selection were resolved via discussion, and disagreements that could not be resolved were consulted with another reviewer (M.L)

Phase 1 selection process involved assessing titles and abstracts. Appropriate articles were considered if their abstracts assessed craniofacial growth or analyzed treatment outcome, but had a control group without treatment. Studies assessing fetal growth only or including syndromic patients were excluded.

Phase 2 involved obtaining full copies of the articles selected in phase 1. In this stage articles were excluded if they did not specifically evaluate posterior cranial-base growth. Articles were also rejected if they were case reports or reviews. The articles selected to continue assessed the growth and development of the posterior cranial-base and surrounding structures.

### ***Data Extraction***

Data was extracted from the selected articles on the following items: study design, population characteristics (sample size, sex, age), method used to analyze cranial base growth, results (linear and angulation changes, shape change), and reliability and validity of reported methods (Table II). The primary outcomes were dimensional changes (quantified as continuous variable) in posterior cranial base and surrounding structures during active craniofacial growth and development timing.

### ***Risk of Bias Assessment***

All selected studies were assessed for potential risk of bias using a non-validated quality assessment tool implemented in a previous systematic review<sup>18</sup> (Table III). Two reviewers (K.C and H.S) separately completed this process separately and articles with a score of 50% or less were categorized as poor or low quality (high risk of bias). Good quality articles had scores over 50% and up to 75% (moderate risk of bias). Any article receiving a score greater than 75% was considered to have high or excellent quality (low risk of bias).

## **1.2.3 Results**

### ***Study Selection***

The selection process at each stage of this systematic review is represented in Figure 1. Initially 524 original articles were considered after duplicates removed. Based on the selection criteria, the titles and abstracts were reviewed (phase 1 selection). From these, 54 articles were retrieved for full-text review (phase 2 selection). A total of 31 articles did not satisfy the selection criteria and were excluded (Appendix 1). Therefore, after this final review phase, only 23 articles satisfied the selection criteria and were included in this systematic review.

### ***Study Characteristics***

Summary of the data and results of the selected articles is shown in Table II. Of the 23 articles, 5 were cross-sectional in design<sup>16,20-23</sup>, while the remaining 18 were cohort studies.<sup>5,24-40</sup> The articles were published between 1955 and 2015 and all were published in English. The sample sizes were between 20 and 397 individuals and consisted of craniofacial measurements from living or deceased postnatal human skulls. Validity of the measurements was not determined in any of the studies, while only 6 reported some form of reliability assessment. All the articles measured multiple time points within the same population or data from multiple age groups.

### ***Risk of Bias within Studies***

Table IV summarizes results of the risk of bias assessment. The methodological quality of the studies ranged from poor to excellent quality. The most common weaknesses were failure to validate the accuracy of the findings (none of the studies reported this), insufficient statistical reporting, and failure to calculate or justify sample size.

### ***Results of Individual Studies***

Upon review of the pertinent information from the selected articles, it appears that there was a change for all posterior cranial base linear measurements (from *Sella* (S) to *Basion* (Ba)), among the various age groups studied.<sup>20,24-26,29,33,38-40</sup> In addition, there were variable changes in length and angulation among and between all stages of development.<sup>16,31</sup>

Knott observed that the largest absolute change in linear dimension over a nine year period, from ages 6 to 15, occurred in the post-sphenoid region with an annual average of 1mm.<sup>39</sup> During a similar age interval, other studies also showed similar age-related changes in the posterior cranial base (*S-Ba*).<sup>35,36</sup> Henneberke and Prah-Anderson also reported constant growth velocity for the posterior cranial base (*S-Ba*) over 7 years from age 7 to 14 years at 1mm/yr and 0.9mm/yr for boys and girls, respectively; the average length of the posterior cranial base was 2.5mm larger in boys than girls.<sup>28</sup> On the other hand, other studies showed slightly different growth rates in different age groups and suggested that cranial base growth is closely related to skeletal age.<sup>24,31</sup> Malta et al. showed that the greatest amount of growth was 2.8mm from time 1 to time 2, which correlated to CS1/2 change in growth to CS3/4.<sup>31</sup>

Five studies showed size and growth differences between males and females as the cranial base dimensions increased,<sup>28,29,32,36,40</sup> whereas the other three studies indicated no difference according to sex.<sup>30,31,35</sup>

Two studies reported the changes in posterior cranial base length in adulthood.<sup>26,30</sup> Bishara observed a significant decrease in the cranial base angle (NSO) and increase in cranial base length from age 26 to 46 years.<sup>26</sup> In a group of adults ranging between the ages of 17 and 50 years, Lewis and Roche reported maximum values for posterior cranial base length at age 34.5

years in men and 35.0 years in women, with a growth rate of 0.3mm/year in men and 0.2mm/year in women.<sup>30</sup>

Growth directions of the posterior cranial base were reported. Downward and backward displacement of *Basion* was observed in one study,<sup>25</sup> which corresponds with the downward and slightly backward movement of the occipital condylar point,<sup>39</sup> downward growth of the *Clivus*<sup>32</sup> as well as downward and backward growth of *Sella Turcica* that was reported in another study.<sup>16</sup>

Changes in the cranial base angulation were also noted. Bjork reported that the cranial base angle gradually bends throughout childhood up to about 10 years or so, at which point the cranial base reaches its final shape and the cranial base angle remains relatively stable.<sup>5,34,36</sup> Conversely, Bishara,<sup>26</sup> Knott,<sup>40</sup> Lewis and Roche<sup>30</sup> reported a slightly decrease with age during adulthood.

A meta-analysis was not justified because the methodologies of the selected articles were too heterogeneous.

#### **1.2.4 Discussion**

This systematic review aimed to analyze published studies that evaluated growth of the posterior cranial base and to evaluate their methodological quality. The results indicate that the posterior cranial base is not a totally stable structure during craniofacial growth, and changes in the posterior cranial base are primarily due to growth activity at the speno-occipital synchondrosis, as well as sutural growth (eg, occipito-mastoid changes) and cortical drift, in which bone is resorbed and deposited along the superior and inferior surfaces of the basicranium.<sup>5,16,17</sup> With no definitive agreement on timing of the cessation of growth and closure of the speno-occipital synchondrosis,<sup>16,17</sup> posterior cranial base growth was reported to continue to grow even by small increments into adulthood and beyond.<sup>26,30</sup>

Most commonly reported was the change in length measured in millimeters in various segments of the posterior cranial base using landmarks in the middle and posterior cranial base. As expected, there is a substantial and significant increase in posterior cranial base length during all study periods from birth to adolescents,<sup>20,24,26,29,38-40</sup> and even small increments into adulthood.<sup>26,30</sup>

Proportional growth was reported<sup>24,29</sup> as well as differential growth rates were also seen. The more significant differential growth rates tended to correlate with pubertal growth spurts and growth potential.<sup>20,24,31,32</sup> A calculated length change over a nine year period (from age 6 to 15) was shown.<sup>39</sup> All these studies support this relationship between posterior cranial base length increase with activity of the spheno-occipital synchondrosis, since their study periods were before the estimated closure of the synchondrosis at about age 11-18 years based on laminagraphy, autopsy and serial sections.<sup>16,17,38</sup> Bjork showed dorsal elongation of the cranial base due to endochondral growth at the *Clivus*.<sup>5</sup>

In reference to direction of change/growth, *Basion* was shown to move backward and downward<sup>5,25</sup>, with an additional point measured in the general area of *Basion*, occipital condyle point (Bolton), also showed downward and backward movement.<sup>39</sup> The anterior reference point for the posterior cranial base, *Sella*, was shown to move down and back as well.<sup>16,18</sup> Although both *Basion* and *Sella* were displaced in the same direction, these changes seem to be due to different mechanisms. Movement of *Basion* can be attributed to synchondrosis growth, whereas movement of *Sella* can be attributed to eccentric growth of the *Sella Turcica* which remains stable at its anterior wall after around age 7. Intrinsic growth of *Sella Turcica* was also shown in a previous systematic review by Afrand et al.<sup>18</sup> As reported by Enlow, development of the endocranium also changes by deposition on the outside and resorption from the inside, also

referred to as cortical drift.<sup>10</sup> This can also explain small changes in location of landmarks from longitudinal cephalograms. Bjork also reported parallel lowering of the *Foramen Magnum*.<sup>5</sup>

Angulation changes of the cranial base showed mixed results. Numerous studies attempt to correlate cranial base angle with facial type, but in this systematic review we solely attempted to address changes due to growth without analyzing its impact on facial characteristics. The longitudinal study by Ohtsuki et al, showed decreases in S-N-Ba angle up to age 18.<sup>38</sup> In contrast, Phelan et al showed that there was no change in cranial base angle measured as SNBa.<sup>34</sup> This was also supported by Thordarson et al who showed no difference in cranial base flexure from age 6 to 16 years.<sup>35</sup> In a longitudinal study by Wilhelm et al, they also reported no difference in cranial base angle between different facial classifications, specifically Class I and Class II.<sup>37</sup> In one of the studies by Knott, she concluded that the decrease in WPO angle (which was defined as the angle between the post-sphenoid line from P to O and the pre-sphenoid line from W to P) and increase in post-sphenoid length corresponded to the movement of the occipital condyle point. She also concluded that angular changes within individuals were small and statistically insignificant changes were present.<sup>39</sup>

When comparing males to females again there is conflicting data for the amount and rate of growth. Ursi et al reported no differences in posterior cranial base length until age 16, when males had larger values and continued to show evidence of growth.<sup>36</sup> In the report by Thordarson et al, no differences were shown between males and females even as the posterior cranial base lengthened.<sup>35</sup> In another study by Knott, when comparing male and female longitudinal growth data, they showed an increase in post-sphenoid length before the age of 6 years and no differences between sexes, but after the age of 12, males showed greater length change.<sup>40</sup> The longitudinal study by Lewis and Roche, which looked at adults up to the age of 50,

showed difference between males and females for maximal growth rate and maximal length of posterior cranial base. Although these values are small, they still show the potential for dimensional change in the posterior cranial base region into adulthood.<sup>30</sup> Overall, the present findings suggest that age-related changes in the craniofacial complex do not stop with the onset of adulthood, but continue, albeit at a significant slower rate, throughout adult life. However, these changes tend to be of small magnitude, so that the clinical relevance is somewhat limited and generally would not significantly influence orthodontic treatment planning.

### ***Limitations***

Even though the commonly accepted techniques for a systematic review were followed, inherent limitations in the search protocol was evident. A significant amount of hand searching recovered 10 of the 23 articles that were chosen for final review. This could be because they were published before the electronic databases began and were not indexed at all or were indexed under different terms.

Another limitation is using a non-validated assessment tool, which was modified to better assess the chosen articles based on a previous systematic review of the anterior cranial base.<sup>18</sup> The use of non-validated assessment tools has its own drawbacks, but with the absence of one validated tool that clearly applies to the type of studies likely to be included, this is inevitable. The studies selected varied significantly in methodological quality. Many were incomplete and considered poor when compared to today's methodological standards, they were also weak in their reporting of findings and their statistical analysis. Inter-examiner and intra-examiner reliabilities were reported in only 20% of the included studies, but should be present to validate the reliability of

landmark identification especially since radiographs were used as the main finding. No authors validated their findings and measurements.

Changes in growth for all studies were reported in millimeters or degrees. Ideally, growth should be reported as a percentage so that one can get an idea of how significant the changes were at any given age. This would also be important when different overall craniofacial sizes are considered.

For growth studies/assessment, long-term longitudinal studies are the best option. Ideal growth studies would follow a large population and obtain records for many years with multiple time points at consistent time intervals. The selected articles varied greatly with regards to the age range studied, developmental stage, data collection technique and data analysis. In addition, 10 out of the 23 selected articles studied subjects from well-known growth studies conducted in North America during the 1930s-1970s. Although they are the best available sample, the same subjects may have been used in multiple studies artificially inflating the overall available data.

Long-term aging studies that include late adulthood are inherently difficult to conduct, and as a result, have a number of limitations such as wide variation in the age of the subjects; different time spans between the examination intervals; and particularly inclusion of 17 to 18 year old subjects for whom later adolescent growth was still possible.<sup>26,30</sup>

In the past, two-dimensional lateral cephalometric radiographs were the most commonly used technique to evaluate growth of the cranial base. The selected articles all used this technique for their analysis of growth and dimensional change in sagittal and vertical dimensions, which lacks assessment of any width (transverse) changes. Measurements in 3D would provide more accurate information on growth changes in the cranial base as a whole. No 3D CBCT studies have yet

been published on the growth of the posterior cranial base. With advances in imaging, landmark identification methods, and ease of use, longitudinal growth studies with CBCT imaging will likely help us better understand growth and stability of the cranial base and craniofacial structures in 3D.

### **Clinical Implications**

This systematic review supports the current evidence and opinions related to posterior cranial base changes. In clinical practice, one must be aware of these changes while diagnosing and treatment planning for orthodontic patients. Superimposition of lateral cephalograms on the posterior cranial base may not be valid given the changes that are demonstrated during craniofacial growth. These findings may help lead to three-dimensional investigation of posterior cranial base growth and development and how these changes should be considered when developing 3D superimposition strategies.

### **1.2.5 Conclusions**

- A significant amount of growth in the posterior cranial base is observed throughout the growth period. Even after pubertal growth has ceased at around 17-18 years, the posterior cranial base is not yet 100% stable and dimensional changes continued into late adulthood although at a small magnitude.
- Growth of the posterior cranial base is generally agreed to be from spheno-occipital synchondrosis growth. Change in length measured from *Sella* to *Basion* is most evident as the posterior cranial base grows.
- *Basion* displaces downward and backward during craniofacial growth.
- *Sella Turcica* moves downward and backward during craniofacial growth.

- The change in cranial base angle (*N-S-Ba*) with age is inconclusive.
- Angulation changes could not be consistently identified among different facial types or malocclusions.

## **Authors' Contributions**

Contributed to study conception and design: KC, HS, DS, ML, CF. Contributed to acquisition of data: KC, DS. Interpreted data: KC, HS, DS, ML, CF. Drafted the paper: KC. Contributed to revisions of manuscript: KC, HS, ML, CF.

## **Funding**

None.

## **Ethics approval**

Not required.

## **Competing Interests**

The authors declare no conflicts of interests.

Table 1.1. Search strategy for MEDLINE via OVIDSP (1950 to present)

#	Searches
1	Exp Maxillofacial development/ OR Growth/ OR human development/
2	Skull/ OR cranial fontanelles/ OR facial bones/ OR pterygopalatine fossa/ OR skull base/ OR sphenoid bone/ OR basion.mp. OR articulare.mp. OR sella turcica/ OR exp cranial fossa, posterior/
3	Exp cephalometry/ab, cl, is, mt, st, sn, td, ut [abnormalities, classification, instrumentation, methods, standards, statistics & numerical data, trends, utilization OR exp Cone-beam computed tomograph/ ae, cl, is, my, st, sn, td, ut OR exp imaging, three-dimensional/ ae, cl, is, mt, st, sn, td, ut OR superimpose*.mp. OR exp methods/ is. Mt, st, ut [instrumentation, methods, standards, utilization]
4	1 AND 2 AND 3
5	4 limited to humans

Table 1.2. Summary of characteristics of included articles

Article	Study Design	Sample size and sex	Age	Measurement Method	Measurement of change reported	Results	Validity/Reliability
Arat et al <sup>24</sup> 2001	Mixed-Longitudinal	78 M=35 F= 43	Group1: 10-12y Group2: 12-15y Group3: 15-17y	- 3 groups divided based on skeletal maturation - Cephalometric and hand wrist films taken - followed for 4 to 7 years	<ul style="list-style-type: none"> <li>Correlated growth potential with growth stage</li> <li>Linear measurement: Tuberculum sella to Basion (T-Ba)</li> <li>Intra- and inter-group differences were examined</li> </ul>	Posterior cranial base (T-Ba) showed substantial increase in all developmental phases and variance among developmental stages - growth differences most evident in group 2 and least in group 3 - group 2 cranial base growth related to growth potential	NR
Arat et al <sup>25</sup> 2010	Longitudinal	30 Class II division 1 M=12 F=18	T1: 11.98 ± 1.30 T2: 15.32± 1.12 T3: 32.12± 6.85	<ul style="list-style-type: none"> <li>Lateral cephalograms</li> <li>Skeletal maturation assessed by CVM</li> <li>Radiographs traced by one operator and superimposed with the new T-W method and common superimposition methods</li> <li>Horizontal and vertical distances of cranial landmarks measured from reference lines</li> </ul>	Graphed displacement (in mm) among superimposition methods	<ul style="list-style-type: none"> <li>Backward movement on Ba in all study periods</li> <li>- Downward displacement of Ba in all study periods</li> </ul>	Same procedures repeated for 10 patients 1 month later -Reliability of measurements calculated by Cronbach alpha reliability test
Bishara et al <sup>26</sup> 1994	Longitudinal	30 M=15 F=15  IOWA growth study	M: 25-45y F: 26-46y	<ul style="list-style-type: none"> <li>Cephalometric analysis,</li> <li>-Linear and angular measurements                             <ul style="list-style-type: none"> <li>dental cast analysis</li> </ul> </li> </ul>	Mean and difference reported: <ul style="list-style-type: none"> <li>Cranial base (NSO) angle</li> <li>Anterior cranial base (S-N)</li> <li>Posterior cranial base (S-O, "O" is occipital point)</li> </ul>	<ul style="list-style-type: none"> <li>Posterior cranial base length (S-O) increased: 1.2mm(F), 1mm (M)</li> <li>Cranial base length (N-O) increased: 1.8mm (F), 1mm(M)</li> <li>Cranial base angle (NSO) decreased more in male: -0.4°(F), -1.2° (M)</li> </ul>	<ul style="list-style-type: none"> <li>Landmarks identified by one investigator and inspected for accuracy by another</li> <li>Each cephalometric measured twice or more until the readings fell within 0.5mm or 0.5 degree error</li> </ul>
Franchi et al <sup>27</sup> 2007	Longitudinal	34 17 Class II div 1 - M (11), F(6) 17 Class I - M (13), F(4)  The university of Michigan & the Denver Child Growth study	<ul style="list-style-type: none"> <li>T1, prepubertal (CS1)-10y</li> <li>T2, postpubertal (CS6)</li> </ul>	<ul style="list-style-type: none"> <li>Lateral Cephalograms</li> <li>Thin-plate Spline analysis</li> <li>Registered at Nasion, Sella, Basion</li> </ul>	Thin-plate Spline analysis -size and shape differences	No significant shape changes in cranial base from T1 to T2 - Centroid size changes were significant for class I and class II patients from T1 to T2	Traced by one investigator and checked by another
Henneberke & Prah Andersen <sup>28</sup> 1994	Mixed - longitudinal	151 Untreated - 76(M), 75(F) 81 Treated - 40(M), 41(F)	7-14y  Age 7-9 yearly radiographs Age 9-14 every 6 months	<ul style="list-style-type: none"> <li>Lateral Cephalograms- Sella, Nasion, Basion</li> <li>Linear measurement of S-N, N-Ba, S-Ba</li> <li>Growth velocity curve for S-N, N-Ba, S-Ba</li> </ul>	Velocity growth curve and growth percentile	<ul style="list-style-type: none"> <li>S-Ba distance increased 7y-14y: 7mm(M), 6mm(F)</li> <li>Growth velocity for S-Ba is constant : 1mm/yr (M), 0.9mm/yr (F)</li> <li>Sexual dimorphism in actual size, timing and amount of growth- boys are larger than girls, differences approximate 2.5mm for N-Ba, 2mm for S-N, 1.5mm for S-Ba</li> <li>Orthodontic treatment does not affect</li> </ul>	Defined a tolerance limits of 0.2-1mm between two tracings and measurements were repeated when tolerance limits were exceeded

<b>Jiang et al<sup>29</sup> 2007</b>	longitudinal	28 M=13 F=15  • Chinese subjects • Normal occlusion	13y - 18y	<ul style="list-style-type: none"> <li>• Lateral Cephalograms</li> <li>• Modified mesh diagram analysis by sex</li> <li>• Superimposed mesh diagrams of 13y and 18y at Nasion</li> </ul>	Proportional analysis Average elaborate mesh diagrams reported	<b>cranial base growth</b> <ul style="list-style-type: none"> <li>• Uniform increase in craniofacial growth between 13-18.</li> <li>• Proportionate growth of posterior cranial base</li> <li>• From 13 to 18 years of age, two sexes with normal occlusion displayed different growth patterns</li> </ul>	<ul style="list-style-type: none"> <li>• Elaborate mesh diagrams of subjects generated 2 times 2-4 weeks apart.</li> <li>• Measurement error – no more than 0.04 from Dahlbergs formula</li> </ul>
<b>Lewis &amp; Roche<sup>30</sup> 1988</b>	Longitudinal	20 M=8 F=12  Fels longitudinal growth collection	17y – 50y -	<ul style="list-style-type: none"> <li>• Lateral cephalograms</li> <li>• Linear measurement: S-N, N-Ba, S-Ba</li> </ul>	Reported total increments, age at maximum rate of growth, maximum rate of growth, age at maximum values	<ul style="list-style-type: none"> <li>• Age at maximum values for S-Ba: 35y (M), 29y(F)</li> <li>• Total increment of S-Ba from 17-18y: 1.5mm (M), 1mm (F)</li> <li>• Maximum rates of growth for S-Ba; 34.5y(M), 35y(F)</li> <li>• Maximum rates of growth of S-Ba (mm/year): 0.3 (M), 0.2 (F)</li> <li>• No difference between sexes</li> </ul>	<ul style="list-style-type: none"> <li>• One observer traced each radiograph and selected points. Measurements between points done by another worker.</li> <li>• Mean interobserver difference : 0.09-0.13mm</li> <li>• Mean interobserver difference: 0.08-0.11mm</li> </ul>
<b>Malta et al<sup>31</sup> 2009</b>	Longitudinal	36 M=15 F=21	10-16y(M), 9-15y(F)  <ul style="list-style-type: none"> <li>• T1 Prepeak (CS1&amp;2): 10y (M), 9.4y(F)</li> <li>• T2 Peak (CS3&amp;4): 13y(M), 11.5(F)</li> <li>• T3 Postpeak (CS5&amp;6): 16y(M), 15y(F)</li> </ul>	<ul style="list-style-type: none"> <li>• Lateral cephalograms</li> <li>• Linear measurement at T1, T2, T3: S-N, Ba-N, Ba-S</li> </ul>	Measurements to represent posterior cranial base (Se-Ba, CC-Ba, CF-Po, Ba-Na)	<ul style="list-style-type: none"> <li>• During all studied periods posterior cranial base showed significant proportional growth increases.</li> <li>• Se-Ba (T1-T3) :3.7mm increase for both sex –no sex difference</li> </ul>	<ul style="list-style-type: none"> <li>• Inter-rater reliability determined for CVM and measurements (ICC &gt; than 0.95)</li> </ul>
<b>Melsen<sup>16</sup> 1969</b>	Cross-sectional	132 skulls (sex unknown)	Grouped according to dental development <ul style="list-style-type: none"> <li>• Deciduous dentition-48</li> <li>• Mixed dentition - 64</li> <li>• Permanent (All 8s erupted)-20</li> </ul>	<ul style="list-style-type: none"> <li>• Direct inspection – Closure of speno-occipital synchondrosis (SOS)</li> <li>• Lateral cephalograms</li> <li>• Tomography for 5 skulls</li> <li>• 22 Linear and 2 angular measurements</li> </ul>	<ul style="list-style-type: none"> <li>• Cranial base measurements: N-S, N-Ba, S-Ba, N-S-Ba, N-S-H (Hormion)</li> </ul>	<ul style="list-style-type: none"> <li>• Sella turcica moves 2mm down and back.</li> <li>• Distance between sella and distal surface of synchondral cartilage continued to increase until second molars fully erupted – interpreted as growth of synchondrosis</li> <li>• Incipient closure of speno-occipital synchondrosis (SOS) occurs after complete eruption of all second molars</li> </ul>	Duplicate measurements on 10 skulls. Renewed markings and new radiographs taken. Students t-test did not reveal any systematic error
<b>Mitani<sup>32</sup> 1973</b>	Longitudinal	30 M=17 F=13	7y -15y	<ul style="list-style-type: none"> <li>• Lateral cephalograms</li> <li>• Linear measurement for cranial base growth: S-Ba, N-Ba, Ba-Ar</li> </ul>	Mean curve of the growth rate -reported time difference in maximum annual increment of posterior cranial base to mandibular length	<ul style="list-style-type: none"> <li>• Total increment for S-Ba was smaller in female : 10.3±1.8mm (M), 7.5±1.7mm (F)</li> <li>• Growth of the posterior cranial base and mandibular condyle showed significant correlation.</li> <li>• Total growth increment of the posterior cranial base was smaller in female than male compared with that of the condyle.</li> <li>• 60% of males and females showed</li> </ul>	NR

						coincidence in timing of maximum increment of posterior cranial base and mandibular length.	
<b>Palomo et al</b> <sup>33</sup> 2005	Longitudinal	32 (Females) 16 Class II div1 16 Class I  -Bolton-Brush growth study	T1= 6y T2=11y T3=15y	Lateral & Frontal cephalograms –use 3D landmark frame	Procrustes analysis -Reported shape change in millimeters	Continuous shape change from 6 to 15in both Class II & Class I samples	Intraoperator reliability – same operator identified all landmarks, 37.5% of total sample was digitized 3 times. Reported average difference of 0.627mm
<b>Phelan et al</b> <sup>34</sup> 2014	Longitudinal	24 M=14 F=10  The university of Michigan & the Denver Child Growth study	T1(CS1-2):8y9m T2(CS2-3):11y8m T3(CS4-5):14y2m T4(CS6):16y8m	<ul style="list-style-type: none"> <li>• Lateral cephalograms</li> <li>• Cervical Vertebral maturation stage</li> </ul>	Reported distances and angles <ul style="list-style-type: none"> <li>• Cranial base measurements: N-S-Ba</li> </ul>	No change in cranial base angle (N-S-Ba) T1=130.3°±5.3 T2=129.9 °±5.1 T3=129.8 °±5.5 T4=129.9 °±6.1	Cephalograms traced by one operator then verified by another
<b>Sejrsen et al</b> <sup>21</sup> 1997	Cross sectional	45 skulls Children=36 Adults=9	Based on Dental stage	<ul style="list-style-type: none"> <li>• Direct skull measurement</li> <li>• Photo measurement</li> </ul>	<ul style="list-style-type: none"> <li>• Reported lengths and widths in mm and plotted on graph.</li> <li>• Measurements of the cranial base – 3 widths and 3 length from external base.</li> <li>• Measured between nerve canal openings</li> </ul>	<ul style="list-style-type: none"> <li>• External cranial base grows in width with increasing dental age.</li> <li>• Cranial length increases with dental age.</li> </ul>	Reliability tested by creating local conversion factors which is ratio between distance to the measurement on the skull and the same distance measured on photo
<b>Singh et al</b> <sup>22</sup> 1997	Cross sectional	142 73 class III 69 class I (equal males and females)	5-11	Pretreatment lateral cephalograms in patients with class III molar and class I molar. -13 cranial landmarks digitized and traced	Thin-plate spline analysis	Changes in morphology if the posterior cranial base in Class III group- highest magnitudes affected Bolton, basion, and articulare. It indicated compression in the horizontal axis in the occipital region of the posterior cranial base in all age group, as well as bending, vertical stretching and narrowing.	Upon duplicate digitation, landmarks with more than 1% discrepancy in x and y coordinates were considered unreliable and excluded
<b>Thordarson et al</b> <sup>35</sup> 2006	longitudinal	182 M=95 F=87	6y- 16y	Lateral Cephalograms - 22 landmarks	Posterior cranial base- angular and linear measurements; N-S-Ba, N-S-Ar S-N, S-Ba, S-Ar, N-Ba	<ul style="list-style-type: none"> <li>• Posterior cranial base dimensions increased significantly from 6 to 16 years and greater changes in boys: S-Ba: 8.7mm(M), 6.3mm (F) N-Ba: 13.7mm(M), 10.2mm(F)</li> <li>• Cranial base flexures decreased significantly in both boys and girls: -1.6° (M), -1.0° (F),</li> <li>• No difference in cranial base flexures between boy and girls, either at 6y or at 16y. At 6y: 130.3±4.6° (M), 129.8±4.8 ° (F) At 16y: 128.7±5.3° (M), 128.8±5.2°(F)</li> </ul>	Reliability – replicate measurement trial performed on 30 cephs of 16 year olds. Intra-observer error – cephs traced in 6 year olds were double-checked by second observer.
<b>Ursi et al</b> <sup>36</sup> 1993	Mixed-longitudinal	32 M=16 F=16  -Bolton-Brush growth study (Bolton standard)	6y-18y  Records at ages 6, 9, 12, 14, 16, 18	Lateral Cephalograms -measurements of cranial base, maxilla and mandible, vertical, dentoalveolar	Posterior cranial base- angular and linear measurements; S-N, S-Ba, N-S-Ba(	<ul style="list-style-type: none"> <li>• Sexual dimorphism not evident until age 16 at posterior cranial base length (S-Ba) when males had larger value. After 12 females did not show large increments. At 6y: 42.1mm (M), 38.6mm(F) ns At 12y: 44.7mm (M), 43.9mm(F) ns At 16y: 47mm (M), 44.9mm(F) ns P&lt;0.05 6y-18y: 6mm(M), 6.2mm(F)</li> </ul>	Cephs traced by one investigator and checked for accuracy by a second

						<ul style="list-style-type: none"> <li>No statistically significant changes in cranial base angle (N-S-Ba) and similar for both with a slight decrease with growth</li> </ul>	
<b>Wilhelm et al</b> <sup>37</sup> 2001	Longitudinal	43 (equal males and females) Class I group=22 Class II group=21  -Fels growth study	1mo- 14y T1: 1month T2: 2 y T3: 14y	Lateral Cephalograms	7 cranial base measurements S-N, Se-N S-Se S-Ba, S-Occ, Ba-Occ N-S-Ba(°)  Se=Sphenoethmoidal point Occ=sphenoccipital point	<ul style="list-style-type: none"> <li>Growth occurred between all age groups with largest increases between 1 month and 2 years.</li> <li>No differences in cranial base linear measurements between class I and II.</li> <li>No differences in cranial base angle between class I and class II</li> </ul>	Reliability assessed by retracing and redigitizing 10 randomly selected radiographs. ICC ranged 0.61-0.97
<b>Bjork</b> <sup>5</sup> 1955	Longitudinal	243 (Males)	12-20y T1: 12 years T2: 20 years	Lateral cephalograms Anterior cranial base superimposition technique	Linear and angular measurements S-N, S-Ba, S-Ar, N-Ba, N-Ar N-S-Ba(°), N-S-Ar(°)	<ul style="list-style-type: none"> <li>Dorsal elongation of cranial base due to endochondral growth at the clivus. 12-20y S-Ba:3.8mm, S-Ar:3.2mm, N-Ba:8.1mm</li> <li>No marked change in shape of cranial base on average to remain stable with age (N-S-Ba (0.7°). however, a marked individual variation with age as regards increased or decreased bending was noted</li> <li>There is parallel lowering of the foramen magnum.</li> <li>Age variations in growth magnitude, growth form, and size. Sphenooccipital synchondrosis acts as center of rotation in medial region of cranial base. Temporal bone and glenoid fossa can be displaced down, up, forward or back depending on cranial base rotation which affects mandibular position.</li> </ul>	NR
<b>Lavalle</b> <sup>23</sup> 1978	Cross-sectional	250 (Males)	7y-15y -Class I, Class II -4 age groups: 7-9 9-11 11-13 13-15	Lateral Cephalograms taken and 177 data points placed. X and y coordinates recorded using strip chart digitizer. Data analyzed and placed into 6 categories (coordinates defining the cranial base are of interest here)	Centroids (standard deviation units of the degree of separation between means)	Cranial Base length contributed most to discrimination between the 3 categories. Craniofacial and facial skeletons are similar to cranial base in sagittal growth	NR
<b>Ford</b> <sup>20</sup> 1958	Cross-sectional	71 dry skulls – sex not specified	0-20 years of age	Dry skulls (measured by divider and ruler). 7 linear measurements Grouped based on eruption of dentition	Linear measurements (mm)	Pituitary point-Basion measurement showed continued growth between all grouped skulls	NR
<b>Ohtsuki et al</b> <sup>38</sup> 1982	Mixed-Longitudinal	397 M=220 F=177  -Fels growth study	0-15 years Grouped into age 0-3, 4-6, 7-18.	Lateral Cephalograms -9 landmarks identified.	Linear and Angular measurements	<ul style="list-style-type: none"> <li>S-Ba length increases constantly but slowly after the age of 2 up to age 18.</li> <li>Basion to sphenooccipital synchondrosis and Sella to sphenooccipital synchondrosis dimensions increase steadily, but Sella to sphenooccipital synchondrosis values are smaller.</li> <li>N-S-Ba angle decreases until age 18</li> </ul>	NR

<b>Knott<sup>39</sup> 1969</b>	Longitudinal	37 females  IOWA growth study	6-15y T1= 6y T2=9y T3=12y T4= 15y	Lateral Roentgenograms -Values obtained by averaging measurements made two anthropometrists on three independent lateral roentgenogram films.	<ul style="list-style-type: none"> <li>• Linear measurements (mm) N-F: Frontal sinus F-W: Ethmoid Presphenoid: W-P Postspenoid :P-O</li> <li>• Angular measurements (°) - 3 cranial base angles :NPO, FPO, WPO</li> </ul> <p>F= frontal sinus point W=Sphenoidal wing point P= pituitary point, anterior wall of sella</p>	<ul style="list-style-type: none"> <li>• Postspenoid segment shows greater dimension change in millimeters between 6 and 12 years of age than anterior portions of cranial base. Annual increase of about 1mm.</li> <li>• Postspenoid segment showed largest absolute change over the nine year period. Average nine-year dimensional change of 17% and averaged 6mm</li> <li>• Downward and backward direction of change for occipital condylar point in relation to sphenoid plane.</li> </ul>	Two anthropometrists measured 3 independent films, averages taken (nearest 0.1mm and 0.1 degree)
<b>Knott<sup>40</sup> 1971</b>	Longitudinal	66 F= 36 M=30  IOWA growth study	6-25y T1= 6y T2=11y T3=15y T4=25y (22-29y)	Lateral Roentgenograms taken at all time points. Data was plotted in millimeters at all time points and descriptive statistics made.	<ul style="list-style-type: none"> <li>• Linear measurements (mm) N-F: Frontal sinus F-W: Ethmoid Presphenoid: W-P Postspenoid :P-O</li> <li>• Angular measurements (°) - 3 cranial base angles :NPO, FPO, WPO</li> </ul> <p>F= frontal sinus point W=Sphenoidal wing point P= pituitary point, anterior wall of sella</p>	<ul style="list-style-type: none"> <li>• Postspenoid segment (P-O) length increases by about 5.3mm from 6 to 12 years At 6y: 40.6mm (M), 39.mm(F) At 12y: 46.0mm (M), 44.6mm(F) At 15y: 48.8mm (M), 45.8mm(F) At 25y: 50.6mm(M), 46.7mm(F)</li> <li>• No differences between sexes at 9-12 years of age. After age 12 the difference in the length of postspenoid segment increases between males and females.</li> <li>• No significant change in cranial base angle (NPO) for females, small decreases for males.</li> </ul>	Two independent measurements made, if differences were greater than 0.2mm, additional determinations were made and averages obtained.

M, males; F, females; T, time point; NR, not reported

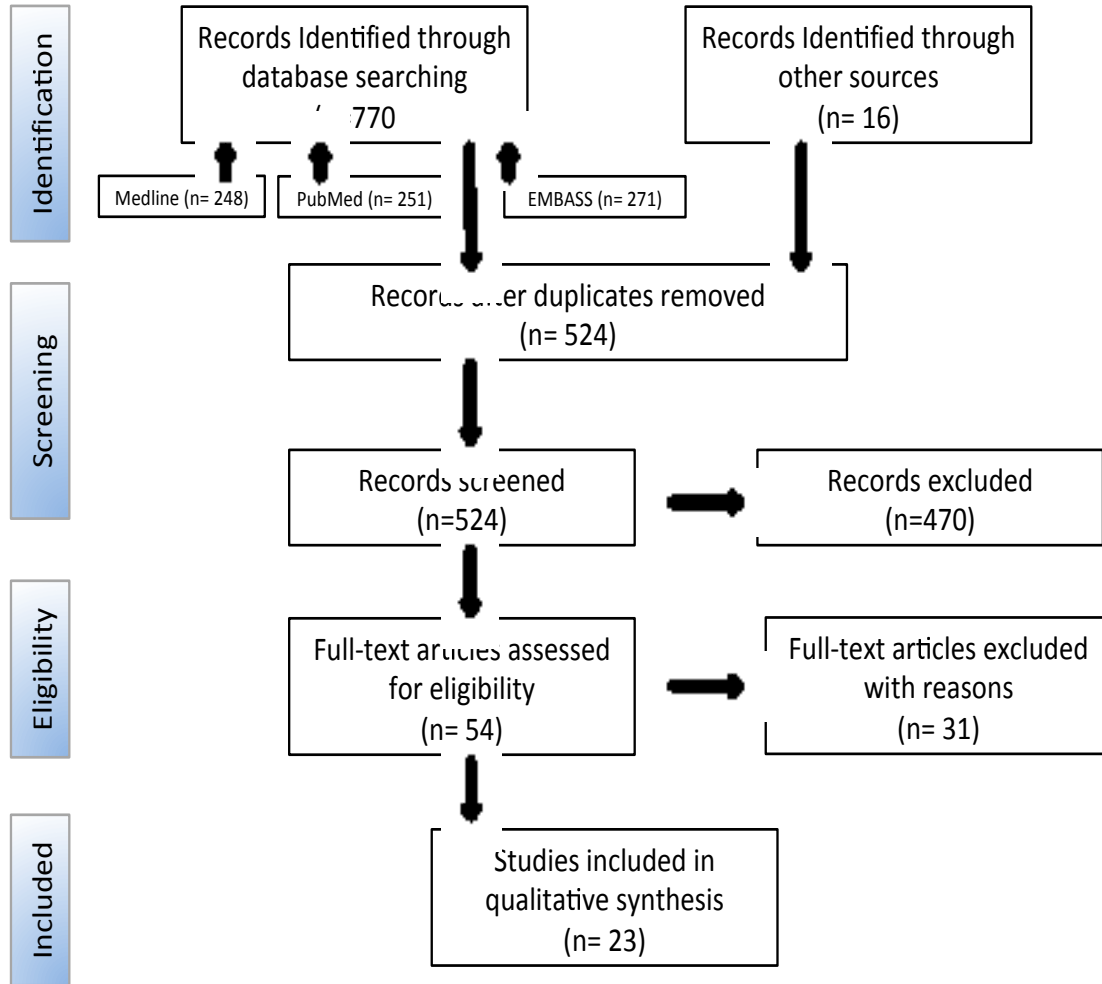
Table 1.3. Methodological scoring for the included studies

<b>Study design (6□Y)</b>
A. Objective clearly defined (Y)
B. Population adequately described (Y)
C. Sample size considered adequate (Y)
D. Selection criteria clearly described (Y) and adequate (Y)
E. Follow up length clearly described (Y)
<b>Study Measurements: (4□✓)</b>
F. Measurement method mentioned (Y) and appropriate (Y)
G. Reliability described (Y)
H. Validity described (Y)
<b>Statistical analysis: (3□Y)</b>
I. statistical analysis appropriate (Y)
J. Presentation of data – exact P value stated (Y), variability measures (SD or CI) stated (Y)
<b>Maximum number of Y= 13</b>

Table 1.4. Risk of bias among the selected articles (Y=yes, N=no, p=partial)

Article	Study Design					Study Measurements			Statistics		Total	% of Total
	A	B	C	D	E	F	G	H	I	J		
<b>Arat 2001</b>	Y	Y	N	Yp	Y	Yp	N	N	Y	YN	7.5	57.7
<b>Arat 2010</b>	Y	Y	N	Yp	Y	Yp	Y	N	Y	NY	9	69.2
<b>Bjork 1955</b>	Y	P	N	NY	Y	YY	Y	N	p	NN	7	53.8
<b>Bishara 1994</b>	Y	Y	N	Yp	Y	YY	Y	N	Y	YY	10.5	80.7
<b>Franchi 2007</b>	Y	Y	N	YY	p	Yp	p	N	Y	YY	9.5	73.1
<b>Henneberke 1994</b>	Y	Y	Y	Yp	N	Yp	p	N	p	pp	8	61.5
<b>Jiang 2007</b>	Y	Y	N	Yp	Y	YY	p	N	p	YY	9.5	73.1
<b>Lavalle 1978</b>	p	Y	Y	Yp	N	Yp	N	N	p	NN	6	46.2
<b>Lewis 1988</b>	Y	p	p	Yp	Y	pp	N	N	p	pN	6.5	50.0
<b>Malta 2009</b>	p	p	N	YY	Y	pp	p	N	Y	YY	8.5	65.4
<b>Melsen 1969</b>	Y	Y	Y	pp	N	pp	N	N	p	NN	5.5	42.3
<b>Mitani 1973</b>	Y	Y	N	Yp	N	Yp	N	N	p	NN	5.5	42.3
<b>Palomo 2005</b>	Y	Y	N	YY	Y	YY	Y	N	p	NN	8.5	65.4
<b>Phelan 2014</b>	Y	Y	N	Yp	Y	YY	Y	N	Y	YY	10.5	80.7
<b>Sejrsen 1997</b>	Y	Y	N	Yp	N	Yp	Y	N	p	NN	6.5	50.0
<b>Singh 1997</b>	Y	Y	N	Yp	N	Yp	Y	N	p	YN	7.5	57.7
<b>Thordarson 2006</b>	Y	Y	Y	YY	Y	YY	Y	N	Y	YY	12	92.3
<b>Ursi 1993</b>	Y	p	N	Yp	N	Yp	Y	N	p	NY	7	53.8
<b>Wilhelm 2001</b>	Y	Y	N	Yp	Y	YY	Y	N	Y	NY	9.5	73.1
<b>Ford 1958</b>	Y	Y	N	YY	N	Yp	N	N	N	NN	5.5	42.2
<b>Ohtsuki 1982</b>	Y	Y	Y	YY	Y	YY	N	N	Y	NY	10	76.9
<b>Knott 1969</b>	p	Y	N	YY	Y	Np	N	N	p	NY	6.5	50.0
<b>Knott 1971</b>	p	Y	N	YY	Y	Np	p	N	p	NY	7	53.8

Figure 1. Flow Diagram of the Study Selection



### 1.2.6 Appendix 1. Articles excluded in phase 2

<b>Author</b>	<b>Reason</b>
Bassed et al. 2010	Did not discuss posterior cranial base
Battagel 1994	Only measured soft tissue and jaws
Bondevik 1995	Did not discuss posterior cranial base
Buschang et al. 1982	Did not measure posterior cranial base
Cevidane and Heymann 2009	Did not discuss posterior cranial base
Cevidane and Styner 2009	Evaluated a method for superimposition
Coben 1998	Did not measure posterior cranial base
Edwards et al 2007	Did not mention posterior cranial base
Esenlik 2014	Did not discuss posterior cranial base
Gao et al. 2012	Did not discuss posterior cranial base
Haffner et al. 1999	Proposed a 3-D analysis technique
Hashemi 2015	Did not discuss posterior cranial bas
Hilloowala et al 1998	Did not measure posterior cranial base
Kean et al 1982	No growth discussion
Klocke et al 2002	Did not discuss changes of posterior cranial base
Kuroe et al. 2004	Discussed cranial bases of different populations
Latrou 2002	Not retrieved in English
Masaki 1980	Not retrieved in English
Moss 1983	Did not discuss posterior cranial base
Nie 2005	No growth measurement
Rosas et al 2008	Growth not discussed
Sielaff 1991	Not retrieved in English
Steuer 1972	Discussed hypophyseal fossa for superimposition
Tallgren 1974	Did not discuss posterior cranial base
Tanabe et al. 2002	Did not discuss posterior cranial base
Thiesen et al. 2013	Only discussed one time-point, not growth of cranial base
Viazis 1991	Could not obtain full article
Walker et al. 1972	Did not discuss posterior cranial base
West et al. 1999	Did not discuss posterior cranial base
Yang et al. 1990	Not retrieved in English, did not measure posterior cranial base
Yavuz et al. 2004	Only measured PA cephs

## **Chapter 2: Reliability and Accuracy of Posterior Cranial base and surrounding area landmarks assessed through CBCT**

### **2.1 Introduction**

The posterior cranial fossa is bound anteriorly via the petrous part of the temporal bone and dorsum sellae of sphenoid bone, posteriorly by the squamous part of the occipital bone and its floor is formed by the occipital bone and temporal bone with a minor contribution from the parietal bone.<sup>41</sup> The posterior cranial base, for orthodontic purposes, has been defined as a line drawn and connecting *Basion* (Ba) to *Sella Turcica* (S) using two-dimensional cephalometric images.<sup>42</sup> The posterior cranial base and surrounding area contain structures which include multiple foramen with various structures passing through, a base upon which the brain sits, and growth centers which are known to elongate the area during craniofacial growth.<sup>41</sup> These growth areas include the intraoccipital synchondrosis and the most notable speno-occipital synchondrosis which is reported to have variable closure and cessation of growth timing.<sup>43</sup>

Cephalometric landmarks have traditionally been identified on two-dimensional lateral cephalometric images. These images have inherent disadvantages which are tough to overcome. In reality, malocclusion is a three dimensional (3D) problem that affects the vertical, transverse and antero-posterior planes.<sup>44</sup> The use of 3D images has opened up the possibility to identify additional landmarks within the posterior cranial fossa to assess normal or abnormal growth and development of this area, as well as assess orthodontic treatment effects.

3D images are advantageous over two-dimensional images (2D) in a number of ways. These new images help to reduce or eliminate magnification error and overlap of structures, represent true anatomical structures in a 1:1 ratio, provide visualization of three-dimensional structures on multi-planar two-dimensional images and allow pinpoint accuracy in landmark placement with proper manipulation of the images and software.<sup>45</sup> Two dimensional images have

inferior accuracy and precision compared with three-dimensional images as reported in the literature.<sup>46,47</sup> Three-dimensional landmark identification provides an unobstructed view of the structures, there is less distortion of the structures, and bilateral superimposition is avoided<sup>47</sup>

Three-dimensional imaging in orthodontics is usually conducted via cone-beam computed tomography (CBCT). Compared to CT scans (another three-dimensional imaging modality), CBCT's are quicker, less expensive and deliver less ionizing radiation to the patient.<sup>48,49</sup> CBCT imaging is becoming more and more popular in day-to-day treatment planning of orthodontic patients and has opened up new areas for study within the anatomical human skull.

When investigating landmarks in a new format, it is important to ensure they are an accurate representation of the true anatomical structure. Accuracy for landmark identification refers to how close the landmark represent the true/actual anatomical location.<sup>50</sup> With any landmark identification, reliability to establish how repeatable the procedure is must also be shown. This involves inter-rater and intra-rater reliability testing. Inter-rater reliability refers to the degree of agreement among the judges/observers under the same conditions, whereas intra-rater reliability refers to the degree of agreement of repeated measurements of a single observer under the same conditions.<sup>51</sup>

Past research has investigated the above parameters. In a meta analysis, it was suggested that the total error in the x coordinate be no more than 0.59mm and 0.56 mm in the y coordinate to be considered acceptable levels of accuracy. While another study stated mean variance in the x axis of 0.07mm and the y axis of 0.08mm,<sup>52</sup> and showed that inter-rater observations were greater than intra-rater observations. With repeated practice of landmark identification, it is

stated that error can be reduced to 0.5mm in 2-D images and consideration of this should be extrapolated to 3-D images.<sup>53</sup>

When comparing within and between raters, intraclass correlation coefficient (ICC) values of over 0.9 were demonstrated for inter and intra observer assessments for three-dimensional landmark identification using CBCT images when proper training and calibration of operators were properly conducted.<sup>54</sup> Similarly, ICC values for inter-rater landmark identification of greater than 0.9 were shown by Gupta, but their results showed a mean error in linear measurements of 2.63mm.<sup>55</sup> In the reliability and accuracy study by Lagravere<sup>56</sup>, they demonstrated intra-examiner mean accuracy on average of 0.5mm with inter-examiner differences of no greater than 1.3mm. In another study by Lagravere et al,<sup>57</sup> when linear measurements were taken from CBCT images, an error of less than 1mm was reported and re-emphasized the 1 to 1 image to reality ratio for CBCT images.

Given these past studies, landmarks with the highest accuracy and reproducibility should be considered for craniofacial studies to reduce the impact of measurement errors and increase validity of cephalometric evaluations. Even the smallest errors in landmark identification could potentially be a source of substantial error in overall treatment process.<sup>58</sup>

To the best of our knowledge, no three-dimensional studies have quantified the growth of the posterior cranial base and surrounding structures. The purpose of this study is to therefore identify anatomical landmarks in the posterior cranial base and surrounding areas that are potentially accurate and reproducible in three-dimensional CBCT derived images. A few landmarks from the middle cranial base are included, as well as newly identified anatomical landmarks deemed appropriate to study. Many of these structures are difficult to identify from a 2D sagittal view due to overlap so are appropriate to be assessed in three dimensions.

### **Research questions:**

Question #1: What posterior cranial base and surrounding area landmarks are reproducible and reliable in three-dimensional images?

Question #2: Are these identified landmarks accurate and representative of true anatomical landmarks?

## **2.2 Materials and Methods**

Ten (10) well-preserved dry skulls were used in this study. Landmarks were identified based on visual inspection of the dry skulls for canals, foramina, projections, and surfaces in the posterior cranial base region as well as surrounding structures that have not previously been investigated. These structures were landmarked using a malleable blockout compound material (Block-Out Compound, 1 lb - Buffalo Dental Mfg Co Inc.) and for further accuracy small pieces of gutta-percha were strategically placed to identify true anatomical landmarks (Appendix 1).

For imaging, the skulls were placed on a Styrofoam block and into a double-layered Plexiglas box with dimensions 26 x 24.6 x 22 cm. Water was filled between the inner and outer compartments to simulate soft tissue attenuation. The Plexiglas box and skull sat on a pedestal to fit inside the CBCT scanner (i-CAT, Image Science International, Hatfield, PA, USA). The ICAT scanner protocol was large field of view, 9in x 12in, voxel size 0.30mm, 120kVp, 23.87mAs, 8.9 seconds and was used for all images. All the skulls were imaged without the mandible or skull cap in place.

Figure 2: Skull set up in ICAT machine



All skulls were imaged two times. Once with the gutta percha in place and a second time without any radiopaque materials. The images were exported into a DICOM file and then uploaded into the Avizo software (version 7.0) for analysis. The Cartesian coordinate system was used with x-y plane representing the axial (superior-inferior) plane, x-z plane representing the coronal (anterior-posterior) plane and y-z plane representing the sagittal (left-right) plane (Appendix 2). The program was modified for surface rendering to more accurately locate the landmarks, and all landmarks were double checked in all three planes of space separately.

A total of 33 landmarks were identified in the posterior cranial base and surrounding area for initial assessment. The sagittal, axial, and coronal views as well as the surface rendered

images for each landmark have been provided in order to standardize their identification in three-dimensions (Appendix 3.1). Visual representation of those landmarks can be seen in Appendix 3.2 in the axial, sagittal and coronal views. The principle investigator (K.C) learned the software and using a spherical marker of 0.25mm placed it on the appropriate landmarks in a specific order from landmark 1-33 as determined by the investigator. The principal investigator marked the landmarks three times on the 10 skull images without gutta percha, with each trial 7 days apart. Two additional investigators (D.S and M.L) each landmarked the same 10 skulls and the 33 landmarks once, in the specific order provided. The investigators were blinded via identifying the images with code and they were analyzed in random order.

Figure 3: Close-up of landmarks



To assess accuracy of the landmarks, the principal investigator marked the images with gutta percha once. One of the previous trial datasets marked by the principal investigator without gutta percha was then randomly selected to compare to the reading with gutta-percha. The skulls

could not be oriented the exact same way in the I-CAT CBCT scanner so their coordinates could not be directly compared. To overcome this, linear measurements were generated using the landmark coordinates and the following equation was used to measure distance between two landmarks with three-dimensional coordinates.

$$d = \sqrt{(x_2 - x_1)^2 + (y_2 - y_1)^2 + (z_2 - z_1)^2}$$

d is the distance (mm) between the two anatomic landmarks and x1, y1, z1 and x2, y2, z2 are the coordinates. The distances between all these landmarks were chosen by K.C and M.L and approved by the remaining committee members as representative of the transverse, vertical and anterior-posterior dimensions. Due to the large number of landmarks, these linear measurements were agreed upon to represent all dimensions without using every landmark in all three planes.

Table 2.1. Definitions of the chosen distances:

Transverse Dimension (right-left)		
1	Foramen magnum width	Distance between left and right rims of foramen magnum (FMR-FML)
2	Right Hypoglossal canal width	Distance between right internal and external points on hypoglossal canal (IHC-R to EHC-R)
3	Left Hypoglossal canal width	Distance between left internal and external points on hypoglossal canal (IHC-L to EHC-L)
4	Internal Hypoglossal canal right to left	Distance from the internal hypoglossal canal points from right to left (IHC-R to IHC-L)
5	Clivus width	Width of the clivus from right occipital bone to left occipital bone point (OBW-R to OBW-L)
6	Right Temporal bone point to sphenoccipital point	Distance between TBP-R and CP
7	Left Temporal bone point to sphenoccipital point	Distance between TBP-L and CP
8	Right sella width point to depth of sella	Distance between Sella-R and Sella depth
9	Left sella width point to depth of sella	Distance between Sella-L and Sella depth
10	Foramen Ovale right to left	Distance between right and left foramen Ovale (FO-R to FO-L)
11	Foramen spinosum right to left	Distance between right and left foramen spinosum (FS-

		R to FS-L)
12	Carotid canal right to left	Distance between CC-R to CC-L
13	Internal auditory meatus right to left	Distance between IAM-R to IAM-L
14	Stylomastoid foramen right to left	Distance between SF-R to SF-L
15	Posterior part of infratemporal fossa right to left	Distance between IF-R to IF-L
16	Porion to internal auditory meatus right	Distance between EAM-R to IAM-R
17	Porion to internal auditory meatus left	Distance between EAM-L to IAM-L
18	Articular eminence to sella right	Distance between AE-R to Sella depth
19	Articular eminence to sella left	Distance between AE-L to sella depth
Vertical Dimension (superior-inferior)		
20	Sella to vomer point	Distance between Sella depth to V
21	Internal hypoglossal to internal auditory meatus right	Distance from IHC-R to IAM-R
22	Internal hypoglossal to internal auditory meatus left	Distance from IHC-L to IAM-L
23	Basion to sphenoccipital synchondrosis point	Distance from Ba to CP
Anterior-posterior Dimension (front-back)		
24	Vomer point to Basion	Distance from V to Ba
25	Infratemporal fossa point to basion right	Distance from IF-R to Ba
26	Infratemporal fossa point to basion left	Distance from IF-L to Ba
27	Articular eminence to stylomastoid right	Distance from AE-R to SF-R
28	Articular eminence to stylomastoid left	Distance from AE-L to SF-L
29	Foramen magnum a/p	Distance from Ba to FMP

### 2.3 Statistical Analysis

The data was analyzed using a standard statistical software program (SPSS version 24 For PC, IBM)

Intra-rater and inter-rater reliability were used to assess reproducibility and repeatability of the 33 selected landmarks. Intra-rater reliability was assessed using Intraclass correlation

coefficient (ICC) that measures agreement between the three trials done by the principal investigator on the skulls without gutta percha. ICC values were obtained for each landmark in the x, y, and z coordinates. In order to ensure consistency in one rater's individual measurement while the subjects were randomly chosen, a single measure with consistency under two-way mixed model was chosen.

To assess inter-rater reliability, ICC was used to measure agreement between the trials of D.S, M.L and one randomly selected readings from the principle investigator (K.C). A single measure with absolute agreement under two-way mixed model was chosen to show that all raters were in agreement while the subjects were chosen randomly.

ICC values were interpreted by the general guidelines presented by Portney and Watkins.<sup>59</sup>

- ICC above 0.90: Excellent agreement
- ICC above 0.75: Good agreement
- ICC between 0.51 and 0.74: Moderate agreement
- ICC below 0.50: Poor agreement

The absolute mean difference of intra and inter rater reliability measurements were reported in millimeters in all axes to help make the data more understandable for the general population.

## **2.4 Results**

Intra-rater reliability:

Intra-rater reliability in the x, y, z coordinates of all the chosen landmarks were excellent.

All values were above 0.946 which demonstrates excellent agreement. Profile plots and scatter plots all show agreement with the high ICC values (appendix 4.1 and 4.2). At this point, none of the landmarks were eliminated.

Table 2.2: ICC of intra-rater reliability for landmarks in X, Y, Z axes.

	Landmark	X			Y			Z		
		ICC	Lower Bound	Upper Bound	ICC	Lower bound	Upper bound	ICC	Lower bound	Upper bound
1	FMP	0.98	0.944	0.955	0.999	0.998	1	0.999	0.997	1
2	FMR	0.996	0.988	0.999	0.996	0.987	0.999	0.998	0.995	1
3	FML	0.998	0.994	0.999	0.995	0.984	0.999	0.999	0.998	1
4	Ba	0.996	0.989	0.999	0.999	0.998	1	1	0.999	1
5	IHC-R	0.992	0.976	0.998	0.999	0.997	1	0.998	0.995	1
6	IHC-L	0.993	0.978	0.998	0.999	0.998	1	0.999	0.998	1
7	EHC-R	0.996	0.988	0.999	0.999	0.997	1	0.999	0.996	1
8	EHC-L	0.994	0.984	0.999	0.994	0.984	0.998	0.999	0.996	1
9	IF-R	0.99	0.972	0.997	0.999	0.997	1	0.999	0.996	1
10	IF-L	0.982	0.949	0.995	0.999	0.998	1	0.999	0.997	1
11	AE-R	0.946	0.851	0.985	0.988	0.965	0.997	0.998	0.995	0.999
12	AE-L	0.961	0.89	0.989	0.983	0.95	0.995	0.999	0.998	1
13	EAM-L	0.995	0.987	0.999	0.97	0.916	0.992	0.998	0.995	1
14	EAM-R	0.998	0.994	0.999	0.972	0.92	0.992	0.999	0.996	1
15	SF-R	0.996	0.989	0.999	0.999	0.998	1	0.996	0.988	0.999
16	SF-L	0.998	0.994	0.999	0.999	0.998	1	0.997	0.991	0.999
17	CC-R	0.998	0.994	0.999	0.999	0.996	1	0.998	0.995	1
18	CC-L	0.995	0.984	0.999	0.999	0.996	1	1	0.999	1
19	Vomer	0.998	0.993	0.999	0.991	0.973	0.997	0.998	0.995	1
20	OBW-R	0.995	0.984	0.999	0.986	0.959	0.996	0.995	0.987	0.999
21	OBW-L	0.99	0.971	0.997	0.988	0.964	0.997	0.994	0.983	0.998
22	FS-R	0.998	0.994	0.999	0.999	0.996	1	0.997	0.991	0.999
23	FS-L	0.998	0.995	1	0.999	0.997	1	0.994	0.983	0.998
24	Sella depth	0.987	0.963	0.997	0.988	0.965	0.997	0.999	0.997	1
25	Sella width-L	0.995	0.984	0.999	0.993	0.979	0.998	0.99	0.971	0.997
26	Sella width-R	0.996	0.998	0.999	0.99	0.97	0.997	0.993	0.981	0.998
27	TBP-L	0.996	0.99	0.999	0.999	0.996	1	1	0.999	1

28	TBP-R	0.995	0.986	0.999	0.997	0.993	0.999	1	0.999	1
29	CP	0.983	0.951	0.995	0.997	0.99	0.999	0.997	0.991	0.999
30	IAM-L	0.997	0.991	0.999	0.999	0.996	1	0.999	0.998	1
31	IAM-R	0.997	0.992	0.999	0.999	0.998	1	0.998	0.995	1
32	FO-R	0.997	0.992	0.999	0.98	0.943	0.995	0.982	0.948	0.995
33	FO-L	0.986	0.959	0.996	0.981	0.947	0.995	0.996	0.988	0.999

Mean error or differences of the landmark identification from the three trials by the same examiner were all less than 1.3mm in all three axes. The largest mean difference was 1.3mm at landmark AE-R (articular eminence right) and was recorded in the x axis. The smallest mean error was 0.1mm for landmark TBP-L (temporal bone point – L) in the z axis.

Table 2.3: Intra-rater absolute mean differences (mm) in X, Y, and Z axes

Landmark	N	x				Y				Z			
		Mean	St. Dev	Min	Max	Mean	St. Dev	Min	Max	Mean	St. Dev	Min	Max
FMP	10	0.66	0.47	0.2	1.4	0.2	0.13	0	0.4	0.2	0.19	0	0.4
FMR	10	0.24	0.13	0	0.4	0.62	0.4	0.2	1.2	0.46	0.28	0	1
FML	10	0.2	0.19	0	0.6	0.92	0.5	0.4	1.8	0.4	0.16	0.2	0.6
Ba	10	0.26	0.13	0.2	0.6	0.18	0.17	0	0.6	0.14	0.1	0	0.2
IHC-R	10	0.4	0.25	0.2	1	0.2	0.19	0	0.6	0.38	0.33	0	1
IHC-L	10	0.34	0.28	0	1	0.16	0.13	0	0.4	0.3	0.14	0.2	0.6
EHC-R	10	0.26	0.21	0	0.8	0.28	0.19	0	0.6	0.4	0.3	0.2	1
EHC-L	10	0.3	0.14	0.2	0.6	0.48	0.49	0	1.6	0.42	0.27	0	1
IF-R	10	0.4	0.35	0	1.2	0.2	0.19	0	0.6	0.34	0.27	0	0.8
IF-L	10	0.54	0.69	0	2.4	0.14	0.1	0	0.2	0.34	0.28	0	1
AE-R	10	1.33	0.61	0.4	2	0.79	0.5	0	1.4	0.36	0.3	0	0.97
AE-L	10	1.2	0.69	0.2	2.33	0.95	0.53	0.4	2	0.32	0.24	0.02	0.79
EAM-L	10	0.29	0.29	0	0.73	0.88	1.14	0	3.99	0.46	0.35	0	1.2
EAM-R	10	0.36	0.36	0	1.20	0.7	1.26	0	4.19	0.38	0.26	0.2	1
SF-R	10	0.21	0.18	0	0.6	0.19	0.19	0	0.6	0.91	0.81	0	2.58
SF-L	10	0.23	0.18	0	0.6	0.19	0.15	0	0.4	0.9	0.66	0.2	2.55
CC-R	10	0.22	0.12	0	0.46	0.25	0.24	0	0.8	0.32	0.28	0	1
CC-L	10	0.3	0.2	0	0.63	0.23	0.23	0	0.66	0.16	0.18	0	0.6
V	10	0.16	0.13	0	0.4	0.56	0.51	0	1.8	0.3	0.29	0	0.8
OBW-R	10	0.32	0.19	0.14	0.8	0.82	0.52	0.2	1.8	0.74	0.42	0.2	1.4

OBW-L	10	0.42	0.37	0	1.2	0.8	0.51	0.2	1.4	0.85	0.52	0.4	1.8
FS-R	10	0.2	0.12	0	0.4	0.28	0.11	0.17	0.42	0.58	0.27	0.2	0.99
FS-L	10	0.19	0.14	0	0.4	0.25	0.17	0	0.6	0.7	0.7	0.2	2.59
Sella depth	10	0.45	0.27	0	1	0.97	0.45	0.2	1.6	0.28	0.21	0	0.8
Sella-L	10	0.24	0.13	0	0.47	0.49	0.42	0	1.4	0.86	0.48	0.4	2
Sella-R	10	0.27	0.23	0	0.6	0.74	0.36	0.22	1.2	0.76	0.43	0.2	1.6
TBP-L	10	0.34	0.21	0.2	0.8	0.24	0.16	0	0.4	0.1	0.1	0	0.2
TBP-R	10	0.3	0.29	0	1	0.24	0.36	0	1.2	0.14	0.1	0	0.2
CP	10	0.48	0.35	0	1.2	0.44	0.24	0.2	1	0.42	0.17	0.2	0.8
IAM-L	10	0.22	0.15	0	0.4	0.26	0.13	0	0.4	0.22	0.17	0	0.6
IAM-R	10	0.2	0.13	0	0.4	0.2	0.09	0	0.4	0.26	0.13	0	0.4
FO-R	10	0.53	0.67	0	2.2	0.76	0.89	0	3.19	0.94	1.14	0.2	3.99
FO-L	10	0.6	0.82	0	2.2	0.75	1.05	0	3.59	0.8	0.46	0.2	1.6

After analysis of these findings, all the landmarks were carried forward in the study. All landmarks were discernable when one observer, after adequate training, identified them on the same 10 skulls 3 times.

Inter-rater reliability:

Inter-rater reliability in the x, y, z coordinates was more variable than intra-rater reliability. All landmarks showed good to excellent reliability in the x-axis except foramen ovale left and right (FO-L and FO-R) which were 0.716 and 0.733 respectively. In the y axis all landmarks demonstrated good to excellent reliability except carotid canal left (CC-L) which showed a moderate agreement of 0.729. In the z axis all landmarks showed good to excellent inter-rater reliability with the lowest value of 0.879 for foramen ovale left (FO-L). Profile plots and scatter plots for excellent ICC values in the x, y, z, axes are shown in appendix 5.1 and 6.1. Profile plots and scatter plots for good and moderate ICC values are shown in the x,y, z axes in appendix 5.2 and 6.2.

Table 2.4: Inter-rater reliability ICC values

	Landmark	X			Y			Z		
		ICC	Lower Bound	Upper Bound	ICC	Lower bound	Upper bound	ICC	Lower bound	Upper bound
1	FMP	0.964	0.873	0.991	0.981	0.945	0.995	0.977	0.934	0.994
2	FMR	0.982	0.951	0.995	0.963	0.901	0.99	0.972	0.922	0.992
3	FML	0.993	0.975	0.998	0.94	0.835	0.984	0.964	0.894	0.99
4	Ba	0.986	0.959	0.996	0.978	0.939	0.994	0.981	0.948	0.995
5	IHC-R	0.981	0.945	0.995	0.974	0.928	0.993	0.963	0.9	0.99
6	IHC-L	0.989	0.962	0.997	0.972	0.924	0.992	0.97	0.917	0.992
7	EHC-R	0.96	0.729	0.991	0.958	0.884	0.988	0.909	0.498	0.98
8	EHC-L	0.943	0.74	0.986	0.949	0.845	0.986	0.911	0.555	0.979
9	IF-R	0.952	0.762	0.989	0.817	0.555	0.946	0.973	0.918	0.993
10	IF-L	0.965	0.9	0.991	0.875	0.66	0.965	0.955	0.876	0.987
11	AE-R	0.845	0.422	0.961	0.83	0.601	0.949	0.977	0.925	0.994
12	AE-L	0.906	0.689	0.975	0.851	0.548	0.96	0.973	0.924	0.993
13	EAM-L	0.994	0.984	0.998	0.897	0.739	0.97	0.96	0.892	0.989
14	EAM-R	0.988	0.966	0.997	0.858	0.641	0.959	0.964	0.895	0.99
15	SF-R	0.972	0.924	0.992	0.868	0.651	0.962	0.941	0.828	0.984
16	SF-L	0.993	0.98	0.998	0.932	0.821	0.981	0.954	0.857	0.988
17	CC-R	0.964	0.903	0.99	0.88	0.698	0.966	0.922	0.797	0.978
18	CC-L	0.92	0.792	0.977	0.729	0.424	0.915	0.928	0.81	0.98
19	Vomer	0.983	0.954	0.995	0.901	0.723	0.972	0.976	0.933	0.993
20	OBW-R	0.957	0.88	0.988	0.925	0.804	0.979	0.907	0.68	0.976
21	OBW-L	0.961	0.891	0.989	0.935	0.827	0.982	0.89	0.709	0.969
22	FS-R	0.996	0.987	0.999	0.92	0.783	0.978	0.968	0.872	0.992
23	FS-L	0.984	0.957	0.996	0.937	0.835	0.982	0.96	0.883	0.989
24	Sella depth	0.956	0.88	0.988	0.927	0.73	0.982	0.973	0.925	0.992
25	Sella width-L	0.876	0.691	0.964	0.885	0.633	0.97	0.861	0.614	0.961
26	Sella width-R	0.939	0.839	0.983	0.892	0.697	0.97	0.914	0.729	0.977
27	TBP-L	0.983	0.951	0.995	0.962	0.891	0.99	0.961	0.894	0.989
28	TBP-R	0.99	0.971	0.997	0.958	0.883	0.988	0.959	0.887	0.989
29	CP	0.978	0.937	0.994	0.996	0.904	0.991	0.947	0.856	0.985
30	IAM-L	0.849	0.635	0.956	0.847	0.635	0.955	0.957	0.882	0.988
31	IAM-R	0.991	0.975	0.998	0.768	0.479	0.929	0.951	0.869	0.986
32	FO-R	0.716	0.114	0.928	0.86	0.484	0.965	0.951	0.862	0.986
33	FO-L	0.733	0.415	0.917	0.823	0.395	0.954	0.879	0.702	0.965

Mean difference for the inter-rater testing was also more variable than intra-rater. As seen in table 4, the mean error in the x axis ranged from 0.26mm to 3.12mm, the y axis ranged from 0.35mm to 3.43mm and z axis from 0.18mm to 1.87mm. The largest differences appeared to come from one examiner and deemed due to vague definition of the landmarks and comparative less training with landmark identification. All landmarks were moved forward due to the relatively minor discrepancies.

Table 2.5: Mean error inter-rater (mm) in X, Y, and Z axes

Landmark	N	x				Y				Z			
		Mean	St. Dev	Min	Max	Mean	St. Dev	Min	Max	Mean	St. Dev	Min	Max
FMP	10	0.79	0.82	0	2.27	0.4	0.27	0.08	0.94	0.22	0.14	0.01	0.43
FMR	10	0.49	0.38	0.03	1.16	1.22	0.71	0.4	2.89	0.52	0.4	0.03	1.36
FML	10	0.59	0.32	0.19	1.12	1.39	0.72	0.47	2.58	1.12	0.58	0.27	2.43
Ba	10	0.44	0.44	0	1.33	0.63	0.51	0.08	1.56	0.39	0.15	0.2	0.62
IHC-R	10	0.59	0.31	0.12	1.24	0.44	0.28	0.03	0.82	0.66	0.34	0.05	1.23
IHC-L	10	0.62	0.19	0.26	0.87	0.62	0.54	0.09	1.97	0.6	0.39	0.2	1.25
EHC-R	10	0.9	0.43	0.31	1.7	1.03	0.68	0.1	2.37	1.83	0.65	1.02	3.04
EHC-L	10	1.12	0.34	0.67	1.65	0.96	0.88	0.17	3.29	1.87	0.67	0.82	2.84
IF-R	10	1.01	0.64	0.26	2	0.35	0.33	0.07	1.06	0.52	0.41	0.07	1.27
IF-L	10	0.82	0.88	0.06	2.67	0.6	1.31	0.07	4.32	0.52	0.24	0.19	1
AE-R	10	1.96	1.12	0.4	4.06	1.36	0.69	0.61	2.61	0.48	0.27	0.13	0.99
AE-L	10	1.59	0.73	0.67	2.75	1.36	1.09	0.07	3.93	0.46	0.29	0.17	1.19
EAM-L	10	0.39	0.32	0.06	0.98	1.21	1.23	0.02	3.96	0.57	0.64	0.02	2.27
EAM-R	10	0.53	0.34	0.01	1.07	0.73	0.43	0.09	1.33	0.89	0.63	0.13	1.93
SF-R	10	0.61	0.43	0.12	1.33	0.93	1.27	0.03	4.37	1.03	1.11	0.26	3.93
SF-L	10	0.48	0.4	0.08	1.33	1.19	1.18	0.15	3.36	1.14	0.91	0.18	3
CC-R	10	0.64	0.7	0.03	2.43	1.23	2.15	0.05	7.16	0.89	1.02	0.22	3.62
CC-L	10	0.95	1.1	0.04	4	2	4.35	0.03	14.15	0.95	1.19	0.2	4.21
V	10	0.48	0.37	0.07	1.33	2.45	1.3	0.73	4.14	0.4	0.26	0.02	0.8
OBW-R	10	0.78	0.66	0.11	2.18	1.55	1.06	0.2	3.33	1.44	0.62	0.4	2.4
OBW-L	10	0.79	0.47	0.07	1.66	1.82	1.09	0.01	3.33	1.5	0.59	0.43	2.4

FS-R	10	0.26	0.28	0.02	0.85	0.35	0.29	0.02	0.67	0.73	0.49	0.2	1.8
FS-L	10	0.53	0.48	0.02	1.33	0.94	0.94	0.01	2.87	0.74	0.24	0.38	1
Sella depth	10	0.81	0.62	0.13	1.93	1.95	0.8	0.86	3.06	0.39	0.2	0.14	0.8
Sella-L	10	1.02	0.96	0.01	3.4	2.34	1.23	0.67	4.8	1.61	0.85	0.41	3.4
Sella-R	10	1.2	0.57	0.62	2	2.21	0.98	1.08	3.73	1.33	0.73	0.33	2.79
TBP-L	10	0.5	0.46	0.06	1.33	0.72	0.68	0.18	2.54	0.18	0.08	0.07	0.33
TBP-R	10	0.34	0.27	0.05	0.76	0.61	0.39	0.07	1.34	0.26	0.16	0.07	0.41
CP	10	0.53	0.33	0	1.01	0.76	0.64	0.15	2.08	0.53	0.33	0.2	1.2
IAM-L	10	1.18	1.51	0.04	4.67	2.43	3.1	0.04	9.33	0.98	0.62	0.4	2.2
IAM-R	10	0.45	0.31	0.04	0.78	2.31	4.18	0.04	10.44	0.81	1.07	0.07	3.4
FO-R	10	2.65	0.93	1.33	4.03	2.92	1.34	0.27	4	0.97	0.65	0.18	2.2
FO-L	10	3.12	1.41	0.32	4.92	3.43	1.6	1.2	6.59	1.21	1.24	0.19	4.52

Accuracy:

The ICC values obtained after analysis of the linear measurements when gutta percha was present and the linear measurements on the bare skulls showed variable and inconsistent results. 13 of the 29 distance measurements showed good to excellent agreement while the remaining 16 showed only moderate or poor agreement.

Table 2.6: ICC for accuracy of linear measurements (\* denotes poor, # moderate agreement,  $\sigma$  denotes good, no symbol denotes excellent agreement)

Distance	Number	Agreement Level	ICC	Lower Bound	Upper Bound
Foramen magnum width (FMR to FML)	1		0.963	0.864	0.991
Hypoglossal canal width right (IHC-R to EHC-R)	2	#	0.722	-0.67	0.944
Hypoglossal canal width left (IHC-L to EHC-L)	3	*	0.334	-0.54	0.774
Internal hypoglossal canal right to left (IHC-L to IHC-R)	4	$\sigma$	0.883	0.538	0.971
clivus right to left (OBW-R to	5	*	0.243	-0.139	0.681

OBW-L)					
Temporal bone point to sphenoccipital right (TBP-R to CP)	6	*	0.422	-0.297	0.821
Temporal bone point to sphenoccipital left (TBP-L to CP)	7	#	0.531	-0.112	0.876
Depth of sella to right (Sella depth to Sella-R)	8	#	0.544	-0.032	0.86
Depth of sella to left (Sella depth to Sella-L)	9	$\sigma$	0.878	0.595	0.968
foramen ovale right to left (FO-R to FO-L)	10		0.981	0.928	0.995
foramen spinosum right to left (FS-R to FS-L)	11	$\sigma$	0.875	0.533	0.968
carotid right to left (CC-R to CC-L)	12		0.959	0.852	0.99
internal auditory right to left (IAM-R to IAM-L)	13	$\sigma$	0.774	0.338	0.938
stylomastoid right to left (SF-R to SF-L)	14		0.984	0.939	0.996
posterior part of infratemporal fossa right to left (IF-R to IF-L)	15		0.937	0.728	0.985
External to internal auditory meatus right (EAM-R to IAM-R)	16	#	0.65	0.051	0.901
External to internal auditory meatus left (EAM-L to IAM-L)	17	#	0.721	0.22	0.922
articular eminence to sella right (AE-R to sella depth)	18	#	0.686	0.179	0.91
articular eminence to sella left (AE-L to sella depth)	19	$\sigma$	0.844	0.511	0.958
sella depth to vomer (Sella depth to V)	20	*	0.329	-0.024	0.776
internal hypoglossal to internal auditory meatus right (IHC-R to IAM-R)	21	#	0.625	0.033	0.892
internal hypoglossal to internal auditory meatus left (IHC-L to IAM-L)	22	#	0.573	-0.064	0.877
basion to sphenoccipital synch (Ba to CP)	23	#	0.653	0.103	0.9
vomer to basion (V to Ba)	24	*	0.385	-0.201	0.739
infratemporal fossa point to basion right (IF-R to Ba)	25	$\sigma$	0.861	0.317	0.968
infratemporal fossa point to	26	$\sigma$	0.768	-0.01	0.948

basion left (IF-L to Ba)					
articular eminence to stylomastoid right (AE-R to SF-R)	27	#	0.558	-0.108	0.884
articular eminence to stylomastoid left (AE-L to SF-L)	28	#	0.593	-0.106	0.896
Foramen magnum a/p (Ba to FMP)	29		0.936	0.717	0.984

The mean differences of the linear measurements between trials with gutta percha and without were all less than 2.62mm. Five difference in distance measurements showed negative values (Internal Hypoglossal canal right to left, Temporal bone point to spheni-occipital left, Foramen spinosum right to left, internal auditory meatus right to left, and Porion to internal auditory meatus right). Mean and standard deviation values can be seen in Appendix 7 for the distance measurements on the skulls with and without gutta percha.

Table 2.7: Mean Error for difference in linear measurements (mm)

Distance	N	Mean	Std. Deviation	Min	Max
Foramen magnum width (FMR to FML)	10	.17	.87	-0.98	1.88
Hypoglossal canal width right (IHC-R to EHC-R)	10	1.63	.74	0.59	2.81
Hypoglossal canal width left (IHC-L to EHC-L)	10	2.62	.93	0.4	3.87
Internal hypoglossal canal right to left (IHC-L to IHC-R)	10	-.49	.72	-2	0.18
clivus right to left (OBW-R to OBW-L)	10	2.61	2.11	-0.03	5.98
Temporal bone point to sphenoccipital right (TBP-R to CP)	10	.12	1.14	-1.8	1.38

Temporal bone point to sphenoccipital left (TBP-L to CP)	10	-1.19	.93	-3.08	-0.01
Depth of sella to right (Sella depth to Sella-R)	10	1.38	1.77	-1.33	3.6
Depth of sella to left (Sella depth to Sella-L)	10	.37	.77	-1.25	1.52
foramen ovale right to left (FO-R to FO-L)	10	.07	.66	-0.92	1.1
foramen spinosum right to left (FS-R to FS-L)	10	-.91	1.42	-4.26	0.96
carotid right to left (CC-R to CC-L)	10	.37	.91	-1.36	2.04
internal auditory right to left (IAM-R to IAM-L)	10	-.45	1.81	-1.98	4.2
stylomastoid right to left (SF-R to SF-L)	10	.14	.75	-1.04	1.21
posterior part of infratemporal fossa right to left (IF-R to IF-L)	10	1.16	1.79	-0.85	5
External to internal auditory meatus right (EAM-R to IAM-R)	10	-.19	2.06	-5.11	2.5
External to internal auditory meatus left (EAM-L to IAM-L)	10	.39	1.68	-3.48	3.02
articular eminence to sella right (AE-R to sella depth)	10	.98	2.75	-2.07	5
articular eminence to sella left (AE-L to sella depth)	10	.54	2.01	-3.72	2.82
sella depth to vomer (Sella depth to V)	10	2.03	.47	1.15	2.72
internal hypoglossal to internal auditory meatus right (IHC-R to IAM-R)	10	1.00	1.26	-0.19	3.85
internal hypoglossal to internal auditory meatus left (IHC-L to IAM-L)	10	1.08	1.08	-1.06	2.75
basion to sphenoccipital synch (Ba to CP)	10	1.20	1.78	-1.59	3.45
vomer to basion (V to Ba)	10	.64	1.41	-0.98	3.9

infratemporal fossa point to basion right (IF-R to Ba)	10	.94	1.03	-0.84	2.51
infratemporal fossa point to basion left (IF-L to Ba)	10	1.24	1.00	0.05	3.13
articular eminence to stylomastoid right (AE-R to SF-R)	10	2.23	1.41	0.33	4.6
articular eminence to stylomastoid left (AE-L to SF-L)	10	2.01	1.34	0.67	4.28
Foramen magnum a/p (Ba to FMP)	10	-.70	1.05	-1.97	1.64

Even with a couple poor ICC values and moderately large mean error values for a few landmarks, all the landmarks and distances were kept as designed due to factors discussed below.

## 2.5 Discussion

### Summary:

As no known three-dimensional CBCT studies have been performed to assess changes in the posterior cranial base and surrounding area, locating reliable and accurate landmarks is the first step. Once landmarks are established, they can potentially be applied to future growth studies to help assess normal growth, stability of landmarks, or changes demonstrated via different treatment modalities. If these landmarks are deemed stable in the coronal, axial and sagittal dimensions, they may be used as reference points when sequential radiographic images need to be superimposed.

In this study, the reproducibility and accuracy of well-established and of newly identified anatomical landmarks were evaluated. In two-dimensional images some landmarks could not be identified which is why they have application in a three-dimensional study. To validate the

landmarks, intra and inter- rater reliability as well as accuracy were assessed using ICC values, mean error measurements and linear distance calculations.

Landmarks should be both reproducible and accurate. Reproducibility means, in general terms, that the experiment can be duplicated, either by the same investigator or someone else.<sup>51</sup> Accuracy, meaning how close the measurements are to what the true value is, should also be high. In this study, we can state that the identification of the landmarks was precise, given the fact that measurements were all very close to each other. Although some linear measurements are less accurate than others but have high reliability and vice versa, have decided to maintain all landmarks in this analysis as true representations of anatomical structures.

*Reliability and accuracy results:*

Intra rater reliability refers to the degree of stability when a measurement is repeated under identical conditions by the same rater. Inter-rater reliability is the same except when done by different investigators.

In this study, in all axis, the ICC for all 33 landmarks for intra-rater were excellent (above 0.90). This means that the principal investigator had knowledge of where the landmark should be and could repeatedly locate the same landmark at different times and on different subjects.

When 3 observers landmarked the 10 dry skulls one time each, the inter-rater measurements were all excellent, except foramen ovale which showed moderate agreement. The lower values for ICC on landmark foramen ovale left and right were attributed to lack of guidance and teaching for one of the observers. The slightly higher mean differences, the highest being 3.43mm for foramen ovale left in the y axis, was attributed again to a single observer as proper calibration and guidance to landmark identification was assumed but not present. This

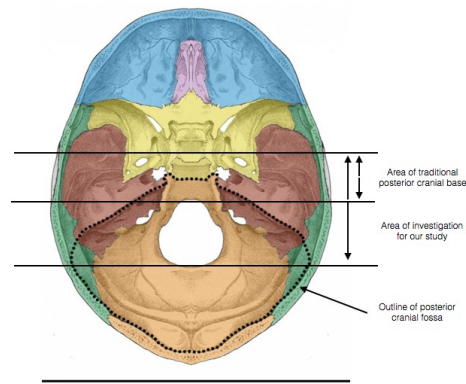
observer may have used a previous definition based on their working knowledge when completing the task as opposed to the exact location as defined for this study.

When the dry skulls were compared with gutta percha and without, linear distances were calculated (accuracy). The difference in these linear differences helped to determine if the landmarks in this study were true representations of actual anatomical locations. As seen above then ICC values were extremely varied while the mean differences were all under 2.62mm. When analyzed, this appears to be a systematic issue with the way the landmarks were identified with gutta percha. Small (but not consistently measured) gutta percha “chunks” were placed into a blockout compound that was sticky enough to attach both to the gutta percha and dry skull. When the thickness of the compound and the size of the gutta percha identifier are taken into account, this appears to be where the larger mean error differences lie. The primary investigator found it difficult to melt gutta-percha and stick it to the landmarks, which is why this technique was developed.

**Specific landmark findings:**

In this study, landmarks in the posterior cranial fossa and surrounding area, as depicted in Figure 4, were considered to check their reliability and accuracy. These landmarks are best visualized in all three planes of space which made them suitable for three-dimensional study. Each landmark will be discussed below.

Figure 4: Posterior cranial area of study



### **Opithsion:**

The most posterior part of the rim of foramen magnum showed excellent intra-rater and inter-rater reliability. The intra-rater mean errors were 0.66 mm in the x axis and 0.2mm in both the y and z axes. In a study by Yoon where they used Opithsion (Op) when constructing reference planes, they showed that Op moved  $2.58 \pm 2.39$  mm. They also stated that Op is one of the most reproducible landmarks in a 3DCT analysis.<sup>60</sup> Based on the results from this study we will agree with their statement as Opithsion is in a location that is very easy to identify in a three dimensional image and in all three planes of space.

### **Foramen magnum left and right:**

The landmarks on the left and right rim of foramen magnum showed excellent inter and intra-examiner reliability. They also showed excellent accuracy when linear measurements were taken between them. In a study measuring foramen magnum (FM) to identify sexual dimorphism, Ilguy et al showed ICC scores of FM measurements for sagittal, transverse, and circumference were 0.95, 0.99, and 0.98, respectively.<sup>61</sup> Given the ease of identifying the

landmarks associated with foramen magnum, and with a little practice, these measurements appear reproducible and accurate in CBCT images of the posterior cranial region.

### **Basion:**

In 2 dimensional images, Basion, is a cornerstone landmark when identifying the posterior cranial base. In this study, it was shown that in 3D images Basion is additionally a viable landmark to study. This landmark demonstrated excellent inter-rater ICC values, excellent intra-rater ICC values and excellent accuracy when used in a linear measurement with Opisthion. As shown in this study, Basion has been demonstrated to be one of the most reliable landmarks on CBCT images.<sup>62</sup> In the study by Lagravere, they showed only moderate intra-rater reliability in the y-axis and mild inter-rater reliability in the y-axis for Basion. They also showed mean differences for Basion at 1.64mm in the y-axis for the same examiner, and when comparing 3 examiners showed mean differences in Basion in the x-axis of 1.46mm and in the y-axis of 2.45mm.<sup>63</sup> Given the results of this study and others, Basion has repeatably shown to be accurate in 3D images.

### **Hypoglossal canal internal/external right and left:**

The hypoglossal canal transmits the hypoglossal nerve and sits above the occipital condyles. In a study on morphometric analysis of the hypoglossal canal they showed this anatomical location should be identified and acknowledged for surgical interventions.<sup>64</sup> In another study the hypoglossal canal was filled with gutta percha and shown to have high intra-examiner reliability and accuracy with mean differences of only 0.79 and 0.56mm for the left and right canals.<sup>56</sup> Our study showed the reliability of identification of both the internal and external hypoglossal canal landmarks showed excellent inter and intra examiner reliability. When these points were used to calculate distances, the ICC values were greatly reduced. As

above, this may be due to the difference in distance when the compound was used versus when the skulls were bare. Additionally, a number of skulls had double canals or bony adhesions dividing the opening, based on where the point was placed, this could greatly affect the accuracy.

#### **Infratemporal fossa right and left:**

This point was chosen based on visual inspection of the dry skulls. It was clearly identifiable based on the curvature and groove of the temporal bone at the anterior portion of the infratemporal fossa. No previous data could be found on this location. In our study we showed this landmark was both reliable and accurate (see tables 2.2 to 2.6). When placing this point, the images must be manipulated and skull re-oriented, but the results show it is very accurate.

#### **Articular eminence right and left:**

The articular eminence is part of the temporal bone and included in the temporomandibular joint complex. It is separated from the condyle by the articular disk. Many studies have investigated the disc in relation to the eminence, or the inclination of the eminence<sup>65-67</sup>, but none could be found that specifically looked at the eminence as a landmark. The specific point in this study was based on examination of the dry skull and appeared reproducible and accurate. The results here back up the original thoughts from the dry skull inspection, but again when landmarked with gutta percha, the values appear less promising due to the error in compound and gutta percha thickness.

#### **External auditory meatus right and left:**

The landmark traditionally associated with external auditory meatus in lateral cephalograms is Porion. However, during evaluation of the dry skulls, this 2D landmark was difficult to decide where to place. The difficulty in deciding where to place this landmark was shown by Ludlow.<sup>47</sup> In our study, the external auditory meatus exits the skull and funnels

inferiorly, this is where a ridge was formed and where the landmark was placed. With proper calibration and training, a single observer and multiple observers were able to reliably place this landmark. Although it was not used for distance measurements, it could be considered in future 3D studies.

#### **Stylomastoid foramen:**

This small foramen is located between the styloid process and mastoid process of the temporal bone and from it emerges the facial nerve.<sup>41</sup> A few studies used the stylomastoid foramen as a starting point to identify the facial nerve and investigate it further. Without this accurate initial anatomical location identified, their research would not have been capable.<sup>68,69</sup> Our study showed that this foramen was easy to identify, reliably landmarked in 3D images and accurate when used in linear measurements

#### **Carotid canal:**

The carotid canal is located in the petrous part of the temporal bone and the structures which pass it include the internal carotid artery, the internal carotid venous plexus and the sympathetic nerve plexus. Its opening varies in shape and it can be divided into ascending petrous, transverse petrous, and ascending cavernous portions.<sup>70,71</sup> The location chosen for the carotid canal point was a consistent fissure on the medial wall from a superior view. This small fissure location proved to be reliable when one observer and 3 observers were identifying it, as well as accurate when used in linear measurements. Although the location of the fissure at the opening of the carotid canal varied from specimen to specimen, it was reliably and accurately located.

#### **Vomer point:**

The point which we refer to as vomer point in this 3D evaluation, appears to be best related in 2D images to the landmark hormion (the posterior border of the vomer connecting to the sphenoid bone).<sup>72</sup> In a CBCT image and using surface rendering, this landmark is easily visualized where the posterior part of the vomer connects to the basilar part of the occipital bone. As seen by the results of this study this location could easily be reproduced by the observers, but the accuracy varied when used for linear measurements. Given the ease of identifying this point in 3D surface rendered and in axial, coronal and sagittal slices, we recommend its further study.

### **Occipital bone:**

These landmarks are located on the lateral surface of the basilar portion of the occipital bone anterior to the foramen magnum. The basilar portion of the occipital bone grows via endochondral ossification<sup>73</sup> and lies inferior and distal to the location of the sphenoccipital synchondrosis. No studies were identified that landmarked the width of the basilar portion. In a growth study by Scott,<sup>74</sup> mention was made about the basilar part of the occipital bone, but nothing was quantified. In our study, identifying this landmark took some finesse and patience, but the results show it can be readily placed with good understanding of its location.

### **Foramen spinosum:**

In a study about the middle cranial fossa, Bumpous showed that foramen spinosum was accurate to 1mm.<sup>75</sup> Foramen spinosum is located at the base of the skull in the greater wing of the sphenoid bone. The middle meningeal artery, vein and nerve pass through it and it has been shown to be about 2.56mm in length and 2.1 mm in width.<sup>76</sup> Identification of this landmark has been shown to be difficult due to its anatomy. Afrand<sup>58</sup> stated that this landmark was the least reliable and difficult to identify, whereas Lagravere<sup>56</sup> concluded this landmark was acceptable for 3D superimpositions. Our study has to agree with Bumpous and Lagravere in that this

landmark was reliable when one or three observers were identifying it and an accurate representation of true anatomy.

#### **Depth of sella:**

Sella Turcica based on traditional cephalometric evaluation as a “free floating” landmark does not transfer well to three dimensions, as placing a landmark on a solid structure is easier. We chose the depth (lowest point) of the hypophyseal fossa to be landmarked for this study. This landmark is located in the sphenoid bone at the base where the pituitary gland sits and above the sphenoid air cells. Previous studies show a large variation in morphology in the floor of sella,<sup>77</sup> but none were identified on accuracy and reliability for landmark placement. Given the results from this study, this landmark may be used for future studies as it is easily identified in 3D images.

#### **Width of sella turcica:**

As above, these landmarks were located lateral to sella turcica in the sphenoid bone on the ridge/rim where foramen lacerum emerges. This landmark proved the need for proper calibration and identification of its location. The ridge upon which it is placed is highly variable and difficult to visualize in a number of cases. The easiest way is to manipulate the software for surface rendering is that is an option (as it was in this study).

#### **Temporal bone tip:**

The temporal bone is made up of squamous, petrous and tympanic portions as well as the mastoid process, styloid process, and zygomatic process.<sup>41</sup> This bone is formed by both intramembranous and endochondral ossification.<sup>78</sup> The landmark chosen in this study can be found along the superior ridge of the petrous part of the temporal bone where it ends and connects with the basioccipital and sphenoid bones. Upon visual inspection, this anatomical

landmark seemed easy to pinpoint. With the excellent ICC values and low mean error values, this landmark location seems suitable for future use.

### **Clivus point:**

In this study, we defined the clivus point as the midpoint of a horizontal line connecting temporal bone tips on the right and left. Clivus point approximately demarcates where the occipital bone meets the sphenoid bone; at the location of sphenoccipital synchondrosis. This is a site of much research with varied conclusions.<sup>79-81</sup> Based solely on the anatomical landmark, our study showed excellent identification by all observers. It is somewhat a constructed point, but can be reliably placed.

### **Internal auditory meatus:**

The internal auditory meatus is located in the petrous part of the temporal bone where the facial and vestibulocochlear nerve pass through.<sup>82</sup> This structure can vary in shape, size and course but the opening is well demarcated.<sup>83</sup> For this study, based on the dry skulls, the posterior margin where the meatus emerges is well defined and easily identifiable. The results agree that with knowledge of where the actual landmark should be, it can be reliably and accurately placed.

### **Foramen ovale:**

Both Afrand<sup>58</sup> and Lagraverre<sup>56</sup> concluded that this location is reliable and accurate for use in three dimensional studies. This landmark in our study showed the poorest results. When the primary observer was locating this point, there were no concerns. When the second and third observers were added, the point became more variable. This could be due to the landmark definition and knowledge of where it should be placed. Given the small diameter marker (0.25mm), and the varied diameter of the foramen, this could add greatly to the discrepancy. Given the results of previous studies, this point and location were kept, and still will be

recommended for future study; as long as its definition is concrete and calibration to find its location is thorough.

### **General discussion:**

As suggested above, the chosen landmarks for our study presented excellent intra-rater reliability and inter-rater reliability and could potentially be used for future craniofacial analysis. In our study foramen ovale showed the weakest identification, but based on previous investigations, we have chosen to keep this landmark as recommended, but with an accurate description as to its location.

All the landmarks show varied anatomy from specimen to specimen, but with good definitions, practice, and calibration/guidance for first time observers, these points can be reliably and accurately placed. It should be noted that when using the landmarks, the vertical, horizontal and A/P positions all demonstrate varied errors. Landmarks with larger errors in the vertical should be avoided when making vertical measurements and so forth for all the different planes.<sup>84</sup>

As applied to our study, Major et al<sup>84</sup> recommended to avoid landmarks with identification error more than 1.5mm and stated errors more than 2.5mm to be unacceptable. Lagravère et al<sup>56</sup> stated variations of less than 1mm for CBCT images to not have any clinical significance while in a study done by Mah<sup>45</sup> they stated variation in landmark identification between 0.5 and 1mm to have possible clinical significance. It should also be noted that landmarks identified at boundaries versus on curvatures or prominences can demonstrate increased variability in measurement error.<sup>58</sup>

Although not applicable to our study given the delicacy of the specimens, but accuracy may be increased by creating small holes into the anatomical landmark and placing a radiopaque fiduciary into this hole for improved accuracy.

Additionally, the negative vs. positive values measured from the differences in distance measurements, may demonstrate an over and underestimation of landmark identification. The measurements were calculated by subtracting the data from the skulls without gutta percha from the ones with gutta percha. Any differences can be attributed to measurement/observation error due to the methodology and technique for placing the gutta percha landmarks.

### **Limitations:**

The number of skulls (10) used in this study can be considered a limitation, but in the literature, this number has been used on numerous occasions so it was deemed suitable for this study as well. A higher number of specimens would be advantageous to increase the power of the study. The fact that dry skulls were used may also affect the reliability of landmark identification on live subjects due to image quality and potential increased soft tissue attenuation or movement.

The experience of the investigator is also a variable. The primary investigator in this study found it easier to use the iso-surface rendering to locate the landmarks, then double-checking them in the 3 planes. New investigators will need to learn to identify the landmarks which is why exact descriptive definitions to locate the landmarks in all three planes is a must. Additionally, two of the observers had a “training” session for landmark identification while the third (who was more experienced) was left to just learn from the definitions. A few of the landmarks showed larger mean differences which can be attributed to improper identification or poor definition of the landmark, but may need to be further studied.

With the software that was used, Avizo, there is a steep learning curve and it takes a lot of time to set up each image for analysis. Manipulation of the software and the images requires proper training and guidance. In our study, all the investigators had previous working knowledge with the program but given the new landmark locations, care had to be taken to orient the images to find the points. With 33 landmarks investigated, the process was very time consuming; reducing the number and focusing certain areas, may have improved the accuracy.

All three planes could not be viewed at the same time, but can be checked separately after the surface rendering was used to identify a landmark. Slight alterations in landmark position were inevitable, as the investigators had to keep switching between planes to properly place the point. Identifying one plane for which the landmark is best represented could be a solution, but why reduce the capabilities of the three-dimensional images back down to one dimension.

Using the blockout compound and small inconsistently cut pieces of gutta percha most surely increased the error for accuracy measurements. In order to get the materials to stay and depending on the location, thicker areas of compound were used, which added to the error. If one piece of gutta percha was 2mm long and the pinpoint for landmark definition was placed at the very tip, this additional distance would clearly increase the accuracy mean error measurements. Additionally, the accuracy was measured from linear distances. This does not show three-dimensional locations of the landmarks and could add additional error.

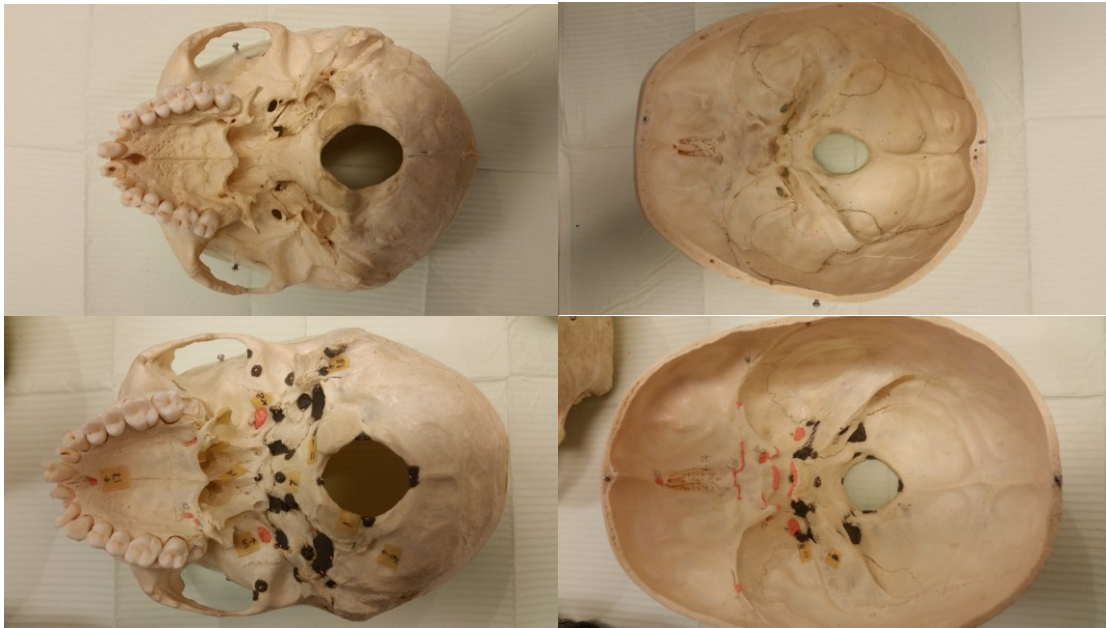
## **2.6 Conclusions**

All the identified structures within the posterior cranial base and surrounding area assessed through CBCT images on dry skulls can be considered reliable and reproducible. The

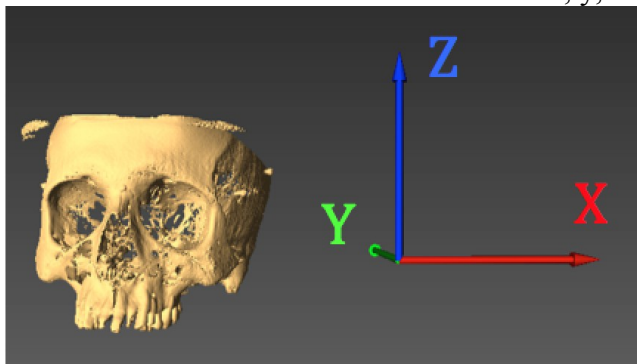
accuracy varied, but this was due to the technique used to place and maintain gutta percha to the dry skulls. All the landmarks used in this study may be used for future studies as long as the definitions are concrete and limitations in landmark identification are known.

## 2.7 Appendices

APPENDIX 1: Dry skulls with (bottom left and right) and without (top left and top) gutta percha on the chosen landmarks

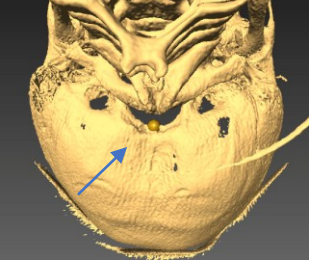
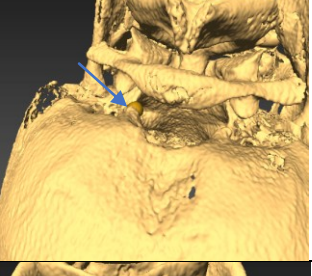
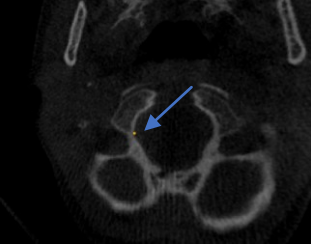
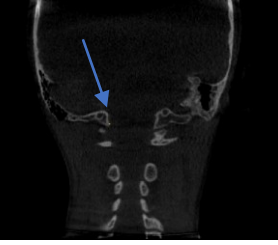
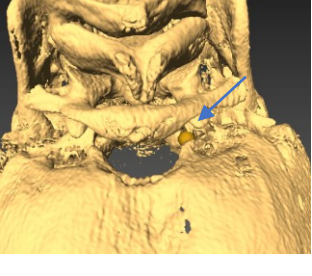
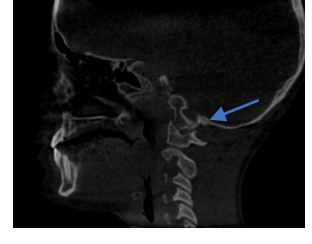
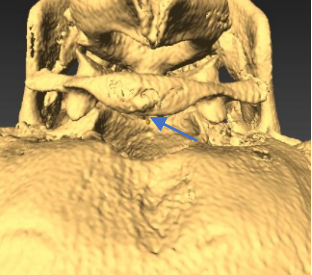
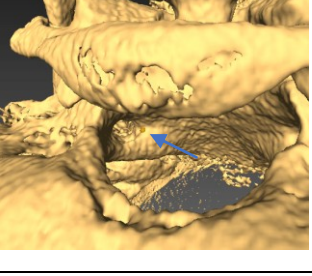
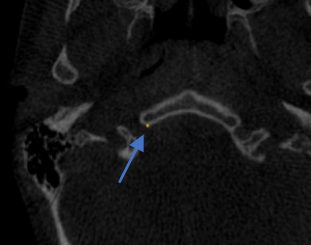


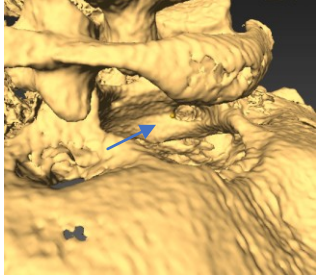
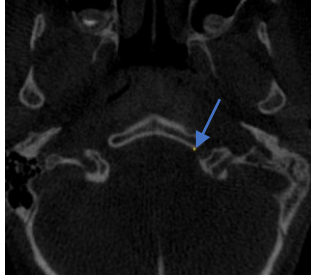
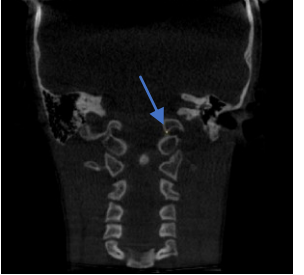
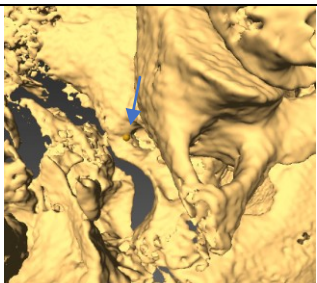
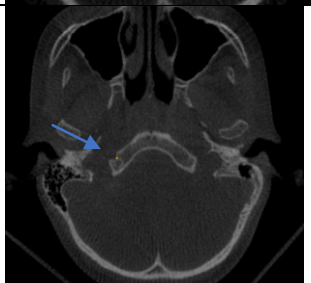
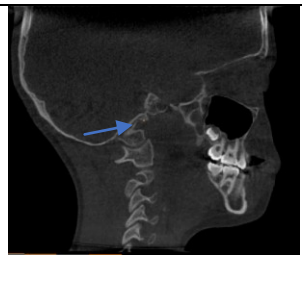
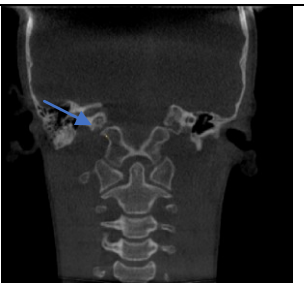
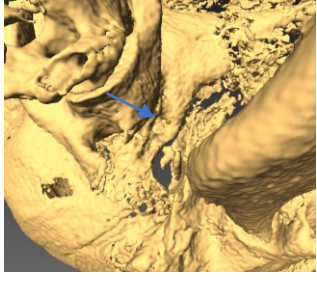
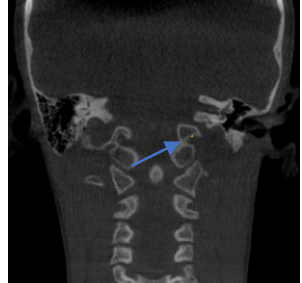
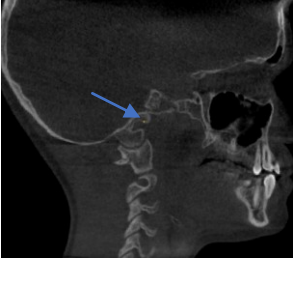
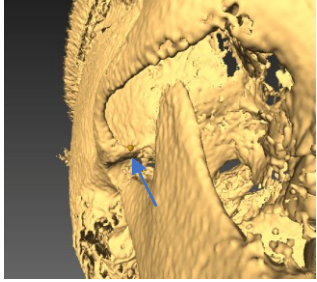
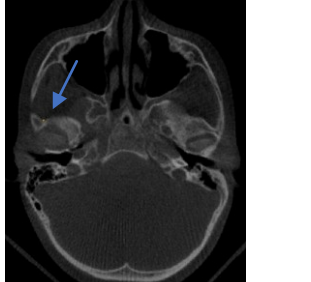
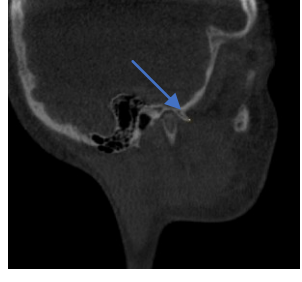
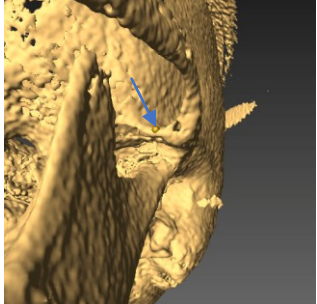
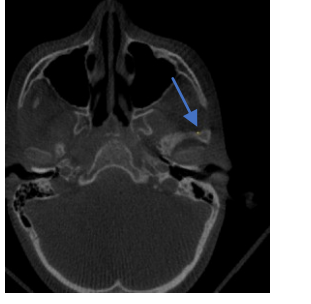
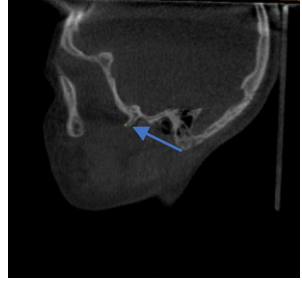
APPENDIX 2: Orientation of skulls with x, y, z axes.

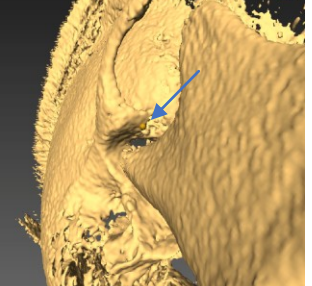
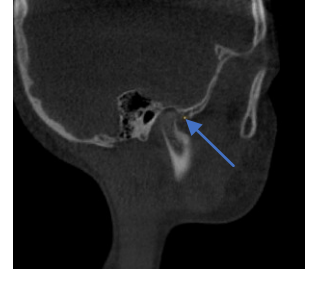
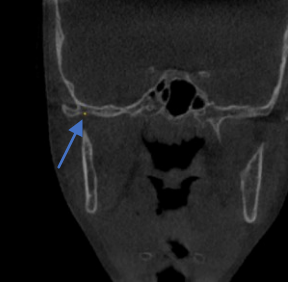
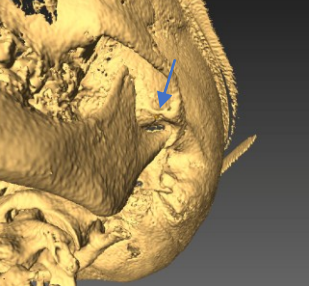
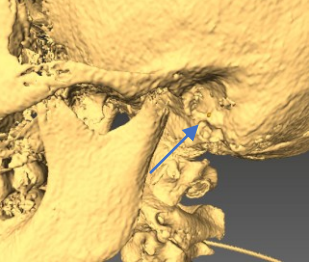
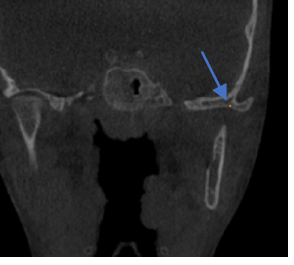
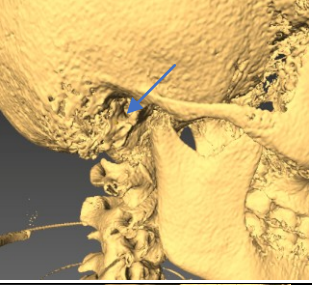
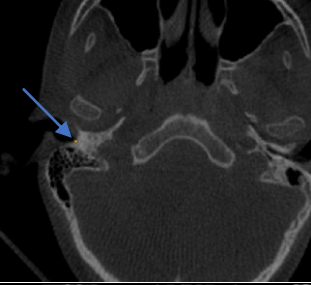
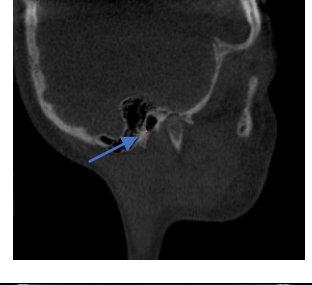
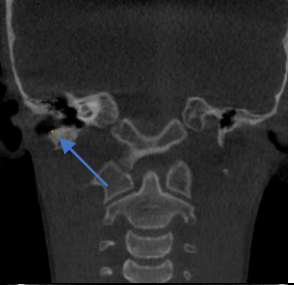
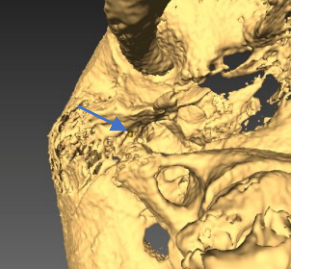


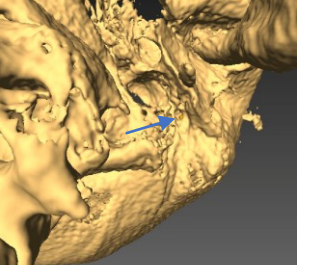
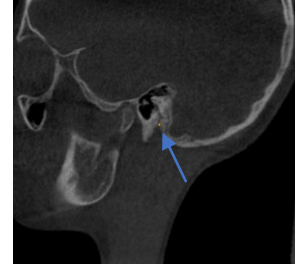
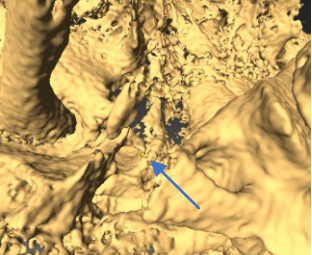
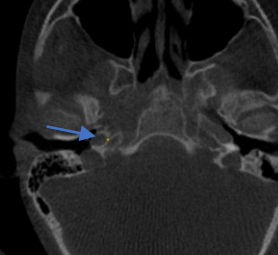
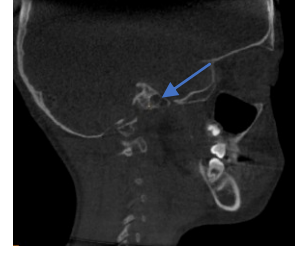
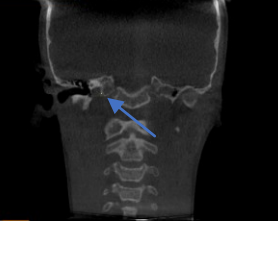
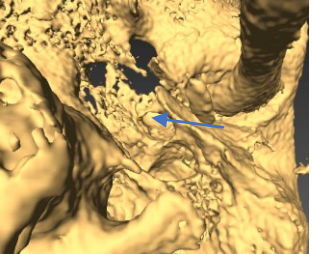
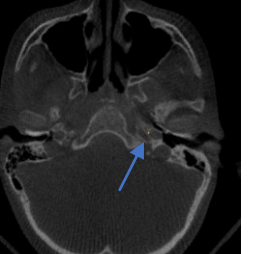
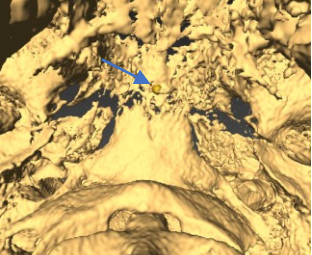
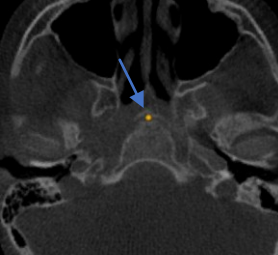
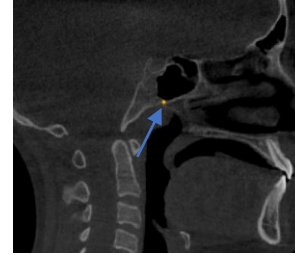
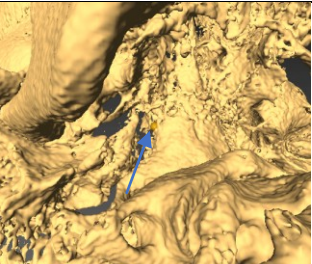
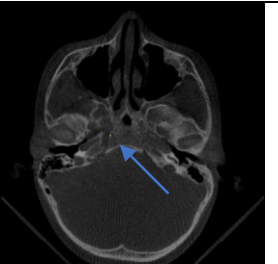
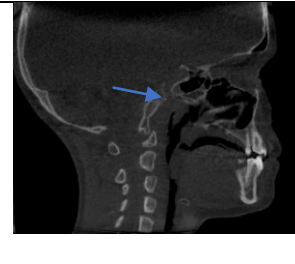
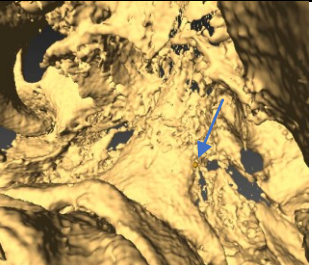
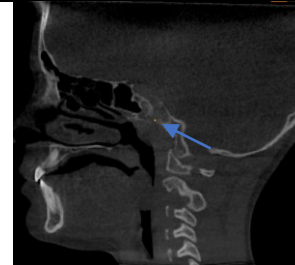
APPENDIX 3.1: Landmark descriptions

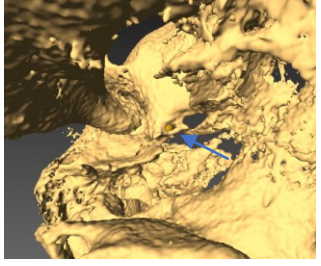
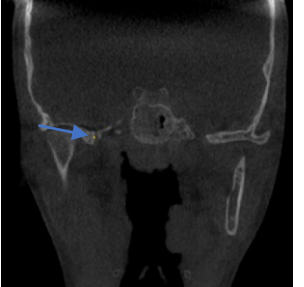
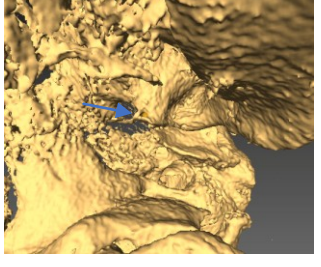
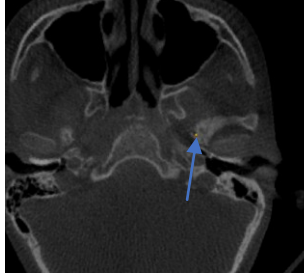
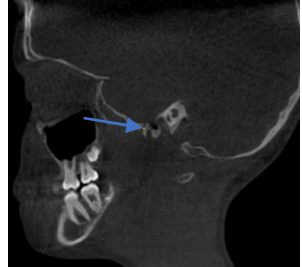
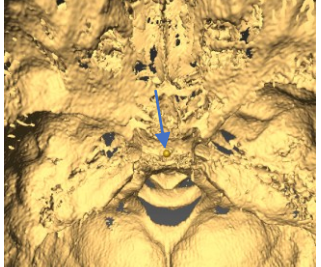
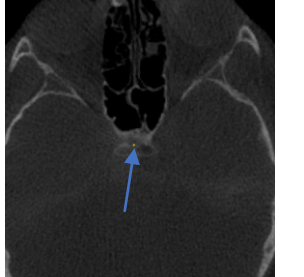
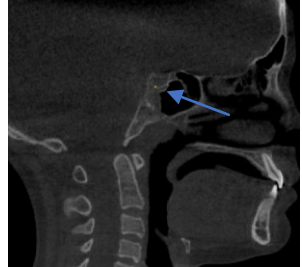
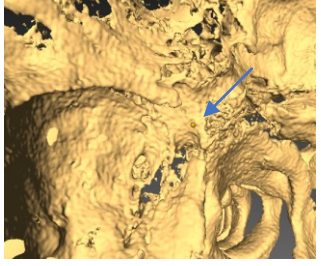
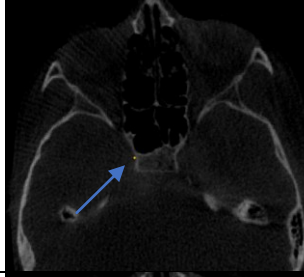
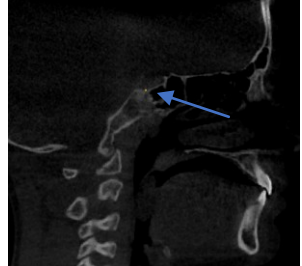
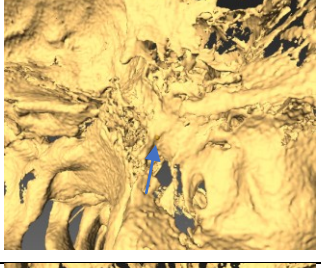
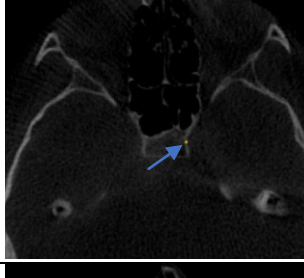
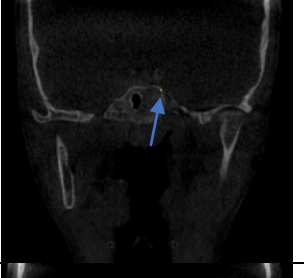
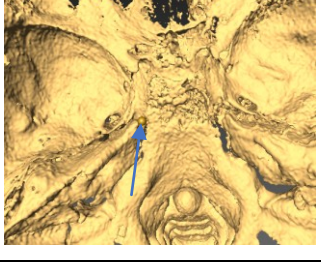
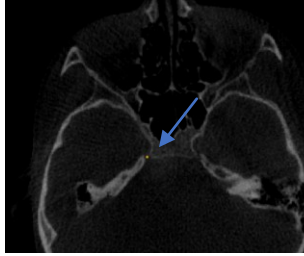
#	Landmark	3D	Axial view (XY)	Sagittal view (YZ)	Coronal view (XZ)
---	----------	----	-----------------	--------------------	-------------------

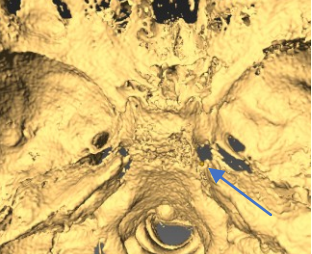
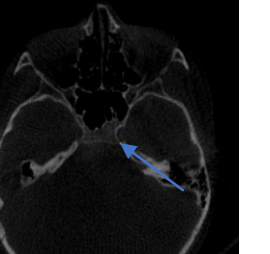
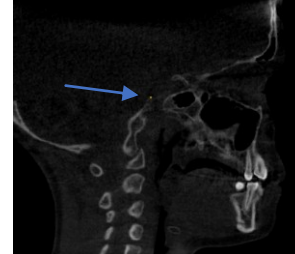
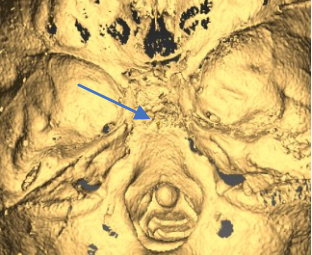
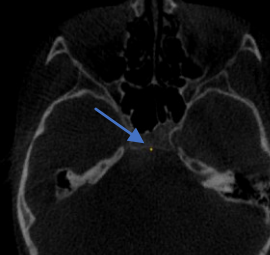
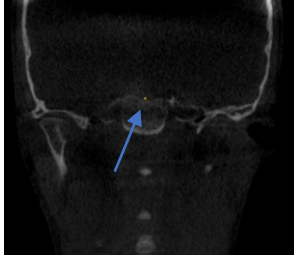
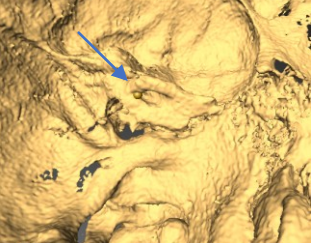
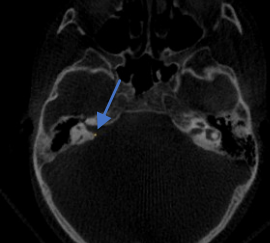
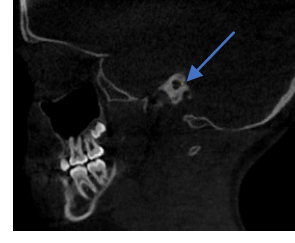
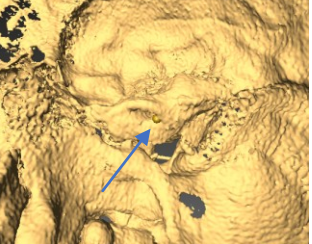
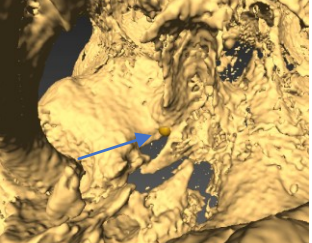
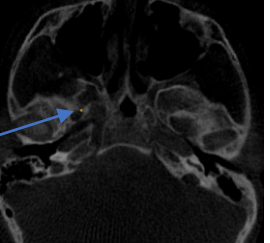
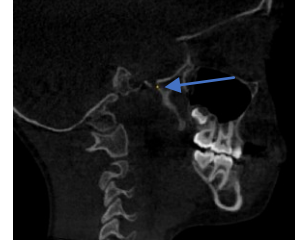
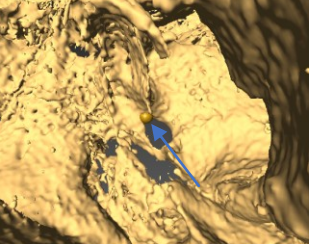
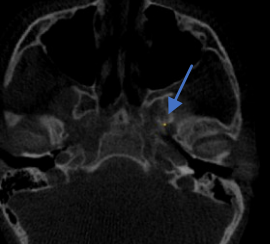
<p>1</p> <p>Posterior Foramen Magnum (FMP)</p> <p>Most posterior curvature of foramen magnum at the most prominent margin from an inferior view</p>				
<p>2</p> <p>Right border of Foramen Magnum (FMR)</p> <p>Right most curvature of Foramen magnum at the most prominent part of the margin of the bone from an inferior view</p>				
<p>3</p> <p>Left border of Foramen Magnum (FML)</p> <p>Left most curvature of Foramen magnum at the most prominent part of the margin of the bone from an inferior view</p>				
<p>4</p> <p>Basion (anterior border of Foramen Magnum) (Ba)</p> <p>Anterior most curvature of foramen magnum at the most prominent part of the margin of the rim from an inferior view</p>				
<p>5</p> <p>Right Internal hypoglossal canal (IHC-R)</p> <p>Most anterior curvature of the internal opening of the hypoglossal canal on patients right</p>				

<p>6</p> <p>Left internal hypoglossal canal (IHC-L)</p> <p>Most anterior curvature of the internal opening of the hypoglossal canal on patients left</p>				
<p>7</p> <p>Right external hypoglossal canal (EHC-R)</p> <p>Most anterior curvature of the rim on the external opening of the hypoglossal canal on patients right</p>				
<p>8</p> <p>Left external hypoglossal canal (EHC-L)</p> <p>Most anterior curvature of the rim on the external opening of the hypoglossal canal on patients left</p>				
<p>9</p> <p>Intratemporal fossa Right (IF-R)</p> <p>Most posterior curvature on the rim of the zygomatic process of the temporal bone on patients right</p>				
<p>10</p> <p>Intratemporal fossa left (IF-L)</p> <p>Most posterior curvature on the rim of the zygomatic process of the temporal bone on patients left</p>				

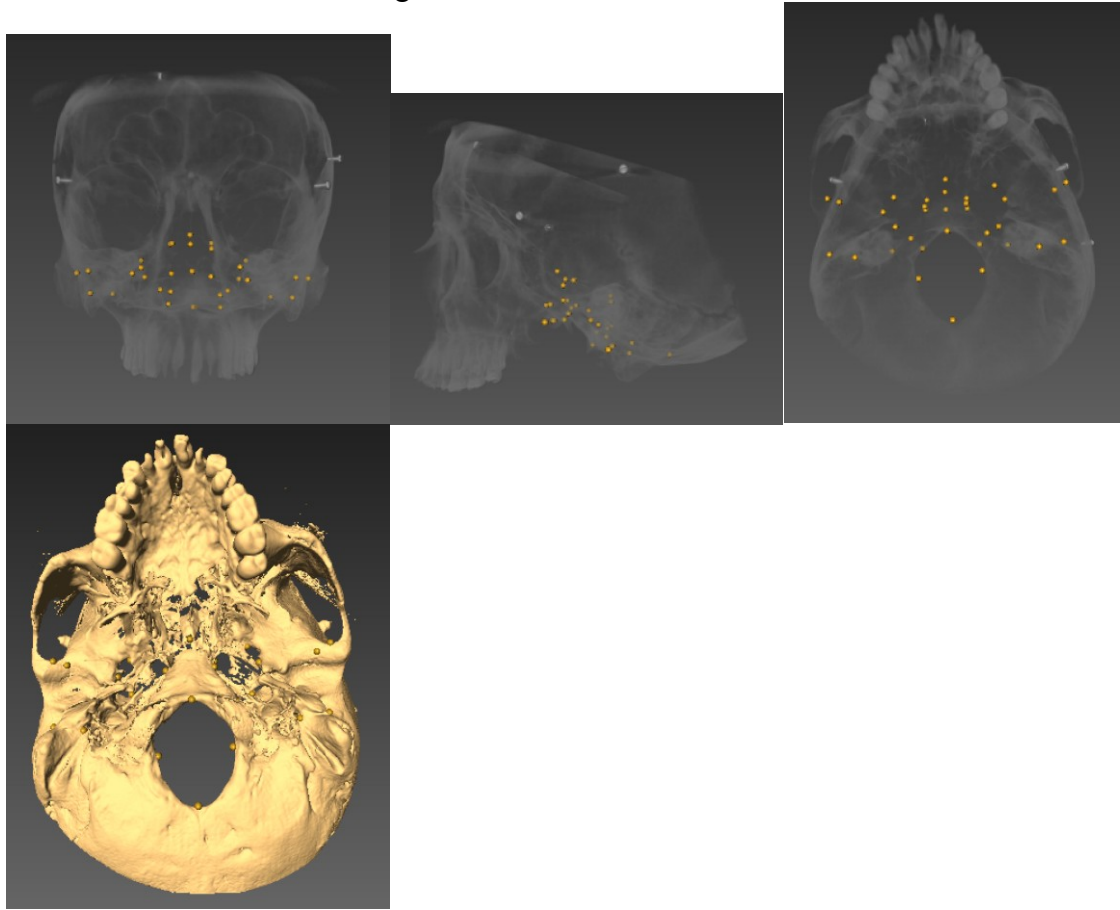
<p>1 1</p> <p>Articular Eminence on patients right (AE-R)</p> <p>Most superior middle portion of the articular eminence on patients right</p>				
<p>1 2</p> <p>Articular eminence on patients left (AE-L)</p> <p>Most superior middle portion of the articular eminence on patients left</p>				
<p>1 3</p> <p>Left External Auditory Meatus (EAM-L)</p> <p>Most inferior external portion of the rim of the external auditory meatus on patients left</p>				
<p>1 4</p> <p>Right External Auditory Meatus (EAM-R)</p> <p>Most inferior external portion of the rim of the external auditory meatus on patients right</p>				
<p>1 5</p> <p>Right stylomastoid foramen (SF-R)</p> <p>Most posterior border as the stylomastoid foramen leaves the skull on patients right</p>				

<p>1 6</p> <p>Left stylomastoid foramen (SF-L)</p> <p>Most posterior border as the stylomastoid foramen leaves the skull on patients left</p>				
<p>1 7</p> <p>Carotid canal right (CC-R)</p> <p>Most inferior point where the carotid canal creates a fissure towards the midline of the skull</p>				
<p>1 8</p> <p>Carotid canal left (CC-L)</p> <p>Most inferior point where the carotid canal creates a fissure towards the midline of the skull</p>				
<p>1 9</p> <p>Vomer point (V)</p> <p>Point where the posterior part of the vomer touches the anterior part of the occipital bone (point is on occipital bone)</p>				
<p>2 0</p> <p>Right occipital bone width (OBW-R)</p> <p>Right most point on the right side of the occipital bone before it begins to widen</p>				
<p>2 1</p> <p>Left occipital bone width (OBW-L)</p> <p>Left most point on the right side of the occipital bone before it begins to widen</p>				

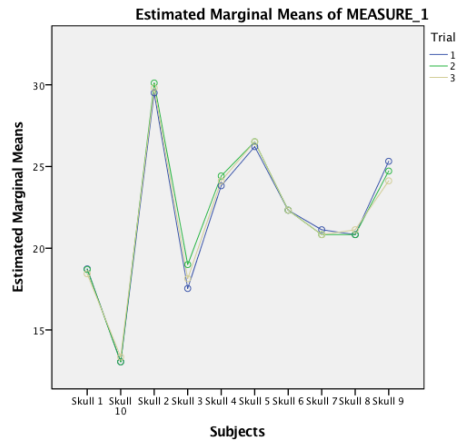
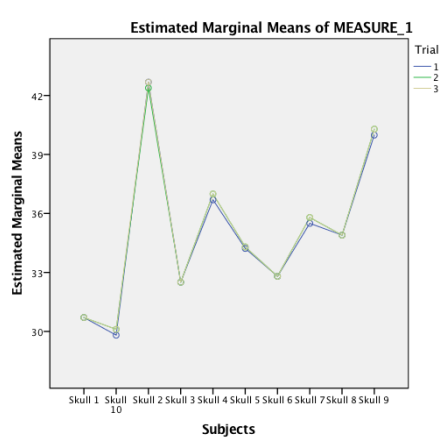
<p>2 2</p> <p>Right Foramen spinosum (FS-R)</p> <p>Most posterior inferior part of the rim of the foramen spinosum where it leaves the skull on patients right</p>				
<p>2 3</p> <p>Left Foramen Spinosum (FS-L)</p> <p>Most posterior inferior part of the rim of the foramen spinosum where it leaves the skull on patients right</p>				
<p>2 4</p> <p>Depth of Sella Turcica (Sella depth)</p> <p>Surface within sella turcica that is the most inferior and middle</p>				
<p>2 5</p> <p>Left width of sella turcica (Sella-L)</p> <p>Left most part where the most superior part of the rim of jugular foramen comes up along near sella</p>				
<p>2 6</p> <p>Right width of sella turcica (Sella-R)</p> <p>Right most part where the most superior part of the rim of jugular foramen comes up along near sella</p>				
<p>2 7</p> <p>Left tip of temporal bone (TBP-L)</p> <p>Point on the tip of the rim of the temporal bone where it meets with sphenoid bone</p>				

<p>2 8</p> <p>Right tip of temporal bone (TBP-R)</p> <p>Point on the tip of the rim of the temporal bone where it meets with sphenoid bone</p>				
<p>2 9</p> <p>Clivus point (CP)</p> <p>Middle most part of clivus when a horizontal line is drawn between the TBP-R and TBP-L</p>				
<p>3 0</p> <p>Left Internal acoustic meatus (IAM-L)</p> <p>Most posterior outer part of the rim of the internal acoustic meatus as it enters the skull</p>				
<p>3 1</p> <p>Right Internal acoustic meatus (IAM-R)</p> <p>Most posterior outer part of the rim of the internal acoustic meatus as it enters the skull</p>				
<p>3 2</p> <p>Right Foramen Ovale (FO-R)</p> <p>Most anterior inferior part of the rim as foramen ovale leaves the skull</p>				
<p>3 3</p> <p>Left Foramen Ovale (FO-L)</p> <p>Most anterior inferior part of the rim as foramen ovale leaves the skull</p>				

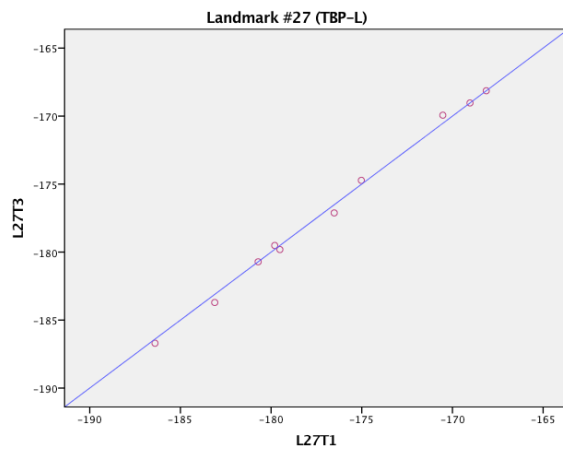
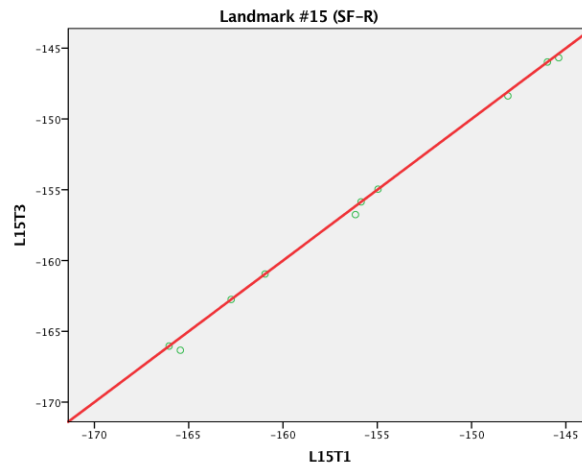
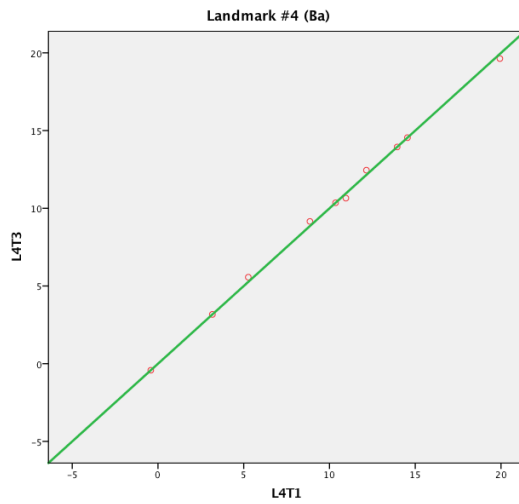
APPENDIX 3.2: Landmarks in coronal, sagittal and axial views (left to right) as well as axial view with 3D surface rendering



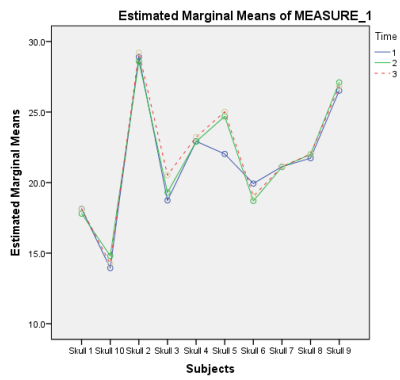
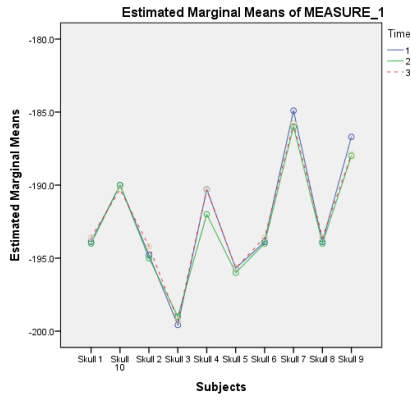
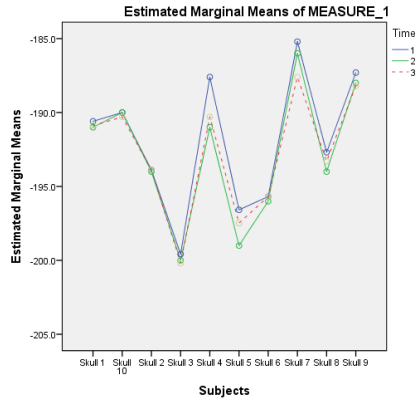
APPENDIX 4.1: Profile plots of intra-rater reliability for the highest (top) and lowest (bottom) ICC values in the x-axis.



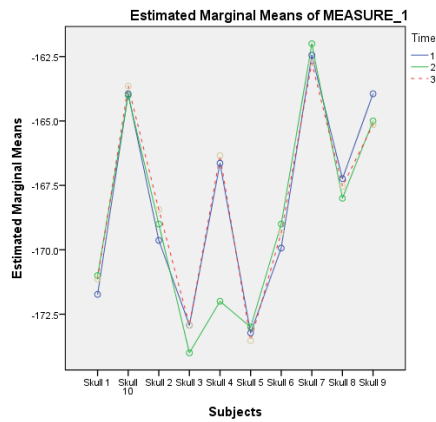
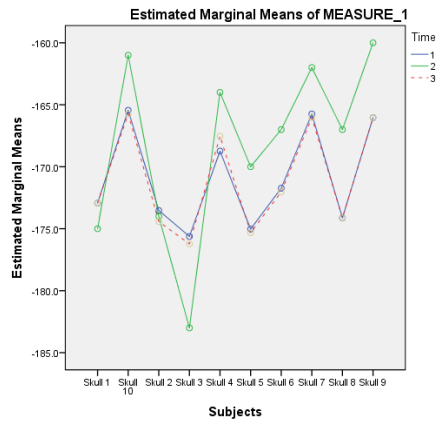
APPENDIX 4.2: Scatter plots with 45 degree line for landmark #4 (x-axis), #15 (y-axis), #27 (z-axis).

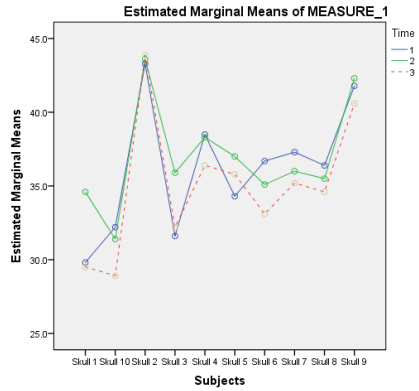


APPENDIX 5.1: Profile plot of inter-rater reliability for excellent ICC values in the x, y, z axes

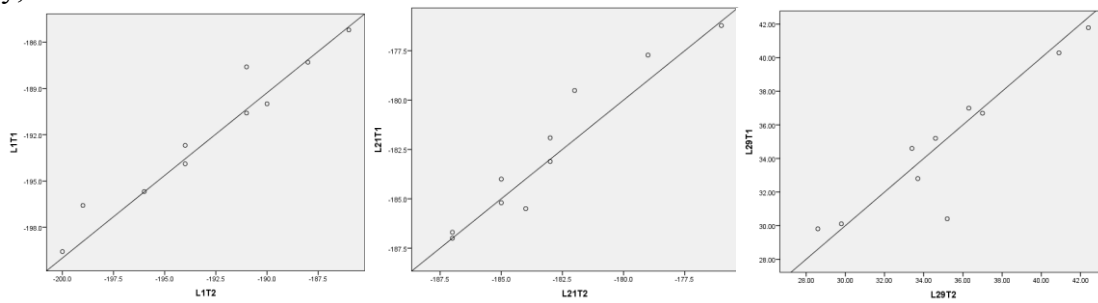


Appendix 5.2: Profile plots for inter-rater reliability with moderate or good ICC in the x, y, z axes

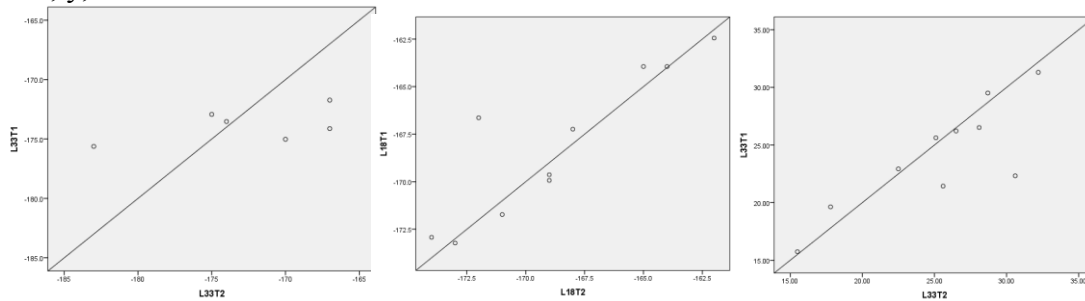




APPENDIX 6.1: Scatter plots with 45 degree line of excellent ICC for inter-rater reliability in x, y, z axes



Appendix 6.2: Scatter plots with 45 degree line of good or moderate ICC for inter-rater reliability in x, y, z axes



Appendix 7: Mean and standard deviation of distance measurements on skulls with and without gutta percha

	N	With Gutta perch		Without Gutta percha	
		Mean	Std. Deviation	Mean	Std. Deviation
Foramen magnum width (FMR to FML)	10	25.23	8.53	25.08	8.53

Hypoglossal canal width right (IHC-R to EHC-R)	10	6.96	2.42	5.48	2.45
Hypoglossal canal width left (IHC-L to EHC-L)	10	7.7	2.15	5.32	1.63
Internal hypoglossal canal right to left (IHC-L to IHC-R)	10	22.78	6.42	23.22	6.59
clivus right to left (OBW-R to OBW-L)	10	20.67	5.69	18.3	4.61
Temporal bone point to sphenoccipital right (TBP-R to CP)	10	10.96	1.94	10.85	1.86
Temporal bone point to sphenoccipital left (TBP-L to CP)	10	10.24	1.43	11.32	2.05
Depth of sella to right (Sella depth to Sella-R)	10	10.71	2.2	9.46	2.03
Depth of sella to left (Sella depth to Sella-L)	10	10.45	1.74	10.11	1.5
foramen ovale right to left (FO-R to FO-L)	10	40.56	10.6	40.5	10.57
foramen spinosum right to left (FS-R to FS-L)	10	53.44	14.3	54.26	14.76
carotid right to left (CC-R to CC-L)	10	46.17	11.81	45.83	11.58
internal auditory right to left (IAM-R to IAM-L)	10	47.83	11.92	48.24	11.86
stylomastoid right to left (SF-R to SF-L)	10	74.38	20.36	74.25	20.38
posterior part of infratemporal fossa right to left (IF-R to IF-L)	10	91.76	26.08	90.71	25.64
External to internal auditory meatus right (EAM-R to IAM-R)	10	25.73	3.99	25.9	3.94

External to internal auditory meatus left (EAM-L to IAM-L)	10	26.55	3.8	26.2	3.71
articular eminence to sella right (AE-R to sella depth)	10	46.34	10.02	45.45	9.64
articular eminence to sella left (AE-L to sella depth)	10	46.25	9.7	45.76	9.45
sella depth to vomer (Sella depth to V)	10	19.15	1.02	17.3	1.39
internal hypoglossal to internal auditory meatus right (IHC-R to IAM-R)	10	21.71	1.76	20.8	1.43
internal hypoglossal to internal auditory meatus left (IHC-L to IAM-L)	10	21.38	1.71	20.4	1.06
basion to sphenoccipital synch (Ba to CP)	10	29.14	3.22	28.05	2.59
vomer to basion (V to Ba)	10	27.9	1.85	27.32	1.59
infratemporal fossa point to basion right (IF-R to Ba)	10	53.93	9.94	53.07	9.54
infratemporal fossa point to basion left (IF-L to Ba)	10	55.21	9.89	54.08	9.54
articular eminence to stylomastoid right (AE-R to SF-R)	10	29.63	2.4	27.61	2.12
articular eminence to stylomastoid left (AE-L to SF-L)	10	29.34	2.34	27.51	1.95
Foramen magnum a/p (Ba to FMP)	10	32.41	3.44	33.04	3.39

## **Chapter 3: Posterior Cranial base and surrounding area changes assessed through CBCT Imaging in adolescents**

### **2.1 Introduction**

Of all the dental specialties, orthodontics may be the most deeply tied to craniofacial growth and development. A large portion of patients enter orthodontic treatment as adolescents. At this age, peak growth of the facial complex and whole body is likely to be taking place.<sup>85</sup> Understanding of craniofacial development is important for any practicing orthodontist, which includes embryonic origins, type of ossification, detailed anatomy and timing of the cephalocaudal gradient of growth.<sup>9</sup>

Application of this knowledge may help guide diagnosis, treatment planning, and treatment modalities. Through the use of growth charts, familiar comparisons, development of secondary sexual characteristics and radiographic analysis, practitioners can make an educated guess as to when treatment should be initiated for certain craniofacial problems. To assist in this, radiographic evaluation using stable and easily identified anatomical landmarks is important.

A systematic review (Chapter 2) showed that the current evidence suggests the posterior cranial base is not totally stable based on traditional cephalometric evaluation and continues to change in dimension even into late adulthood. This systematic review concluded these results based on a lateral/sagittal view of the posterior cranial base (*Sella to Basion*). Given that the head is a 3D structure, knowledge of its growth in all three planes (sagittal, axial, coronal) would be beneficial in order to confirm or refute these findings.

Much of the change shown in conventional 2D images has been attributed to growth at the spheno-occipital synchondrosis. This structure is a cartilaginous connection between the basilar part of the occipital bone and the body of the sphenoid.<sup>43</sup> Growth of the entire cranial base is via endochondral ossification, while areas adjacent form through intramembranous

ossification.<sup>78</sup> The middle and posterior cranial fossa have numerous sutures and synchondroses that contribute to transverse, vertical and anteroposterior growth, each with differing ossification times.<sup>86</sup> Additionally, in a study using MRI images, the posterior cranial fossa was said to show a concentric (ring like) pattern of growth.<sup>87</sup>

As mentioned, growth is a three-dimensional phenomenon. Using cone-beam computed tomography (CBCT) images has allowed visualization of the craniofacial complex in all planes of space. With the use of specialized software, these images can be manipulated to visualize specific structures or anomalies, achieve pinpoint accuracy in landmark identification and measure distances and angles between structures.<sup>88</sup> Using distances between locations and at multiple time-points one can show stability or growth of a certain area. Thus, stable landmarks should be established and used in order to superimpose sequential images and assess growth or treatment results.

To the best of our knowledge, CBCT growth analysis of the posterior cranial base has not been carried out. In this study, the posterior cranial base and surrounding area will be studied for structural changes in an adolescent population sample using CBCT. If stable, certain structures may be used for future superimposition and any observed changes in this area may be attributed to continued growth and development.

#### Research Question:

- 1) Are the previously determined landmarks (Chapter 2) in the posterior cranial base and surrounding area stable during adolescent years in the horizontal, vertical and antero-posterior dimensions?

## **2.2 Methods and Materials**

This study is a retrospective observational longitudinal study approved by the University of Alberta research ethics board.

The patient CBCT images for this growth assessment were part of a randomly selected patient pool obtained from a database of images acquired for a clinical trial. CBCT images were taken on the patients both before and after they received orthodontic treatment. The images were acquired using an ICAT scanner (Image Science International, Hatfield, PA, USA). The ICAT scanner protocol was large field of view, 9in x 12in, voxel size 0.30mm, 120kVp, 23.87mAs, 8.9 seconds. Sixty (60) patients were assessed in this study and their two CBCT images were taken at an average of 17.5 months apart. The mean, standard deviation, minimum and maximum values for Age at T1, T2 and difference are shown in Table 3.1. The sample included 21 males and 39 females. The principle examiner (K.C) marked the 60 time 1 images and the 60 time 2 images.

Table 3.1.1: Mean, standard deviation, minimum, maximum at T1, T2 and difference (in years)

	N	Mean	Std Deviation	Minimum	Maximum
Age at T1	60	13.1	1.1	11.0	15.5
Age at T2	60	14.6	1.0	12.7	17.0
T2-T1 (years)	60	1.5	0.18	1.1	1.9

Table 3.1.2: Male and Female Demographics

	Number	Average Age at T1	Average Age at T2	Average Difference
Male	21	13.4	14.9	1.5
Female	39	12.9	14.4	1.4

The landmarks determined in a previous study to have acceptable reproducibility and accuracy were marked on the patient images pre-treatment (T1) and post-treatment (T2). Twenty-nine (29) linear measurements were determined upon visual inspection of dry skulls. (Table 2.5) An attempt was made to include each landmark in multiple planes but an emphasis was placed on horizontal (left to right) measurements as this has previously been the least investigated dimension due to the scarcity of frontal cephalograms. Nineteen distances were measured in the horizontal, four in the vertical, and six in the anterior-posterior. The twenty-nine linear measurements were generated using the equation:

$$d = \sqrt{(x_2 - x_1)^2 + (y_2 - y_1)^2 + (z_2 - z_1)^2}$$

D is the distance in millimeters between the two landmarks and x1, y1, z1 and x2, y2, z2 are the coordinates of the landmarks used for the linear measurements.

Table 3.2 Linear measurements

Transverse Dimension (right-left)		
1H	Foramen magnum width (FMW)	Distance between left and right rims of foramen magnum (FMR-FML)
2H	Right Hypoglossal canal width	Distance between right internal and external points on hypoglossal canal (IHC-R to EHC-R)
3H	Left Hypoglossal canal width	Distance between left internal and external points on hypoglossal canal (IHC-L to EHC-L)
4H	Internal Hypoglossal canal right to left	Distance from the internal hypoglossal canal points from right to left (IHC-R to IHC- L)
5H	Clivus width	Width of the clivus from right occipital bone to left occipital bone point (OBW-R to OBW-L)
6H	Right Temporal bone point to sphenoccipital point	Distance between TBP-R and CP
7H	Left Temporal bone point to sphenoccipital point	Distance between TBP-L and CP
8H	Right sella width point to depth of sella	Distance between Sella-R and Sella depth
9H	Left sella width point to depth of sella	Distance between Sella-L and Sella depth

10H	Foramen Ovale right to left	Distance between right and left foramen Ovale (FO-R to FO-L)
11H	Foramen spinosum right to left	Distance between right and left foramen spinosum (FS-R to FS-L)
12H	Carotid canal right to left	Distance between CC-R to CC-L
13H	Internal auditory meatus right to left	Distance between IAM-R to IAM-L
14H	Stylomastoid foramen right to left	Distance between SF-R to SF-L
15H	Posterior part of infratemporal fossa right to left	Distance between IF-R to IF-L
16H	EAM-R to internal auditory meatus right	Distance between EAM-R to IAM-R
17H	EAM-L to internal auditory meatus left	Distance between EAM-L to IAM-L
18H	Articular eminence to sella right	Distance between AE-R to Sella depth
19H	Articular eminence to sella left	Distance between AE-L to sella depth
<b>Vertical Dimension (superior-inferior)</b>		
20V	Sella to vomer point	Distance between Sella depth to V
21V	Internal hypoglossal to internal auditory meatus right	Distance from IHC-R to IAM-R
22V	Internal hypoglossal to internal auditory meatus left	Distance from IHC-L to IAM-L
23V	Basion to sphenoccipital synchondrosis point	Distance from B to CP
<b>Anterior-posterior Dimension (front-back)</b>		
24AP	Vomer point to Basion	Distance from V to B
25AP	Infratemporal fossa point to basion right	Distance from IF-R to B
26AP	Infratemporal fossa point to basion left	Distance from IF-L to B
27AP	Articular eminence to stylomastoid right	Distance from AE-R to SF-R
28AP	Articular eminence to stylomastoid left	Distance from AE-L to SF-L
29AP	Foramen magnum a/p	Distance from B to FMP

### 2.3 Statistical Analysis

The data was analyzed using a standard statistical software package (SPSS version 24 for PC, IBM). A sample size power analysis was not completed, but a sample size of sixty (60) was

selected based on a previous study<sup>58</sup>. Sixty cases is two times more than the recommended number to determine significance under these research settings.<sup>58,89</sup>

The calculated distances between landmarks at T1 and T2 are continuous dependent variables. The distances from T1 were subtracted from T2 to calculate their difference (which will be referred to as growth). The percentage change was also calculated. The descriptive statistics for the distances and percentages change can be found in Appendix 1.

To answer research question #1, a repeated measures MANOVA was first run for both growth and percentage change. Patients' ages at initial imaging was considered as a covariate. A multivariate analysis of covariance (MANCOVA) was then run for both growth and percentage change. The covariate is used to control for the difference in age of the subjects at time 1 and avoid misleading results. This covariate removes the variability of age across individuals at the time of the initial CBCT. After this, treatment time was substituted as a covariate. This was to see if there was a difference in growth for those that had shorter or longer treatment times. MANOVA hypothesis tests can be seen in Appendix 2.

Prior to completing the significance testing, model assumptions were evaluated for both difference and percentage change. All data was checked for multivariate normality visually via Q-Q plot and box plot of the Mahalanobis distance of the difference between T1 and T2 (dependent variable) for each distance and percentage change for each distance (Appendix 3). Percentage change had 1 outlier, which was kept because it was within one and a half time the maximum value. Assumption of linearity of repeated measures was met as assessed by bivariate scatter plots (Appendix 4). The sphericity assumption was not applicable. Multicollinearity was assessed by regression analysis on age (covariate) and difference. Age was not well correlated with any of the response variables (Appendix 5). Appendix 6 shows a boxplot of the difference

in distance and percentage change. Appendix 7 shows an estimated marginal means graph for T1 and T1 over all the difference in distance measurements.

The percentage change and difference data were compared between males and females using repeated measures MANOVA to determine if sex would affect the results.

In addition, the data was “converted” and run through the MATLAB software as described in detail by Lagravere et al.<sup>90</sup> This was used to assess the change in position of all the landmarks in all three planes of space using a global coordinate system and reference planes.

## 2.4 Results

Running the multivariate MANOVA analysis, when all the distances were considered jointly, got a statistically significant difference of the dependent variables,  $F(29,31) = 4.517$ ,  $p < 0.001$ ; Wilk's  $\Lambda = 0.191$ ; partial  $\eta^2 = 0.809$  was obtained. This indicates that there is some statistically significant change in distance of several measurements. Adding age at T1 as a covariate got a non-statistically significant result, indicating age at time of initial CBCT image does not affect the potential growth,  $F(29,30) = 0.876$ ,  $p = 0.639$ ; Wilk's  $\Lambda = 0.542$ ; partial  $\eta^2 = 0.458$ . When using treatment time (difference in age when starting treatment and finishing treatment) as a covariate, reveals suggestive, but inconclusive results,  $F(29,30) = 1.827$ ,  $p = 0.053$ ; Wilk's  $\Lambda = 0.362$ ; partial  $\eta^2 = 0.638$ .

Since age at T1 did not show significance, it was removed, but still considered in the discussion. Table 3.3 presents the pairwise comparisons of the mean of the measurements that showed significant changes from time 1 to time 2.

Table 3.3: MANOVA pairwise comparisons for growth

Distance (difference in distances)	Mean difference T2- T1 (in mm)	Standard deviation	P value	95% Confidence interval for distance	
				Lower bound	Upper bound
Diffd5H	0.482	1.353	0.008	0.133	0.832
Diffd10H	0.359	0.811	0.001	0.150	0.569
Diffd11H	0.712	1.188	<0.0001	0.405	1.019
Diffd14H	0.893	1.236	<0.0001	0.574	1.212
Diffd15H	1.323	1.444	<0.0001	0.950	1.696
Diffd16H	1.002	2.077	<0.0001	0.466	1.539
Diffd17H	0.562	1.397	0.003	0.201	0.923
Diffd18H	0.857	1.258	<0.0001	0.532	1.182
Diffd19H	0.852	1.429	<0.0001	0.482	1.221
Diffd20V	0.625	1.889	0.013	0.136	1.113
Diffd23V	0.827	1.194	<0.0001	0.518	1.135
Diffd24AP	0.602	2.006	0.023	0.084	1.121
Diffd25AP	0.857	1.047	<0.0001	0.587	1.128
Diffd26AP	0.869	0.878	<0.0001	0.642	1.096
Diffd29AP	-0.182	0.533	0.010	-0.320	-0.045

The same MANOVA was run with percentage change values. When all the percentage change values were considered jointly, there was a statistically significant difference,  $F(29,31) = 5.157$ ,  $p = <0.0001$ ; Wilk's  $\Lambda = 0.172$ ; partial  $\eta^2 = 0.828$ . Tables 3.4 shows the pairwise comparisons of the values that showed significance when MANOVA testing for percentage change. Again age at T1 was used as the covariate with results showing no evidence of its significance,  $F(29,30) = 0.879$ ,  $p = 0.635$ ; Wilk's  $\Lambda = 0.541$ ; partial  $\eta^2 = 0.541$ . Age at T1 as a covariate was removed. Using the treatment time as a covariate yielded,  $F(29,30) = 1.672$ ,  $p =$

0.084; Wilk's  $\Lambda = 0.382$ ; partial  $\eta^2 = 0.618$  (see table 4). The covariate of treatment time (difference in time from start of treatment to finish) was also removed.

Table 3.4: MANOVA Pairwise comparisons for percentage change.

Distance (percentage change in distances)	Mean difference T2- T1	Standard deviation	P value	95% Confidence interval for distance	
				Lower bound	Upper bound
%changeD5	2.437	6.540	0.005	0.747	4.126
%changeD10	0.849	1.891	0.001	0.360	1.337
%changeD11	1.207	1.888	<0.0001	0.719	1.694
%changeD14	1.051	1.404	<0.0001	0.688	1.414
%changeD15	1.322	1.439	<0.0001	0.951	1.694
%changeD16	4.307	10.209	0.002	1.670	6.944
%changeD17	2.219	5.529	0.003	0.790	3.647
%changeD18	1.657	2.419	<0.0001	1.032	2.282
%changeD19	1.650	2.741	<0.0001	0.942	2.358
%changeD20	4.580	17.656	0.049	0.020	9.142
%changeD21	1.391	5.075	0.038	0.080	2.703
%changeD23	2.698	4.052	<0.0001	1.651	3.745
%changeD24	2.403	7.602	0.017	0.439	4.367
%changeD25	1.485	1.804	<0.0001	1.019	1.952
%changeD26	1.511	1.538	<0.0001	1.114	1.909
%changeD29	-0.464	1.422	0.014	-0.832	-0.098

Table 3.5: pairwise comparisons that showed statistical significance for growth (difference in distances from T1 to T2) when treatment time was considered as a covariate

Distance (difference in distances)	Mean difference T2- T1 (in mm)	Standard deviation	P value	95% Confidence interval for distance	
				Lower bound	Upper bound
Diffd17H	0.562	1.397	0.018	0.216	0.909
Diffd22V	0.128	1.041	0.044	-0.134	0.391
Diffd27AP	0.238	1.089	0.052	-0.036	0.513

Having set the clinical significance for difference and percentage change at 1.5mm and 5% respectively, none of the mean values surpassed these numbers. Appendix 8 shows scatter plots of distance 17 (EAM-L to IAM-L) which showed significant findings when treatment time was used as a covariate. It was noted that as the treatment time was longer, there was more growth. Appendix 9 shows a scatter plot for distance 7 that showed no relation between growth and treatment time. The lower horizontal line showing that as treatment time was longer, no further growth was present.

Additionally, using the repeated measures MANOVA with sex as a fixed factor, there was no significant difference between males and females for the percentage change and difference values.

As seen in table 3.6, the “converted” data via the MATLAB software showed the mean changes in the x, y and z coordinates for all landmarks. This data used fixed landmarks to measure spatial movement of the other landmarks. Some significant movement was observed especially in the z axis.

Table 3.6: Matlab values in all axis (in mm). Highlighted values were above the clinically significant value of 1.5mm.

	X Axis (tansverse)		Y axis (A/P)		Z axis (vertical)	
	Mean	Std. Deviation	Mean	Std. Deviation	Mean	Std. Deviation
FMP	-0.05	1.24	0.13	1.69	-5.04	7.41
FMR	0.14	1.22	-0.75	2.3	-3.47	5.02
FML	-0.16	1.12	-0.64	2.22	-3.29	4.99
Ba	0	0	0.02	0.16	-0.16	1.05
IHC-R	0.05	0.93	-0.12	1.14	-2.15	2.88
IHC-L	0.01	1.14	-0.07	1.41	-2.17	3.28
EHC-R	0.19	0.86	-0.07	1.33	-1.97	2.3
EHC-L	0	1.18	-0.02	1.45	-1.58	2.51
IF-R	0.81	0.93	-0.07	1.39	0.57	3.11
IF-L	-0.33	1.39	0.19	1.43	0.97	2.17
AE-R	0.78	1.11	-0.1	1.32	0.4	2.73
AE-L	-0.52	1.63	0.31	1.37	0.65	2.34
EAM-L	0.01	0.12	0.07	0.5	0	0
EAM-R	0	0.02	0.02	0.16	0	0
SF-R	0.43	0.79	0.22	1.49	-2.31	3.62
SF-L	-0.33	1.31	0.68	1.78	-2.13	4.14
CC-R	0.54	1.18	0.15	1.54	-1.46	2.08
CC-L	0.15	1.62	0.67	1.78	-0.8	3
V	0.33	1.05	0.1	2.14	1.14	2.61
OBW-R	0.23	0.93	0.39	1.72	-0.49	1.62
OBW-L	-0.24	1.16	0.4	1.93	-0.31	1.42
FS-R	0.38	0.56	-0.08	0.75	0.04	1.53
FS-L	-0.38	0.56	0.08	0.75	-0.04	1.53
Sella depth	0.2	1.56	1.64	2.64	0.48	2.03
Sella-L	0.36	1.37	1.47	2.44	0.34	2.3
Sella-R	0.04	1.21	1.28	2.06	0.2	2.25
TBP-L	0.24	1.56	1.5	2.3	-0.45	1.24
TBP-R	0.08	1.44	1.38	2.35	-0.51	1.63
CP	0.12	1.41	1.67	2.27	-0.46	1.3
IAM-L	0.09	1.64	1.48	2.77	-1.84	2.78

IAM-R	0	2.22	1.44	2.64	-2.23	2.69
FO-R	0.34	0.82	0.15	1.02	0.48	1.97
FO-L	0.01	1.03	0.2	0.85	0.14	1.83

Overall, though statistically significant results were present, transferring this to a clinical setting needs to be explored further.

## 2.5 Discussion

Knowledge on whether a patient is growing or not is vital to orthodontic treatment planning. In order to assess this, previously used techniques revolved around monitoring stature<sup>91</sup>, familiar growth patterns, development of secondary sexual characteristics, shoe size, hand wrist radiographs<sup>92</sup>, and sequential serial cephalograms with superimposition<sup>93</sup>. Commonly used superimposition techniques require stable structures that the orthodontist knows will not change or move to a large extent, and are easily and accurately identifiable.

Traditionally, in 2D, the anterior cranial base has been used as a stable plane upon which superimposition to assess growth has been based.<sup>94</sup> This study aimed to assess the growth changes of the posterior cranial base and surrounding area on human adolescent skulls using 3D CBCT images in the horizontal, vertical and antero-posterior dimensions over an average treatment period of 17.5 months. The findings in the AP dimension agree with the previous 2D studies. Given some statistically significant values, the results should be interpreted with caution due to a number of factors that may affect their significance.

CBCT images have inherent drawbacks. Accuracy measurements between distances may be affected by soft-tissue attenuation, patient movement, and artifacts.<sup>95</sup> Variation in voxel size

the images were taken at is another factor. The images in this study were taken at a voxel size of 0.4mm. This means that an error of anywhere between 0 and 0.8mm could be shown at the linear measurements. The voxel size is defined by height, width, and depth which is equal to pixel size in 2D images. Smaller voxel sizes have been shown to increase radiation dose. Increasing the voxel resolution does not result in increased accuracy of the CBCT measurements.<sup>96</sup> Although the images are sharper and “prettier”, it may not be worth the extra radiation dose to get about the same diagnostic resolution.<sup>97</sup>

Soft-tissue attenuation can affect accuracy as well.<sup>98</sup> The Avizo software was manipulated so that the overlying soft tissue was “removed” so that the underlying skeleton and landmarks could be identified. All the images required small manipulations in order best see the skeleton. This variation may affect the accuracy of measurements, even in the same patient at different time points.

Measurement error is another aspect that should be considered. This consists of random error and systematic error. Variations on landmark identification as well as manipulating the software to identify the landmarks are sources of measurement error. Even identifying the landmarks in 3D contributes to added error. When considering the multiple variables, settings, and possibility of error, it may be possible that the accuracy of 3D measurements would be reduced on patient images.<sup>95</sup>

Patient’s age at time 1 was considered as a covariate. This was to control for systematic variance across individual patients at initial CBCT image. The changes in distance were not affected by the patient’s age, so it was subsequently removed from the analysis. This was unexpected as typically age is highly correlated with growth<sup>99</sup>, but perhaps at a smaller scale in the posterior cranial base during the short time frame our study measured. A second covariate of

treatment time (the difference in time from initial CBCT to final CBCT) was addressed. Interestingly, this factor showed some significant results, despite initial age not being a factor. One would expect that the longer the time interval between images, the more potential there is for growth/changes.

In this study, percentage change was as a measurement. This becomes relevant when changes that may appear significant are seemingly insignificant when placed in context. For example, a change of 5mm may seem like a large number, if it was on a distance of 20mm, then it most certainly is; but if it was on a distance of 100mm, its significance is greatly reduced. In this study, distance 15 (IF-R to IF-L) showed a 1.3mm change, but as a percentage of the total distance, this was only 1.3%, which overall has little clinical significant.

When the results showed statistical significance, this relation to clinical significance does not transfer over. Exact data and standards do not exist to determine clinical significance (especially in the posterior cranial base), but numbers suggested from an experienced orthodontist were used as a guide. For the difference in distances measured between time 1 and 2, a clinically significant value of 1.5mm was used. For percentage change in distance, a clinically significant value of 5% was used. These values were used because anything larger that this may impact diagnosis and/or treatment planning. Despite coming close to these values on only a few distances, the majority of the values fell well below this clinically significant cut off, despite being statistically significant in reporting. This is a valid point for use of this study. Despite showing some significance based on the numbers, in a clinical setting caution should be weighed as these changes in the posterior cranial base may not affect treatment decisions based on timing or modality of treatment.

In this study, the posterior cranial base was assessed in three planes and the measurements were divided as such for ease of identification of each plane. The different planes and distances will be discussed below. Of note, the largest percentage change, which turned out to be in the vertical dimension, was distance 20, sella to vomer point. It showed an increase of 4.6%. The largest distance change, was distance 15, posterior part of infratemporal fossa right to left, which was in the transverse dimension and gave a value of 1.3mm.

### **Anterior-posterior measurements**

In this study there were 6 distance measurements that attempted to show changes in the antero-posterior dimension (Table 3.2). From them 4 of the measurements used the landmark *Basion*. From the previous systematic review, this landmark is known to be displaced down and back. Interestingly, all 4 of these linear measurements showed statistical significant results for both difference and percentage change (see Tables 3.3 and 3.4). Since *Basion* has been reported to be displaced this parallels our findings in this study. As stated previously, this change in distance (growth) and increase in percentage change can be attributed to the spheno-occipital synchondrosis and its activity.<sup>99-101</sup>

### **Vertical measurements**

Only 4 measurements attempted to quantify vertical changes (see Tables 3.2, 3.3 and 3.4). From them 2 of these distances demonstrated statistically significant results. Distance 20 which involved the depth of *sella* point and vomer point and distance 23 which involved *Basion* again and the constructed point that related to the location of spheno-occipital synchondrosis. As shown in the systematic review on changes in the anterior cranial base<sup>18</sup>, *Sella Turcica*

demonstrates downward and backward movement. This may translate to our study since this measurement involved Sella. As for the second vertical measurement, again it involved *Basion* and the changes can be correlated to growth at the speno-occipital synchondrosis itself. Interestingly, distance 21 which was measured from the internal hypoglossal canal to internal auditory meatus showed a significant percentage change, but not difference change.

### **Transverse measurements**

The final dimension studied was the transverse. A total of 19 measurements were reviewed. Since traditional 2D imaging could not address changes in the transverse dimension, multiple measurements would be beneficial when 3D imaging was used. Only 9 of the 19 measurements showed significant results for difference as well as percentage change, but similar to the other dimensions, these were only significant in a statistical context. Over the short time frame this study observed, none of the transverse measurements demonstrated clinically significant changes. In respect to the skull, Moss<sup>102</sup> reported that the medial areas of the skull base finish growth sooner while the lateral areas undergo prolonged change. Friede<sup>86</sup> also reported width development in the middle and posterior cranial fossae is by numerous bones, synchondroses and sutures. Similar to the study by Afrand,<sup>22</sup> in the transverse dimension they showed small increases in dimension between foramen spinosum and foramen ovale, similar to the findings here. Further study may be beneficial in this dimension.

It should also be noted that some values were negative, indicating “shrinkage”, which should not happen unless the landmarks were growing in opposite directions or there was addition of bone to one surface or both. Given the small scale, these negative values can be

attributed to measurement error and the inherent errors in landmark identification when using 3D imaging.

### **Sex differences**

In regards to differences in males vs. females, Ursi et al<sup>36</sup> showed that anterior cranial base length was larger in males, but cranial base angle, maxillary and mandibular length, and facial growth direction were all similar between the sexes. Suguros<sup>87</sup> reported that before 5 years of age there were growth differences between males and females, but after 5, these differences diminished. As above, this study indicates that during adolescents, no difference is observed between males and females for growth differences and percentage of change.

### **Matlab data**

As utilized by Lagravère et al. (10), the Matlab software used anatomical landmarks as origin locations (with coordinates 0, 0, 0). The software then measured the spatial movement in all 3 planes of space of the remaining landmarks. This data showed significant movement of 3 landmarks in the y axis (sella depth, TBP-L, and CP) and 11 landmarks in the z axis (FMP, FMR, FML, IHC-R, IHC-L, EHC-R, EHC-L, SF-R, SF-L, IAM-L, IAM-R). The significant values in the z axis were all negative indicating movement downwards while the significant values in the y axis were positive indicating forward movement. If certain anatomical landmarks were used as the origin points, and movement occurred in front or below, these changes would be justified. It should be kept in mind that these landmarks may have shown growth/movement themselves so any values may be distorted. This software should be used with other points as origins or with additional data to confirm or dispute the changes shown here.

## Limitations:

In this study, the CBCT images were taken over a relatively short period of time by growth standards. The 17.5 months average treatment time may not have been enough time span to demonstrate clinically significant growth/changes. Ideally a longer time for observation with longer intervals between CBCT images would improve the downfall of the limited observation time. Growth studies with multiple time points (T1, T2, T2 etc.) over many years would show the most accurate and significant changes if present.

It should also be noted that the linear measurements used to assess growth were derived from landmarks plotted on the CBCT images. These landmarks were used in multiple distance measurements, so when considering measurement error for the landmarks identification, this would be increased for the multiple distances an individual landmark was used for.

The manipulation of the radiographic software also has a learning curve. The easiest method for landmark placement was use of isosurface rendering (which was checked via axial, coronal and sagittal slices). When placing the landmarks, sometimes they did not register and had to be moved to the “correct” position. The difference in density of the surface rendering compared to the greyscale image may have produced inaccurate landmark identification as well as the need to “remove” the soft tissue until the skull was visible. Even slight changes when adjusting the surface rendering, could have moved the landmark location and affected the results on a small scale.

One observer was responsible for all the data gathering. This observer became quite proficient in landmark identification and software manipulation so it might be beneficial to repeat the study with observers that are “less experienced” to see if the results are repeated.

The number of landmarks per image also may have affected the results. The average time to landmark each image took about 25 minutes. This was very time consuming and not applicable for every day practice life, especially because these landmarks were limited to one area. Utilizing a few easily identifiable, accurate and reliable landmarks may improve future studies.

It should also be noted that the subjects received orthodontic treatment. The modality of treatment was unknown and may need further exploration as to whether it could have affected the results

## **2.6 Conclusions**

The horizontal, vertical and anterior-posterior dimensions of the posterior cranial base and surrounding area showed a few statistically-significant changes over the 17.5 month study time frame. The measurements which took *Basion* into consideration all showed changes, most likely due to speno-occipital synchondrosis growth and previously demonstrated changes in *Basion* position.

The magnitude of the changes was relatively small over the 17.5 treatment duration but consistent with previous 2D studies. Given the observed changes, extrapolated over years of growth, significant growth changes may continue throughout. This study or one similar should be completed on another sample to confirm the results observed here.

## **2.7 Appendices**

Appendix 1: Descriptive statistics of difference (above) and percentage change (below) of repeated measures for each distance:

### Descriptive Statistics

	N	Minimum	Maximum	Mean	Std. Deviation
diffd1H	60	-2.709	3.769	.25966	1.087894
diffd2H	60	-2.555	2.666	.12179	.944306
diffd3H	60	-2.921	3.846	.00359	1.171318
diffd4H	60	-1.627	1.603	.04404	.847668
diffd5H	60	-3.253	4.620	.48241	1.353054
diffd6H	60	-1.999	1.706	-.03649	.772315
diffd7H	60	-1.690	1.991	-.11364	.865591
diffd8H	60	-2.365	3.066	-.15740	.911705
diffd9H	60	-3.410	2.185	-.17070	1.136987
diffd10H	60	-1.468	2.742	.35980	.811489
diffd11H	60	-3.433	4.514	.71207	1.188090
diffd12H	60	-4.786	5.789	.41720	1.881090
diffd13H	60	-10.185	2.223	-.08358	2.133376
diffd14H	60	-3.230	2.899	.89319	1.235536
diffd15H	60	-2.054	4.466	1.32309	1.443946
diffd16H	60	-1.949	11.106	1.00227	2.076866
diffd17H	60	-1.924	6.850	.56237	1.397326
diffd18H	60	-3.648	3.705	.85735	1.257709
diffd19H	60	-3.343	3.866	.85181	1.429631
diffd20V	60	-2.573	11.717	.62460	1.889709
diffd21V	60	-4.929	2.044	.29294	1.183081
diffd22V	60	-3.380	1.947	.12866	1.041992
diffd23V	60	-2.475	3.473	.82665	1.194064
diffd24AP	60	-6.352	8.243	.60244	2.005906
diffd25AP	60	-1.671	3.396	.85719	1.046646
diffd26AP	60	-.968	3.119	.86915	.877813
diffd27AP	60	-2.679	2.561	.23839	1.089009
diffd28AP	60	-7.584	1.852	.24691	1.569615
diffd29AP	60	-1.496	1.493	-.18213	.532551
Valid N (listwise)	60				

### Descriptive Statistics

	N	Minimum	Maximum	Mean	Std. Deviation
%changeD1	60	-7.88	10.81	.8800	3.41454
%changeD2	60	-28.26	64.46	3.2524	14.47746
%changeD3	60	-30.30	57.76	1.0010	16.16922
%changeD4	60	-5.83	6.16	.2421	3.21637
%changeD5	60	-13.09	23.84	2.4369	6.54038
%changeD6	60	-16.43	15.19	-.0604	7.00350
%changeD7	60	-14.90	19.67	-1.0260	7.81252
%changeD8	60	-19.77	31.77	-1.1469	9.27352
%changeD9	60	-26.82	21.98	-1.2946	11.56651
%changeD10	60	-3.48	6.85	.8486	1.89058
%changeD11	60	-5.30	7.48	1.2065	1.88816
%changeD12	60	-8.73	13.05	.9201	3.82156
%changeD13	60	-16.47	4.51	-.0527	3.55638
%changeD14	60	-3.45	3.33	1.0510	1.40358
%changeD15	60	-2.05	4.42	1.3227	1.43914
%changeD16	60	-6.70	54.83	4.3072	10.20898
%changeD17	60	-6.63	30.47	2.2187	5.52911
%changeD18	60	-7.28	6.79	1.6572	2.41941
%changeD19	60	-6.22	7.15	1.6503	2.74123
%changeD20	60	-14.50	129.34	4.5808	17.65652
%changeD21	60	-18.78	11.80	1.3916	5.07590
%changeD22	60	-14.01	8.28	.6470	4.49646
%changeD23	60	-10.72	11.10	2.6981	4.05290
%changeD24	60	-18.88	38.52	2.4029	7.60274
%changeD25	60	-2.82	6.17	1.4855	1.80429
%changeD26	60	-1.61	5.58	1.5116	1.53803
%changeD27	60	-8.11	8.53	.8569	3.53924
%changeD28	60	-19.11	6.43	1.0028	4.44471
%changeD29	60	-3.64	4.19	-.4649	1.42210
Valid N (listwise)	60				

#### Appendix 2: MANOVA hypothesis tests

Ho: The difference in distances of the landmarks between T1 and T1 are equal to 0

Ha: The difference in distances of the landmarks between T1 and T2 are not equal to 0

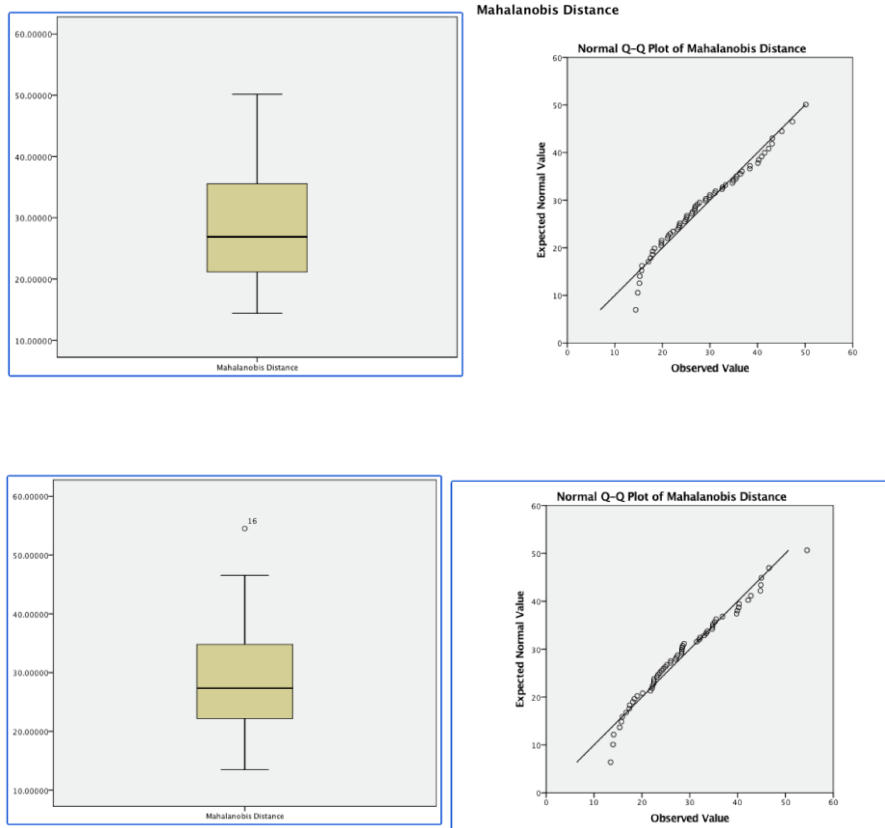
The repeated measures MANCOVA hypothesis tested were:

$H_0$ : The mean of the twenty nine linear measurements, when considered jointly, were the same at T1 and T2, when age (and treatment time) were used as a covariate.

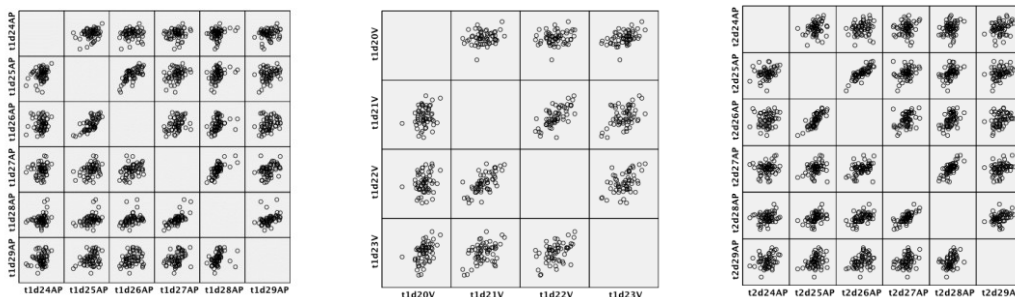
$H_a$ : The mean of the twenty nine different linear measurements, when considered jointly, were not the same at T1 and T2, when age (and treatment time) were considered as a covariate

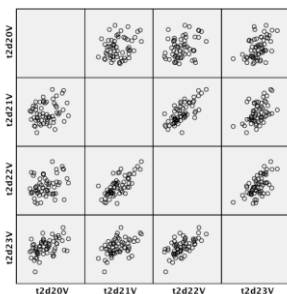
A p value of less than 0.05 was considered as significant.

Appendix 3: Boxplot and Q-Q plot of the Mahalanobis distance for difference in millimeters above and percentage change below:



Appendix 4: Bivariate Scatter plots of measurements at T1 (above) and T2 (below) for A/P and Vertical distances. All variables not included because the table would be unreadable.

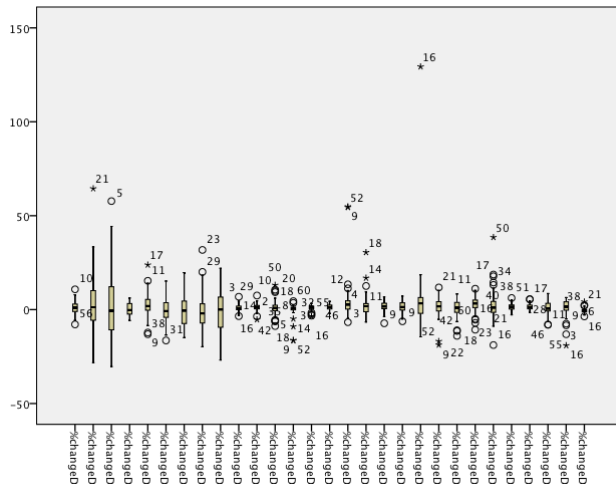
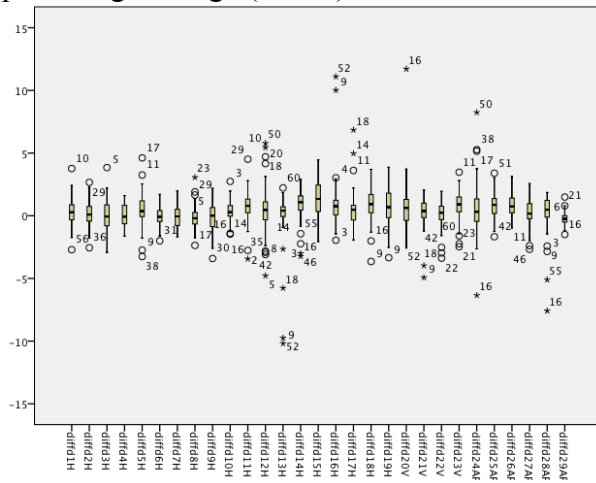




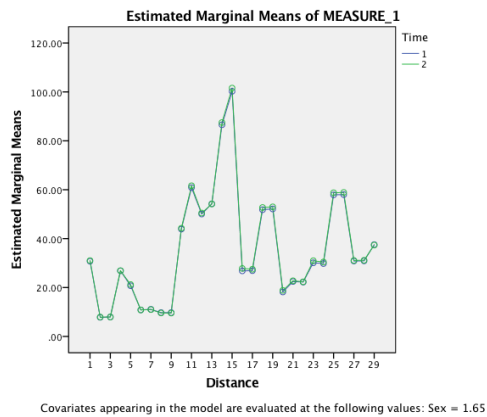
Appendix 5: Test for multicollinearity for age and difference in distance from T1 to T2

Distance difference (T2-T1)	Pearson Correlation (r)
D1H	0.110
D2H	-0.033
D3H	-0.112
D4H	-0.015
D5H	0.007
D6H	-0.154
D7H	0.002
D8H	-0.120
D9H	-0.213
D10H	-0.078
D11H	-0.018
D12H	0.227
D13H	-0.031
D14H	-0.065
D15H	-0.050
D16H	-0.171
D17H	0.305
D18H	0.077
D19H	0.025
D20V	0.193
D21V	0.108
D22V	-0.261
D23V	0.045
D24AP	-0.064
D25AP	0.129
D26AP	-0.085
D27AP	-0.252
D28AP	0.006
D29AP	-0.222

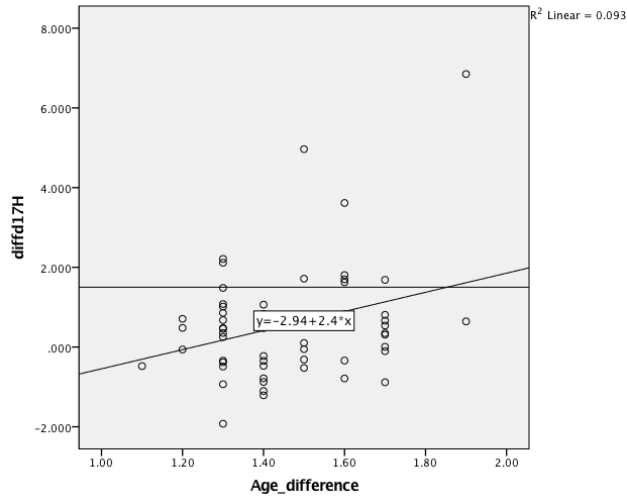
Appendix 6: Boxplot of the difference between T1 and T2 calculated distances (above) and percentage change (below):



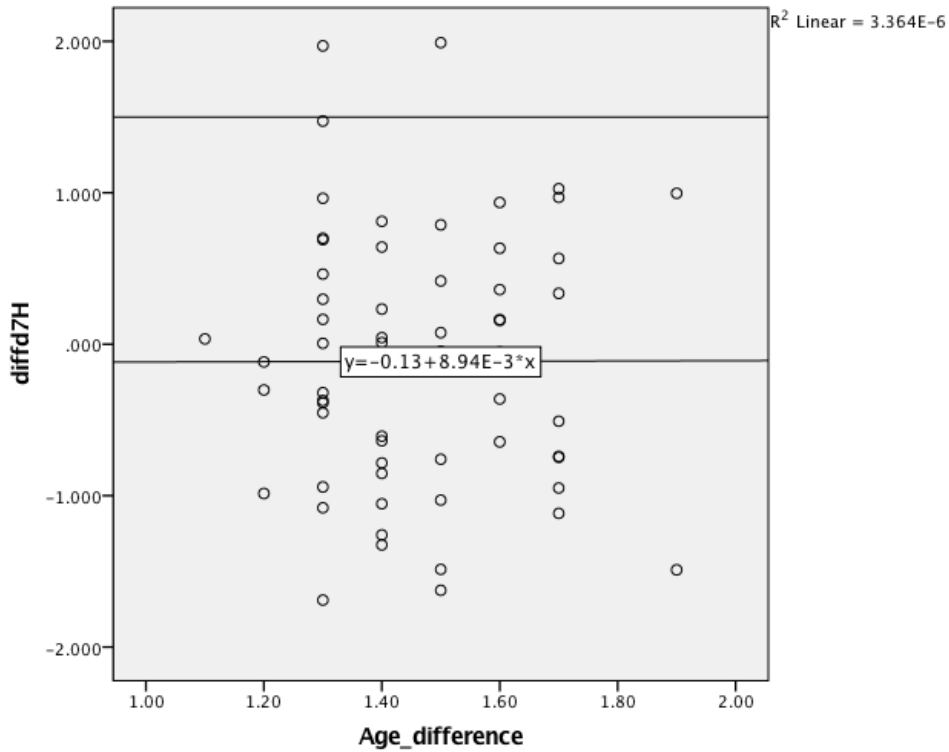
Appendix 7: Estimated marginal means for T1 and T2 for the difference in distance measurements.



Appendix 8: Scatter plot of difference in distance 17 that had a statistically significant result when treatment time used as covariate. Horizontal line set at 1.5mm for clinical significance.



Appendix 9: Scatter plot of difference in distance for distance 7 that showed no relation between treatment time and growth. Upper horizontal line set at clinically significant value of 1.5mm



## CHAPTER 4: General Discussion

### 4.1 Discussion

This study aimed to evaluate natural growth and developmental changes in the posterior cranial base and surrounding area during adolescence. Two research questions were identified after a systematic review of the literature was completed to show how changes in the posterior cranial base have previously been reported.

Question #1:

- a) Within the posterior cranial base and surrounding area, which identified landmarks are reproducible and repeatable when viewed in 3D CBCT images?
- b) Are these landmarks accurate and representative of true anatomical structures?

Question #2:

Are structures within the posterior cranial base and surrounding area dimensionally stable during the adolescent years?

To determine acceptable landmarks in the posterior base and surrounding area, visual inspection of dry human skulls identified 33 landmarks. Most of the landmarks are not commonly used in traditional cephalometry, and were identified solely for the purpose of 3D analysis. Accuracy and reliability were tested using the chosen landmarks. Although some statistically significant results were calculated, there were no clinically significant results concluded. All the landmarks were carried forward in the study.

The Matlab data, using previously defined landmarks as the origins, showed some significant spatial movement of 11 landmarks in the z axis and 3 in the y axis. This should be

interpreted with caution as the origin landmarks may have shown movement as well, but are consistent with potential growth at the spheno-occipital synchondrosis.

As stated above, the main objective was to evaluate potential growth and development changes in the posterior cranial base. The previously accepted landmarks were then used in evaluating adolescent CBCT images taken from two time points averaging 17.5 months apart. Both difference (represented by growth) and percentage change were evaluated as calculated from linear measurements between the landmarks and between the two image times. In all planes of space (sagittal, coronal, and horizontal) there showed neither clinically significant changes for percentage change nor growth (difference). Although some minor changes were demonstrated, continued growth at the spheno-occipital synchondrosis may be responsible as well as these changes may be reflective of measurement error and limitations within the measuring process. Even though the changes observed were minor, similar growth over an entire lifespan may contribute to more clinically significant observations.

## **4.2 Limitations**

Reliability chapter:

Minimizing the factors that may affect results is a goal of any investigation. This study was conducted with 10 previously used dry human skulls. A Plexiglas box and water was used to simulate soft tissue. Although deemed adequate for this study, using more samples and live specimens would be advantageous.

Differences in raters experience, precision and patience when landmarking, and familiarity with the software and landmark locations all contribute to potential reduction in reliability and accuracy results. Since locating the landmarks took time, one rater may have

found it easier to identify in one plane vs other raters comfort when identifying the same landmark in a different plane. Locating the landmarks and increasing reliability may increase with further recommendations into the best plane to localize the structure. Orientation sessions may be an advantage so all the raters know what to do and where to find the landmarks.

Becoming familiar with the Avizo software that was used for this study requires time and patience. Each rater felt more comfortable using different tools within the software to locate the landmarks based on the definitions. Significant time was also required to check the other planes and the isosurface rendering to ensure accurate landmark placement. Viewing the landmark in all three planes would be a nice addition during the landmarking process.

The technique used for hand placing the gutta percha on the dry skulls needs improving. The use of the block-out compound and gutta percha “chucks” appeared very accurate but the increase in thickness to get the block-out compound to stick and inconsistent sizes of the gutta percha may have influenced the accuracy of the landmark placement. Drilling holes into the skulls and placing a marker is more invasive to the specimens, but would significantly increase accuracy.

Growth chapter:

For the growth assessment chapter, the CBCT images that were analyzed were taken on an average of 17.5 months apart. Having more time-points and over a longer period of time would give a better picture to actual growth or size changes. Unfortunately the data available limited us to this time frame.

The sample used also contained more females than males (39 vs. 21). Although the analysis confirmed no differences between males and females, taking a sample with a more

even number would be beneficial. On the other hand, increasing the difference should show similar results.

Again, the use of the Avizo software has its limitations on this human population. Significant time was needed to adjust the images in all three planes as well as for surface rendering in order to adequately locate the landmarks and penetrate/eliminate soft tissue interference. Additionally, the areas deep within the skull (the posterior cranial base) showed significant variability in the resolution of the images. Some images were very sharp at the chosen landmarks whereas others were more difficult to identify.

#### **4.3 Future recommendations**

1. Numerous landmarks that were used in this study were identified solely for 3D analysis. It would be recommended that these landmarks be verified in subsequent studies before concrete recommendations on their use as stable structures.
2. This study used dry skulls when identifying the landmarks and performing reliability and accuracy assessment. It is recommended that if possible, human CBCT images be used for this step. This will eliminate landmark identification differences due to absent soft tissue.
3. It is recommended to add additional measurements in the transverse, vertical and anteroposterior to verify these dimensions in potentially growing and even non-growing populations.
4. Adding CVM as a parameter. Separating the sample based on CVM may yield interesting results.

5. Investigation as to whether the posterior cranial base has constant growth or a peak velocity of growth as other areas are shown to have.
6. Continuing this study or starting a new study with more time-points and/or longer growth assessment period is recommended. To better assess the posterior cranial base, growth assessment studies should follow patients over a longer period of time and with more evaluations.

#### References:

- 1 Steuer, I. The cranial base for superimposition of lateral cephalometric radiographs. *American journal of orthodontics* **61**, 493-500 (1972).
- 2 Ghafari, J., Engel, F. E. & Laster, L. L. Cephalometric superimposition on the cranial base: a review and a comparison of four methods. *American Journal of Orthodontics and Dentofacial Orthopedics* **91**, 403-413 (1987).
- 3 Buschang, P., LaPalme, L., Tanguay, R. & Demirjian, A. The technical reliability of superimposition on cranial base and mandibular structures. *The European Journal of Orthodontics* **8**, 152-156 (1986).
- 4 Nie, X. Cranial base in craniofacial development: developmental features, influence on facial growth, anomaly, and molecular basis. *Acta odontologica Scandinavica* **63**, 127-135, doi:10.1080/00016350510019847 (2005).
- 5 Björk, A. Cranial base development. *American Journal of Orthodontics* **41**, 198-225, doi:10.1016/0002-9416(55)90005-1.
- 6 Thiesen, G. *et al.* Comparative analysis of the anterior and posterior length and deflection angle of the cranial base, in individuals with facial Pattern I, II and III. *Dental press journal of orthodontics* **18**, 69-75 (2013).
- 7 Moore W. J, L. C. L. B. Growth of the facial skeleton in the hominoidea. *New York: Academic* (1974).
- 8 Farman, A. G. & Scarfe, W. C. The Basics of Maxillofacial Cone Beam Computed Tomography. *Seminars in Orthodontics* **15**, 2-13, doi:10.1053/j.sodo.2008.09.001.
- 9 Proffit, W. R., Fields, H. & Sarver, D. *Contemporary Orthodontics 5th Edition*. (Elsevier, 2013).
- 10 Enlow, D. H. *The Human Face: An Account of the Postnatal Growth and Development of the Craniofacial Skeleton*. (Harpers & Row, 1968).
- 11 Bastir, M., Rosas, A. & O'Higgins, P. Craniofacial levels and the morphological maturation of the human skull. *Journal of anatomy* **209**, 637-654, doi:10.1111/j.1469-7580.2006.00644.x (2006).

- 12 Goldstein, J. A. *et al.* Earlier Evidence of Spheno-Occipital Synchondrosis Fusion Correlates with Severity of Midface Hypoplasia in Patients with Syndromic Craniosynostosis. *Plastic and reconstructive surgery* **134**, 504-510, doi:10.1097/prs.0000000000000419 (2014).
- 13 Bassed, R. B., Briggs, C. & Drummer, O. H. Analysis of time of closure of the spheno-occipital synchondrosis using computed tomography. *Forensic Science International* **200**, 161-164, doi:10.1016/j.forsciint.2010.04.009.
- 14 Hoyte, D. A. The cranial base in normal and abnormal skull growth. *Neurosurg Clin N Am* **2**, 515-537 (1991).
- 15 Powell, T. V. & Brodie, A. G. Closure of the spheno-occipital synchondrosis. *The Anatomical Record* **147**, 15-23, doi:10.1002/ar.1091470104 (1963).
- 16 Melsen, B. Time of closure of the spheno-occipital synchondrosis determined on dry skulls. A radiographic craniometric study. *Acta odontologica Scandinavica* **27**, 73-90 (1969).
- 17 Thilander, B. & Ingervall, B. The human spheno-occipital synchondrosis. II. A histological and microradiographic study of its growth. *Acta odontologica Scandinavica* **31**, 323-334 (1973).
- 18 Afrand, M., Ling, C. P., Khosrotehrani, S., Flores-Mir, C. & Lagravere-Vich, M. O. Anterior cranial-base time-related changes: A systematic review. *American journal of orthodontics and dentofacial orthopedics : official publication of the American Association of Orthodontists, its constituent societies, and the American Board of Orthodontics* **146**, 21-32 e26, doi:10.1016/j.ajodo.2014.03.019 (2014).
- 19 Liberati, A. *et al.* The PRISMA statement for reporting systematic reviews and meta-analyses of studies that evaluate health care interventions: explanation and elaboration. *Journal of Clinical Epidemiology* **62**, e1-34.
- 20 Ford, E. Growth of the human cranial base. *Am J Orthod* **44**, 498-506 (1958).
- 21 Sejrsen, B., Jakobsen, J., Skovgaard, L. T. & Kjaer, I. Growth in the external cranial base evaluated on human dry skulls, using nerve canal openings as references. *Acta odontologica Scandinavica* **55**, 356-364 (1997).
- 22 Singh, G. D., McNamara Jr, J. A. & Lozanoff, S. Thin-plate spline analysis of the cranial base in subjects with Class III malocclusion. *European journal of orthodontics* **19**, 341-353 (1997).
- 23 Lavelle, C. L. A study of the craniofacial skeleton. *The Angle orthodontist* **48**, 227-234, doi:10.1043/0003-3219(1978)048<0227:asotcs>2.0.co;2 (1978).
- 24 Arat, M., Koklu, A., Ozdiler, E., Rubenduz, M. & Erdogan, B. Craniofacial growth and skeletal maturation: a mixed longitudinal study. *European journal of orthodontics* **23**, 355-361 (2001).
- 25 Arat, Z. M., Turkkahraman, H., English, J. D., Gallerano, R. L. & Boley, J. C. Longitudinal growth changes of the cranial base from puberty to adulthood. A comparison of different superimposition methods. *The Angle orthodontist* **80**, 537-544, doi:10.2319/080709-447.1 (2010).
- 26 Bishara, S. E., Treder, J. E. & Jakobsen, J. R. Facial and dental changes in adulthood. *American journal of orthodontics and dentofacial orthopedics : official publication of the*

- American Association of Orthodontists, its constituent societies, and the American Board of Orthodontics* **106**, 175-186 (1994).
- 27 Franchi, L., Baccetti, T., Stahl, F. & McNamara Jr, J. A. Thin-plate spline analysis of  
craniofacial growth in class I and class II subjects. *Angle Orthodontist* **77**, 595-601 (2007).
- 28 Henneberger, M. & Prah-Andersen, B. Cranial base growth for Dutch boys and girls: a  
multilevel approach. *American journal of orthodontics and dentofacial orthopedics :  
official publication of the American Association of Orthodontists, its constituent  
societies, and the American Board of Orthodontics* **106**, 503-512 (1994).
- 29 Jiang, J., Xu, T., Lin, J. & Harris, E. F. Proportional analysis of longitudinal craniofacial  
growth using modified mesh diagrams. *Angle Orthodontist* **77**, 794-802 (2007).
- 30 Lewis, A. B. & Roche, A. F. Late growth changes in the craniofacial skeleton. *The Angle  
orthodontist* **58**, 127-135 (1988).
- 31 Malta, L. A., Ortolani, C. F. & Faltin, K. Quantification of cranial base growth during  
pubertal growth. *Journal of orthodontics* **36**, 229-235 (2009).
- 32 Mitani, H. Contributions of the posterior cranial base and mandibular condyles to facial  
depth and height during puberty. *The Angle orthodontist* **43**, 337-343,  
doi:10.1043/0003-3219(1973)043<0337:cotpcb>2.0.co;2 (1973).
- 33 Palomo, J. M., Hunt, D. W., Jr., Hans, M. G. & Broadbent, B. H., Jr. A longitudinal 3-  
dimensional size and shape comparison of untreated Class I and Class II subjects.  
*American Journal of Orthodontics & Dentofacial Orthopedics* **127**, 584-591 (2005).
- 34 Phelan, A., Franchi, L., Baccetti, T., Darendeliler, M. A. & McNamara Jr, J. A. Longitudinal  
growth changes in subjects with open-bite tendency: A retrospective study. *American  
Journal of Orthodontics and Dentofacial Orthopedics* **145**, 28-35 (2014).
- 35 Thordarson, A., Johannsdottir, B. & Magnusson, T. E. Craniofacial changes in Icelandic  
children between 6 and 16 years of age - A longitudinal study. *European journal of  
orthodontics* **28**, 152-165 (2006).
- 36 Ursi, W. J., Trotman, C. A., McNamara Jr, J. A. & Behrents, R. G. Sexual dimorphism in  
normal craniofacial growth. *The Angle orthodontist* **63**, 47-56 (1993).
- 37 Wilhelm, B. M., Beck, F. M., Lidral, A. C. & Vig, K. W. A comparison of cranial base  
growth in Class I and Class II skeletal patterns. *American Journal of Orthodontics &  
Dentofacial Orthopedics* **119**, 401-405 (2001).
- 38 Ohtsuki, F., Mukherjee, D., Lewis, A. B. & Roche, A. F. A factor analysis of cranial base  
and vault dimensions in children. *Am J Phys Anthropol* **58**, 271-279,  
doi:10.1002/ajpa.1330580305 (1982).
- 39 Knott, V. B. Ontogenetic change of four cranial base segments in girls. *Growth* **33**, 123-  
142.
- 40 Knott, V. B. Change in cranial base measures of human males and females from age 6  
years to early adulthood. *Growth* **35**, 145-158.
- 41 Netter, F. H. *Atlas of Human Anatomy*. (Elsevier Health Sciences, 2010).
- 42 Radiographic cephalometry: From basics to video imaging. *Journal of Oral and  
Maxillofacial Surgery* **54**, 1378, doi:10.1016/S0278-2391(96)90517-0.
- 43 Krishan, K. & Kanchan, T. Evaluation of spheno-occipital synchondrosis: A review of  
literature and considerations from forensic anthropologic point of view. *Journal of  
Forensic Dental Sciences* **5**, 72-76, doi:10.4103/0975-1475.119764 (2013).

- 44 Nervina, J. M. Cone beam computed tomography use in orthodontics. *Australian Dental Journal* **57**, 95-102, doi:10.1111/j.1834-7819.2011.01662.x (2012).
- 45 Mah, J. K., Huang, J. C. & Choo, H. Practical Applications of Cone-Beam Computed Tomography in Orthodontics. *The Journal of the American Dental Association* **141**, Supplement 3, 7S-13S, doi:<http://dx.doi.org/10.14219/jada.archive.2010.0361> (2010).
- 46 Baumrind, S. & Frantz, R. C. The reliability of head film measurements. 1. Landmark identification. *Am J Orthod* **60**, 111-127 (1971).
- 47 Ludlow, J. B., Gubler, M., Cevitanes, L. & Mol, A. Precision of cephalometric landmark identification: Cone-beam computed tomography vs conventional cephalometric views. *American Journal of Orthodontics and Dentofacial Orthopedics* **136**, 312.e311-312.e310, doi:<http://dx.doi.org/10.1016/j.ajodo.2008.12.018> (2009).
- 48 Liang, X. *et al.* A comparative evaluation of Cone Beam Computed Tomography (CBCT) and Multi-Slice CT (MSCT): Part I. On subjective image quality. *European Journal of Radiology* **75**, 265-269, doi:<http://dx.doi.org/10.1016/j.ejrad.2009.03.042> (2010).
- 49 Angelopoulos, C., Scarfe, W. C. & Farman, A. G. A Comparison of Maxillofacial CBCT and Medical CT. *Atlas of the Oral and Maxillofacial Surgery Clinics of North America* **20**, 1-17, doi:10.1016/j.cxom.2011.12.008.
- 50 Schlicher, W. *et al.* Consistency and precision of landmark identification in three-dimensional cone beam computed tomography scans. *European journal of orthodontics* **34**, 263-275, doi:10.1093/ejo/cjq144 (2012).
- 51 Gwet, K. L. *Handbook of inter-rater reliability: The definitive guide to measuring the extent of agreement among raters.* (Advanced Analytics, LLC, 2014).
- 52 Kamoen, A., Dermaut, L. & Verbeeck, R. The clinical significance of error measurement in the interpretation of treatment results. *European journal of orthodontics* **23**, 569-578, doi:10.1093/ejo/23.5.569 (2001).
- 53 Lou, L., Lagravere, M. O., Compton, S., Major, P. W. & Flores-Mir, C. Accuracy of measurements and reliability of landmark identification with computed tomography (CT) techniques in the maxillofacial area: a systematic review. *Oral Surgery, Oral Medicine, Oral Pathology, Oral Radiology, and Endodontology* **104**, 402-411, doi:<http://dx.doi.org/10.1016/j.tripleo.2006.07.015> (2007).
- 54 de Oliveira, A. E. F. *et al.* Observer reliability of three-dimensional cephalometric landmark identification on cone-beam computerized tomography. *Oral Surgery, Oral Medicine, Oral Pathology, Oral Radiology, and Endodontology* **107**, 256-265, doi:<http://dx.doi.org/10.1016/j.tripleo.2008.05.039> (2009).
- 55 Gupta, A., Kharbanda, O. P., Sardana, V., Balachandran, R. & Sardana, H. K. Accuracy of 3D cephalometric measurements based on an automatic knowledge-based landmark detection algorithm. *International Journal of Computer Assisted Radiology and Surgery* **11**, 1297-1309, doi:10.1007/s11548-015-1334-7 (2016).
- 56 Lagravère, M. O. *et al.* Cranial base foramen location accuracy and reliability in cone-beam computerized tomography. *American Journal of Orthodontics and Dentofacial Orthopedics* **139**, e203-e210, doi:<http://dx.doi.org/10.1016/j.ajodo.2009.06.027> (2011).
- 57 Lagravère, M. O., Carey, J., Toogood, R. W. & Major, P. W. Three-dimensional accuracy of measurements made with software on cone-beam computed tomography images.

- American Journal of Orthodontics and Dentofacial Orthopedics* **134**, 112-116, doi:<http://dx.doi.org/10.1016/j.ajodo.2006.08.024> (2008).
- 58 Afrand, M., Oh, H., Flores-Mir, C. & Lagravère-Vich, M. O. Growth changes in the anterior and middle cranial bases assessed with cone-beam computed tomography in adolescents. *American Journal of Orthodontics and Dentofacial Orthopedics* **151**, 342-350.e342, doi:<http://dx.doi.org/10.1016/j.ajodo.2016.02.032> (2017).
- 59 Portney, L. G. & Watkins, M. P. *Foundations of clinical research: applications to practice*. Vol. 2 (Prentice Hall Upper Saddle River, NJ, 2000).
- 60 Yoon, K. W. *et al.* Deviation of landmarks in accordance with methods of establishing reference planes in three-dimensional facial CT evaluation. *Imaging Science in Dentistry* **44**, 207-212, doi:10.5624/isd.2014.44.3.207 (2014).
- 61 İlgüy, D., İlgüy, M., Ersan, N., Dölekoğlu, S. & Fişekçioğlu, E. Measurements of the Foramen Magnum and Mandible in Relation to Sex Using CBCT. *Journal of Forensic Sciences* **59**, 601-605, doi:10.1111/1556-4029.12376 (2014).
- 62 Zamora, N., Llamas, J. M., Cibrián, R., Gandia, J. L. & Paredes, V. A study on the reproducibility of cephalometric landmarks when undertaking a three-dimensional (3D) cephalometric analysis. *Medicina Oral, Patología Oral y Cirugía Bucal* **17**, e678-e688, doi:10.4317/medoral.17721 (2012).
- 63 Lagravère, M. O. *et al.* Intraexaminer and interexaminer reliabilities of landmark identification on digitized lateral cephalograms and formatted 3-dimensional cone-beam computerized tomography images. *American Journal of Orthodontics and Dentofacial Orthopedics* **137**, 598-604, doi:<http://dx.doi.org/10.1016/j.ajodo.2008.07.018> (2010).
- 64 Parvindokht, B., Reza, D. M. & Saeid, B. Morphometric analysis of hypoglossal canal of the occipital bone in Iranian dry skulls. *Journal of Craniovertebral Junction & Spine* **6**, 111-114, doi:10.4103/0974-8237.161591 (2015).
- 65 Ren, Y.-F., Isberg, A. & Westesson, P.-L. Steepness of the articular eminence in the temporomandibular joint. *Oral Surgery, Oral Medicine, Oral Pathology, Oral Radiology, and Endodontology* **80**, 258-266, doi:[http://dx.doi.org/10.1016/S1079-2104\(05\)80380-4](http://dx.doi.org/10.1016/S1079-2104(05)80380-4) (1995).
- 66 Shahidi, S., Vojdani, M. & Paknahad, M. Correlation between articular eminence steepness measured with cone-beam computed tomography and clinical dysfunction index in patients with temporomandibular joint dysfunction. *Oral Surgery, Oral Medicine, Oral Pathology and Oral Radiology* **116**, 91-97, doi:<http://dx.doi.org/10.1016/j.oooo.2013.04.001> (2013).
- 67 Panmekiate, S., Petersson, A. & Akerman, S. Angulation and prominence of the posterior slope of the eminence of the temporomandibular joint in relation to disc position. *Dentomaxillofacial Radiology* **20**, 205-208, doi:10.1259/dmfr.20.4.1808008 (1991).
- 68 Ishibashi, M. *et al.* The ability to identify the intraparotid facial nerve for locating parotid gland lesions in comparison to other indirect landmark methods: evaluation by 3.0 T MR imaging with surface coils. *Neuroradiology* **52**, 1037-1045, doi:10.1007/s00234-010-0718-1 (2010).

- 69 Miloro, M., Redlinger, S., Pennington, D. M. & Kolodge, T. In Situ Location of the Temporal Branch of the Facial Nerve. *Journal of Oral and Maxillofacial Surgery* **65**, 2466-2469, doi:<http://dx.doi.org/10.1016/j.joms.2007.04.013> (2007).
- 70 Naidoo, N., Lazarus, L., Ajayi, N. O. & Satyapal, K. S. An anatomical investigation of the carotid canal. *Folia Morphologica* (2016).
- 71 Berlis, A., Putz, R. & Schumacher, M. Direct and CT measurements of canals and foramina of the skull base. *The British journal of radiology* **65**, 653-661 (1992).
- 72 Jeffery, N. Cranial base angulation and growth of the human fetal pharynx. *The Anatomical Record Part A: Discoveries in Molecular, Cellular, and Evolutionary Biology* **284A**, 491-499, doi:10.1002/ar.a.20183 (2005).
- 73 Arnold, M. A. *et al.* MEF2C Transcription Factor Controls Chondrocyte Hypertrophy and Bone Development. *Developmental Cell* **12**, 377-389, doi:<http://dx.doi.org/10.1016/j.devcel.2007.02.004> (2007).
- 74 Scott, J. H. The growth in width of the facial skeleton. *American Journal of Orthodontics* **43**, 366-371, doi:[http://dx.doi.org/10.1016/0002-9416\(57\)90103-3](http://dx.doi.org/10.1016/0002-9416(57)90103-3) (1957).
- 75 Bumpous, J. M., Curtin, H. D., Prokopakis, E. P. & Janecka, I. P. Applications of image-guided navigation in the middle cranial fossa: an anatomic study. *Skull base surgery* **6**, 187-190 (1996).
- 76 Lang, J., Maier, R. & Schafhauser, O. Postnatal enlargement of the foramina rotundum, ovale et spinosum and their topographical changes. *Anatomischer Anzeiger* **156**, 351-387 (1983).
- 77 Zada, G. *et al.* The neurosurgical anatomy of the sphenoid sinus and sellar floor in endoscopic transsphenoidal surgery: Clinical article. *Journal of neurosurgery* **114**, 1319-1330 (2011).
- 78 Sperber, G. H., Guttman, G. D. & Sperber, S. M. *Craniofacial Development (Book for Windows & Macintosh)*. Vol. 1 (PMPH-USA, 2001).
- 79 Okamoto, K., Ito, J., Tokiguchi, S. & Furusawa, T. High-resolution CT findings in the development of the sphenoccipital synchondrosis. *American Journal of Neuroradiology* **17**, 117-120 (1996).
- 80 Ingervall, B. & Thilander, B. The human sphenoccipital synchondrosis I. The time of closure appraised macroscopically. *Acta odontologica Scandinavica* **30**, 349-356 (1972).
- 81 Powell, T. V. & Brodie, A. G. Closure of the sphenoccipital synchondrosis. *The Anatomical Record* **147**, 15-23 (1963).
- 82 Portmann, M. *The internal auditory meatus: anatomy, pathology, and surgery*. (Churchill Livingstone, 1975).
- 83 Visvanathan, V. Anatomical variations of the temporal bone on high-resolution computed tomography imaging: how common are they? *The Journal of Laryngology & Otology* **129**, 634-637 (2015).
- 84 Major, P. W., Johnson, D. E., Hesse, K. L. & Glover, K. E. Landmark identification error in posterior anterior cephalometrics. *The Angle orthodontist* **64**, 447-454 (1994).
- 85 Tanner, J., Whitehouse, R., Marubini, E. & Resele, L. The adolescent growth spurt of boys and girls of the Harpenden growth study. *Annals of human biology* **3**, 109-126 (1976).

- 86 Friede, H. Normal development and growth of the human neurocranium and cranial base. *Scandinavian journal of plastic and reconstructive surgery* **15**, 163-169 (1981).
- 87 Sgouros, S., Natarajan, K., Hockley, A., Goldin, J. & Wake, M. Skull base growth in childhood. *Pediatric neurosurgery* **31**, 259-268 (1999).
- 88 van Vlijmen, O. J. *et al.* Comparison of cephalometric radiographs obtained from cone-beam computed tomography scans and conventional radiographs. *Journal of Oral and Maxillofacial Surgery* **67**, 92-97 (2009).
- 89 Springate, S. The effect of sample size and bias on the reliability of estimates of error: a comparative study of Dahlberg's formula. *The European Journal of Orthodontics* **34**, 158-163 (2012).
- 90 Lagravere, M., Major, P. & Carey, J. Sensitivity analysis for plane orientation in three-dimensional cephalometric analysis based on superimposition of serial cone beam computed tomography images. *Dentomaxillofacial Radiology* (2014).
- 91 TANNER, J. A History of the Study of Human Growth. *ANNALS OF HUMAN BIOLOGY* **8**, 404 (1981).
- 92 Major, P. W. Use of Skeletal Maturation Based on Hand-Wrist Radiographic Analysis as a Predictor of Facial Growth: A Systematic Review. *Angle Orthodontist* **74** (2004).
- 93 Nanda, R. S. The rates of growth of several facial components measured from serial cephalometric roentgenograms. *American Journal of Orthodontics* **41**, 658-673 (1955).
- 94 Cevidane, L. H., Motta, A., Proffit, W. R., Ackerman, J. L. & Styner, M. Cranial base superimposition for 3-dimensional evaluation of soft-tissue changes. *American Journal of Orthodontics and Dentofacial Orthopedics* **137**, S120-S129 (2010).
- 95 Periago, D. R. *et al.* Linear accuracy and reliability of cone beam CT derived 3-dimensional images constructed using an orthodontic volumetric rendering program. *The Angle orthodontist* **78**, 387-395 (2008).
- 96 Damstra, J., Fourie, Z., Slater, J. J. H. & Ren, Y. Accuracy of linear measurements from cone-beam computed tomography-derived surface models of different voxel sizes. *American Journal of Orthodontics and Dentofacial Orthopedics* **137**, 16. e11-16. e16 (2010).
- 97 Spin-Neto, R., Gotfredsen, E. & Wenzel, A. Impact of Voxel Size Variation on CBCT-Based Diagnostic Outcome in Dentistry: a Systematic Review. *Journal of Digital Imaging* **26**, 813-820, doi:10.1007/s10278-012-9562-7 (2013).
- 98 Brown, A. A., Scarfe, W. C., Scheetz, J. P., Silveira, A. M. & Farman, A. G. Linear accuracy of cone beam CT derived 3D images. *The Angle orthodontist* **79**, 150-157 (2009).
- 99 Bastir, M., Rosas, A. & O'Higgins, P. Craniofacial levels and the morphological maturation of the human skull. *Journal of anatomy* **209**, 637-654 (2006).
- 100 Enlow, D. H. & Hans, M. G. *Essentials of facial growth*. (WB Saunders Company, 1996).
- 101 Cunningham, C., Scheuer, L. & Black, S. *Developmental juvenile osteology*. (Academic Press, 2016).
- 102 Moss, M. L. & Greenberg, S. N. Postnatal growth of the human skull base. *The Angle orthodontist* **25**, 77-84 (1955).